Revisiting Polymyxin B: Pharmacokinetics, Biodistribution and Mechanism(s) of Intrarenal Transport

---

A dissertation

Presented to

The Department of Pharmacological and Pharmaceutical Sciences

University of Houston

In Partial Fulfillment of

The Requirement for the Degree of

Doctor of Philosophy

By

Pooja Manchandani

November, 2016

DEDICATED To

My Grandmother, Mrs. Saraswati Devi

A spiritual, gentle soul who taught me to believe in God and myself

My Mother, Mrs. Meena Manchandani

For being my first teacher and giving me her endless love

My Father, Dr. R. K. Manchandani

For teaching me the valuable lessons of hard work and perseverance

My Brother, Lt. Cdr. Punit Ravi Raj

For being a beacon of inspiration and constant motivation

My Beloved Husband, Mr. Sivashankar Rathinakumar

For his patience, understanding and unconditional love towards me

Revisiting Polymyxin B: Pharmacokinetics, Biodistribution and Mechanism(s) of Intrarenal Transport

By

_____

Pooja Manchandani

Approved by:

_____

Vincent H. Tam, Pharm.D. BCPS (Advisor)
Department of Pharmacological and Pharmaceutical Sciences (PPS), College of Pharmacy, UH

_____

Diana S-L Chow, Ph.D.
PPS, College of Pharmacy, UH

_____

Ming Hu, Ph.D.
PPS, College of Pharmacy, UH

_____

Jason Eriksen, Ph.D.
PPS, College of Pharmacy, UH

_____

Jeffery Sherer, Pharm.D.
Department of Pharmacy Practice and Translational Research, College of Pharmacy, UH

_____

Luan D. Truong, MD.
Methodist Hospital and Research Institute, Houston

_____

Lamar Pritchard, Ph.D.
Dean, College of pharmacy, UH

ACKNOWLEDGEMENT

I would like to express my heartfelt appreciation and deepest gratitude to my advisor, Dr. Vincent H. Tam for his immense support, guidance and constant mentoring throughout the pursuit of my doctoral research. He is an excellent scientist and continually conveyed his passion for science which greatly helped me grow as a researcher. His dedication, enthusiasm, and his quest for knowledge have been very instrumental in the successful accomplishment of my research goals. His advice on both scientific as well as career front has been tremendously helpful. This dissertation would not have been possible without his guidance and persistent support.

I would extend my sincere thanks to all my committee members for their insightful suggestions and brilliant comments. I am hugely indebted to Dr. Luan D. Truong from Methodist Hospital and Research Institute for being so kind to provide his technical expertise as well as resources throughout my research. I am extremely thankful to Dr. Diana Chow who has been a constant source of motivation and support as I navigated through various impediments of this graduate program. I am highly indebted to Dr. Jason Eriksen for his extreme patience in training me the techniques of immunohistochemical staining. He always took the time to engage himself in scientific discussions which developed

more conceptual clarity in me. I would also like to thank Dr. Ming Hu for helping me build my knowledge on the important concepts of transporter studies and for his insightful comments on the project. Lastly, I would like to express my special appreciation to Dr. Jefferey Sherer for educating me on the clinical nuances of this research. Thank you all for your valued contribution towards this project.

My gratitude goes to the entire PPS faculty for teaching and imparting wisdom in me so passionately. I am very grateful to my labmates and friends, especially to Dr. Kamilia Abdelraouf, Kimberly Ledesma, Dr. Kai-Tai Chang, Henrietta Abodakpi, Dr. Jessica T. Babic, Jian Zhou, Dr. Song Gao, Dr. Weiqun Wang, Dr. Rashim Singh, Dr. Odochi Nwoko, Dr. Jaspal Singh, Yu Jin Kim and Craig Vollet for their immense help and support. I would also like to express my special appreciation to my friends outside the department, particularly to Hafsa, Jera, Swati, Vijayshree, Radha, Krithika, Priya, Roshan Nirup, Ratheesh, Srikrishna, Manikandan and Saravanan. I am thankful to Dr. Kapil Joshi and Dr. Abhay Asthana, my teachers during the undergraduate program for providing their never-ending encouragement.

A good support system is very critical for surviving through the obstacles of graduate school and accomplishing research goals. I was fortunate to have one such vital support system: ‘my loving family.' My express my deepest gratitude to my family members for their constant motivation; this dissertation would not have

been possible without their support. I dedicate this thesis to my beloved grandmother, Mrs. Saraswati Devi; my loving mother, Mrs. Meena Manchandani who has given me their unconditional love and endless support. My father, Dr. R. K. Manchandani for being the strongest pillar of my life. My brother, Lt. Cdr. Punit Ravi Raj who has always been a beacon of light, encouragement, and lifelong inspiration to me. He offered his constant support and was instrumental in instilling confidence in me throughout my doctoral studies. I would also like to thank my sister-in-law Dr. Sarika Sharma for providing her support and encouragement. I would extend my heartfelt thanks to my dearest husband, soul-mate and best friend, Mr. Sivashankar Rathinakumar for his patience, endless love and all the sacrifices he has made for me. I thank him for sticking by my side, even when I was not in my best shape. He provided me the strength and perseverance to finish this project. I immensely value his understanding and non-judgemental attitude towards me. I am also thankful to my father-in-law, Capt. Rathinakumar Thangavelu and mother-in-law, Mrs. Jothimani Rathinakumar for their love and support. I love you all dearly!

Finally, I thank God, for giving me strength to endure all the challenges and guiding me every single day of my life. I extend my heartfelt appreciation to all those who have been associated directly and indirectly with this dissertation. Thank you all.

Revisiting Polymyxin B: Pharmacokinetics, Biodistribution and Mechanism(s) of Intrarenal Transport

---

An Abstract

Presented to

The Department of Pharmacological and Pharmaceutical Sciences

University of Houston

In Partial Fulfillment of

The Requirement for the Degree of

Doctor of Philosophy

By

Pooja Manchandani

November, 2016

ABSTRACT

Objectives: Despite dose-limiting nephrotoxic potentials, polymyxin B has re-emerged as the last line of therapy against multidrug-resistant Gram-negative bacterial infections. However, the pharmacokinetic, pharmacodynamic and nephrotoxic properties of polymyxin B are still not thoroughly understood. The objectives of this study were to provide additional insights to the overall biodistribution and disposition of polymyxin B; to evaluate the impact of renal polymyxin B exposure on nephrotoxicity; to delineate the underlying transport mechanism(s) responsible for the intrarenal drug accumulation.

Methods: A comparative pharmacokinetic profile of various polymyxin B components following intravenous administration was derived in rats. The overall drug biodistribution in various organs (brain, heart, lungs, liver, spleen, kidneys and skeletal muscle) was assessed. Intrarenal distribution of polymyxin B was evaluated at the cellular level. Drug disposition was quantified in rat urine/ bile. Renal drug accumulation was assessed at different polymyxin B dosing levels, and the onset of polymyxin B-induced nephrotoxicity was correlated to the renal drug exposure. The role of megalin, a renal endocytic receptor was evaluated in the renal accumulation of polymyxin B.

Results: The pharmacokinetic profiles of individual polymyxin B components were comparable. Among all the organs evaluated, polymyxin B distribution was highest in the kidneys. Within kidneys, the highest drug accumulation was observed in the proximal tubular cells. Less than 5% of administered dose (or pharmacologically active metabolites, if any) were recovered in the urine over 48 h, but all four major polymyxin B components were detected in the bile over 4 h. The higher daily dose of polymyxin B resulted in greater renal accumulation. The onset of nephrotoxicity was correlated to the daily dose of polymyxin B. The megalin-mediated renal uptake of polymyxin B could be disrupted.

Conclusions: The individual components of polymyxin B demonstrate similar pharmacokinetics. The biodistribution findings corroborate our previous results that polymyxin B is highly accumulated in the kidneys, but the elimination is likely via a non-renal route. Biliary excretion could be one of the possible routes of polymyxin B elimination, which should be further explored. The onset of polymyxin B-induced nephrotoxicity is correlated to the renal drug exposure. In addition, megalin appears to play a pivotal role in the renal accumulation of polymyxin B, which might contribute to nephrotoxicity.

TABLE OF CONTENTS

LIST OF FIGURES

LIST OF TABLES

CHAPTER 1

INTRODUCTION

1.1 Background

The emergence of antimicrobial resistance is a major global public health crisis (Chen, Ko, & Hsueh, 2013; Clark, Zhanel, & Lynch, 2016; Zavascki, Goldani, Li, & Nation, 2007). Gram-negative bacilli, in particular, present with high levels of intrinsic resistance and a tendency to acquire additional modes of resistance. Thus, they are formidable pathogens commonly implicated in nosocomial infections (Ali, Mumtaz, Naz, Jabeen, & Shafique, 2015; Artiaco, Cicero, Bellomo, & Bianchi, 2012; Bergamasco et al., 2012). These infections are associated with high risk of mortality and morbidity (Alp, Coruh, Gunay, Yontar, & Doganay, 2012; Baijal et al., 2014; Lye et al., 2012; Tumbarello et al., 2015). As a result of the escalating multidrug-resistance (MDR) among these pathogens, many currently available antibiotics used for these infections are rendered ineffective. Furthermore, there are few antibacterial agents in the advanced stages of the drug development process against this ensemble of resistant pathogens. Under these dire circumstances, it has become increasingly challenging to treat these life-threatening infections, particularly in intensive care

unit settings where multidrug-resistant Gram-negative bacilli are highly prevalent (Costa Pde, Atta, & Silva, 2015; Lye et al., 2012; Pradhan, Bhat, & Ghadage, 2014). In response to this clinical need, there has been a resurgence of old antibiotics, such as the polymyxins, as the last treatment resort against infections caused by multidrug-resistant Gram-negative pathogens (Arnold, Forrest, & Messmer, 2007; Bergen, Landersdorfer, Lee, Li, & Nation, 2012; Zavascki et al., 2007).

1.1.1 Agents of Last Resort

Polymyxins [polymyxin B and polymyxin E (colistin)] are increasing used as a last-line option for the treatment of MDR Gram-negative bacteria. Polymyxins are cyclic polypeptide antibiotics introduced for clinical use in the 1950s. However, their use diminished considerably in the early 1970s due to nephrotoxicity concerns (Keirstead et al., 2014; Nandha, Sekhri, & Mandal, 2013; Ouderkirk, Nord, Turett, & Kislak, 2003). Despite being available for over 50 years, the correlation between the pharmacokinetics and toxicodynamic profiles of polymyxin B is still not thoroughly understood. We have very limited information regarding *in vivo* biodistribution, cellular disposition, elimination pathways and transport characteristics of polymyxin B. This knowledge gap often hinders the optimal clinical use of polymyxin B. Therefore, studies to delineate

the pharmacokinetic, pharmacodynamic and toxicodynamic profiles of polymyxin B are warranted. Undoubtedly, such information will play a pivotal role in designing optimal polymyxin B dosing strategies, which will maximize the clinical efficacy as well as safety for its use.

1.1.2 Chemistry and Structure

Polymyxins are amphiphilic cationic polypeptide antibiotics isolated from various strains of *Bacillus polymyxa*. Polymyxin B and polymyxin E (colistin) are the only two clinically used antibiotics from this class and they are active against a wide spectrum of Gram-negative bacteria. Commercially available polymyxin B is a mixture of several structurally related cyclic amphiphilic analogs, primarily polymyxin B1, B2, B3 and isoleucine B1 (Orwa et al., 2001). The relative abundance of each component in the USP mixture is reported to be 61.2%, 25.4%, 5.6% and 7.7% for polymyxin B1, B2, B3, and isoleucine B1 respectively. The proportion of these four primary components in the USP mixture has been shown to be relatively consistent among various polymyxin B formulations procured from different vendors/ manufacturers (He, Ledesma, et al., 2010).

The basic structure of polymyxins consists of a seven-membered polypeptide cationic ring and linear tripeptide chain connected terminally to a fatty acyl moiety. The only structural variation that differentiates polymyxin B from polymyxin E is the replacement of D-phenylalanine with D-Leucine in the seven-membered cyclic polycationic ring as shown in Figure 1.1 (A. L. Kwa, Lim, et al., 2008). Polymyxin B1, B2, and B3, the three major components of the polymyxin B mixture vary at the fatty acid terminus. The fatty acid moiety in polymyxin B1 contains 6-methyloctanoic acid; B2 6-methylheptanoic acid, B3 octanoic acid. Isoleucine polymyxin B1 is an isomer of polymyxin B1 where L-leucine is replaced L-isoleucine in the cyclic ring as represented in Figure 1.2 (Zavascki, Goldani, Li, & Nation, 2007).

Figure 1.1: Structures of Various Polymyxins (Orwa et al., 2001)

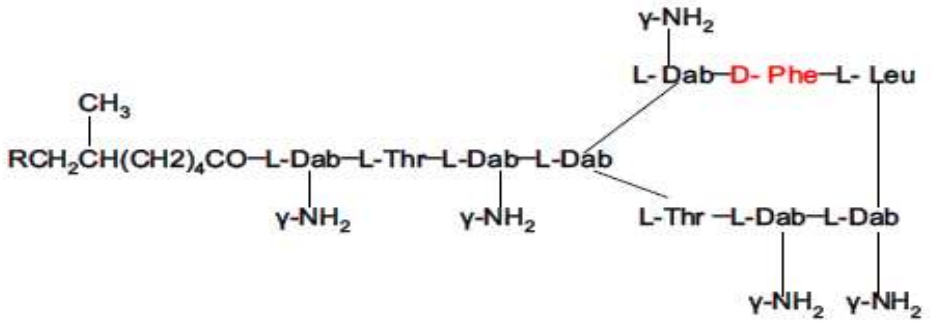

A. Polymyxin B

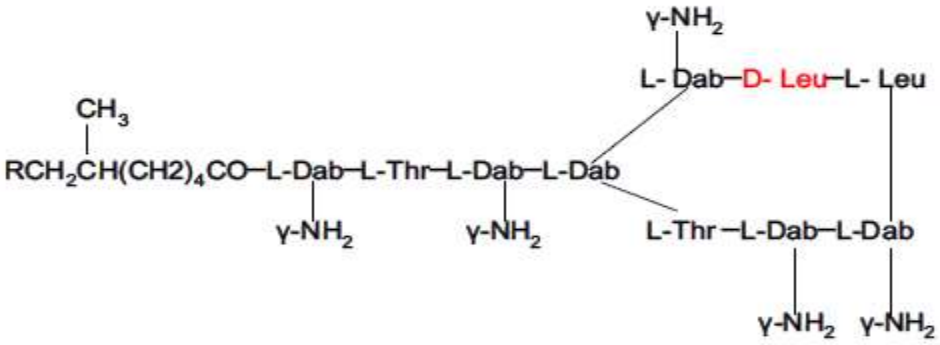

B. Polymyxin E (Colistin)

Figure 1.2: Structure of Major Components of Polymyxin B (Orwa et al., 2001)

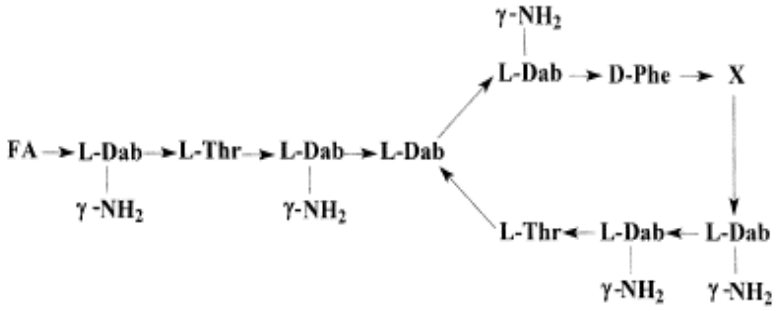

Polymyxin	Fatty acid (FA)	Amino acid (X)	Molecular weight
PMB1	6-methyloctanoic acid	L-leucine	1202
Ile-PMB1	6-methyloctanoic acid	L-isoleucine	1202
PMB2	6-methylheptanoic acid	L-leucine	1188
PMB3	Octanoic acid	L-leucine	1188

1.1.3 Commercial Formulation and Route of Administration

Polymyxin B is primarily formulated as a sulfate salt and administered parenterally. Colistin, however, is formulated as colistin sulfate and colistimethate sodium for oral, topical and parenteral use. Colistin is administered parenterally as colistimethate sodium, a prodrug of colistin which undergoes hydrolysis in plasma to the pharmacologically active moiety (Bergen, Li, Rayner, & Nation, 2006). Colistin sulfate is administered both orally and topically (A. Kwa, Kasiakou, Tam, & Falagas, 2007).

1.1.4 Spectrum of Activity

Polymyxin B and colistin are reported to exhibit comparable pharmacodynamic activity (Tam, Cao, Ledesma, & Hu, 2011). They have an identical spectrum of activity which includes most Gram-negative bacilli, such as *Pseudomonas aeruginosa, Klebsiella pneumoniae,* and *Acinetobacter baumannii,* which are intrinsically susceptible to polymyxins. Various Enterobacteriaceae, such as *Escherichia coli, Salmonella spp., Shigella spp., and Klebsiella spp.* are resistant to a large variety of antibiotics but are susceptible to polymyxins. Additionally, polymyxins possess potent antibacterial activity against *Neisseria spp., Haemophilus influenzae* and *Bordetella pertussis*. However, polymyxins lack activity against Gram-positive bacteria, anaerobic

bacteria, and fungi (A. L. Kwa, Tam, & Falagas, 2008; Yuan & Tam, 2008; Zavascki et al., 2007).

1.1.5 *In vitro* susceptibility of Polymyxins in Clinical Isolates

To date, the most elaborately compiled data evaluating the minimum inhibitory concentrations (MICs) of polymyxins come from the SENTRY Antimicrobial Surveillance Program (2006-2009), summarized in Table 1.1.

Table 1.1: *In vitro* susceptibility of Polymyxin B in Clinical Isolates of Gram-Negative Bacteria from SENTRY Antimicrobial Surveillance Program (2006-2009) (Gales, Jones, & Sader, 2011)

Polymyxins	MIC method	Species (no.of isolates)	MIC_{50} (μg/ml)	MIC_{90} (μg/ml)	Susceptible (%)
Polymyxin B	Broth microdilution	*Acinetobacter spp.* (4686)	≤0.5	≤0.5	99.2
		E coli (17,035)	≤0.5	≤0.5	99.6
		Klebsiella spp. (9774)	≤0.5	≤0.5	98.6
		P. aeruginosa (9130)	1.0	1.0	99.8
Colistin	Broth microdilution	*Acinetobacter spp.* (4686)	≤0.5	1.0	98.6
		E coli (17,035)	≤0.5	≤0.5	99.8
		Klebsiella spp. (9774)	≤0.5	≤0.5	98.5
		P. aeruginosa (9130)	1.0	1.0	99.6

As per Clinical and Laboratory Standard Institute (CLSI) guidelines, the susceptibility breakpoints for polymyxin B and colistin tested for *P. aeruginosa, Acinetobacter spp.* and *Enterobacteriaceae spp.* are identical; MIC of ≤ 2 μg/ml is regarded as susceptible. However, the susceptibility guidelines reported by the European Committee on Antimicrobial Susceptibility Testing (EUCAST) are ≤ 4 μg/ml for *Pseudomonas* spp. and ≤ 2 μg/ml for *Acinetobacter* spp.as well as Enterobacteriaceae (Bergen et al., 2012).

1.1.6 Pharmacodynamics of Polymyxins

Both polymyxin B and colistin are reported to display similar pharmacodynamic characteristics. Tam et al. examined the effect of dose fractionation on the bactericidal activity of polymyxin B against *Pseudomonas aeruginosa* using an *in vitro* hollow fiber infection model. The wild-type and MDR strain of *P. aeruginosa* Polymyxin B were exposed to polymyxin B using three different dosing regimens (8, 12 and 24-hourly administration of the same daily dose) to simulate the steady-state polymyxin B pharmacokinetics in patients. This *in vitro* model was designed to expose the fluctuating concentrations of polymyxin B to the bacterial population over time with linear elimination and repeated dosing for 4 days. With all three dosing regimens against both strains, a rapid bacterial killing was observed in a concentration-dependent manner

followed by the regrowth (as early as 6 hours after first exposure). It was concluded that the most important factor was the total daily dose whereas dose fractionation or alteration in dosing frequency had no significant impact on the overall bactericidal activity of polymyxin B. They found that the *in vitro* bactericidal activity was well correlated with the ratio of area under the concentration-time curve to the minimum inhibitory concentration (AUC/MIC), which was the best-fitted pharmacokinetic/pharmacodynamic index for polymyxin B (Tam et al., 2005). Polymyxin B was also reported to exhibit similar pharmacodynamics with initial rapid bactericidal activity *in vitro* against *A. baumannii* and *K. pneumoniae* followed by a regrowth phase (Abdul Rahim et al., 2015; Tran et al., 2016).

Colistin exhibits very similar pharmacodynamics to that of polymyxin B, with similar initial rapid bactericidal activity followed by a quick regrowth phase (as early as 2 h after first drug exposure). Several *in vitro* time-kill studies reported concentration-dependent bacterial killing by colistin against *A. baumannii* and *K. pneumoniae* and *P. aeruginosa* (Bergen et al., 2010; Owen, Li, Nation, & Spelman, 2007; Poudyal et al., 2008). Another study investigated the pharmacodynamics of colistin in the mice thigh and lung infection models directed against several strains of Gram-negative bacteria. Similar to polymyxin B, it was found that the pharmacokinetic/ pharmacodynamic index that best fitted

the efficacy of colistin was fAUC/MIC ratio (Dudhani, Turnidge, Coulthard, et al., 2010; Dudhani, Turnidge, Nation, & Li, 2010). Collectively, these findings suggest that the total daily exposure is related to the bactericidal activity of polymyxins.

1.1.7 Dosage Guidelines

The currently used dosing guidelines for polymyxins are based on total body weight and the renal function of patients. These dosing recommendations for polymyxin B are empirical and may need to be re-evaluated. The current dosing recommendations for the polymyxins are summarized in Table 1.2.

Table 1.2: Current Dosing Guidelines for Intravenous Polymyxin B and Colistimethate Sodium (Landman, Georgescu, Martin, & Quale, 2008; Yuan & Tam, 2008)

A. Polymyxin B dosing for adults and children older than two years

Renal function	Dosing recommendation
Normal renal function (CrCl > 80 ml/min)	1.5 – 2.5 mg/kg/day (15,000 – 25,000 IU/kg) in two divided doses
Mild renal insufficiency (CrCl 30 - 80 ml/min)	2.5 mg/kg of loading dose on day 1; then 1 -1.5 mg/kg/day
Moderate renal insufficiency (CrCl < 30 ml/min)	2.5 mg/kg of loading dose on day 1; then 1 -1.5 mg/kg/day every 2-3 days
Anuria	2.5 mg/kg of loading dose on day 1; then 11.5 mg/kg/day every 5-7 days

B. Colistimethate Sodium (Colomycin) Dosing for Adults

Renal function	Dosing recommendation
Normal renal function (CrCl > 50 ml/min)	4 - 6 mg/kg/day colistimethate in three divided doses (50,000-75,000 IU for patients ≤ 60 kg); 80 – 160 mg colistimethate every 8 h (1 – 2 million IU for patients > 60 kg)
Mild renal insufficiency (CrCl 20 - 50 ml/min)	80 - 160 mg/kg/day (1 -2 million IU) colistimethate every 8 h
Moderate renal insufficiency (CrCl 10 - 20 ml/min)	80 mg/kg/day (1 million IU) colistimethate every 12 - 8 h
Severe renal insufficiency (CrCl < 10 ml/min)	80 mg/kg/day (1 million IU) colistimethate every 18 - 24 h

1.1.8 Nephrotoxicity of polymyxins: Prevalence and Risk Factors

Dose-dependent nephrotoxicity is the most prevalent adverse effect which hinders the clinical use of polymyxins. With the acceptance of RIFLE (risk, injury, failure, loss and end-stage kidney disease) criteria in 2004, a consensus definition of nephrotoxicity has been developed (Wertheim et al., 2013). Thereafter, some noteworthy attempts have been made in assessing the rate of nephrotoxicity associated with polymyxins using this criterion. A recent retrospective study reported the nephrotoxicity rates evaluated in 173 critically ill patients receiving intravenous colistin and polymyxin B were 60.4% and 41.8%, respectively (Akajagbor et al., 2013). Another study from our lab reported 45.8% as the overall prevalence rate of nephrotoxicity with parenteral use polymyxin B (Dubrovskaya et al., 2015). Similarly, in recent studies conducted utilizing the RIFLE criteria, the prevalence of colistimethate-associated nephrotoxicity was estimated to be approximately 45% (Hartzell et al., 2009; Pogue et al., 2011). Furthermore, among the various independent risk factors evaluated, the total daily dose of polymyxins (both, polymyxin B and colistimethate) was identified as an independent risk factor correlated with the onset of nephrotoxicity (Phe et al., 2014).

A careful review of recent literature on the polymyxin nephrotoxicity revealed a higher rate of nephrotoxicity associated with colistin/ colistimethate sodium (55.3%) as compared to polymyxin B (21.1%) (Phe et al., 2014). Owing to the lower rate of nephrotoxicity but similar antibacterial activity, polymyxin B was our preferred therapeutic agent against MDR infections. Therefore, after a thorough, extensive and careful appraisal of polymyxins, our later investigations into the intricacies of pharmacokinetics, toxicodynamics and mechanism(s) of intrarenal uptake were solely carried out using polymyxin B. To begin with, we focused on identifying the existing knowledge gap in the current understanding of polymyxin B pharmacokinetics and toxicity profile in our literature review.

1.2 Knowledge Gap: Current Understanding of Pharmacokinetics, Biodistribution, Transport Mechanisms and Toxicodynamics of Polymyxin B

There is a paucity of published reports correlating pharmacokinetics and toxicodynamic profiles of polymyxin B. Moreover, we lack a deep understanding of the in vivo biodistribution, disposition, cellular transport, and mechanism(s) of intrarenal uptake of polymyxin B. This knowledge gap hinders the design of optimal dosing strategies. Nephrotoxicity concerns are escalating with the ongoing usage of current polymyxin B dosing approaches. These dosing schemes are commonly associated with a high incidence of nephrotoxicity. Previously, few studies have provided evidence suggesting that polymyxin B is non-renally eliminated (Abdelraouf, He, Ledesma, Hu, & Tam, 2012; Zavascki et al., 2008). A follow-up pharmacokinetic study in the same rat model, however, illustrated prolonged residence of polymyxin B in the kidneys. These results revealed that polymyxin B persisted in the rat kidneys long after the serum concentration was below the lower limit of quantification (Abdelraouf, He, Ledesma, Hu, & Tam, 2012). This prolonged persistence in the kidneys might contribute to its nephrotoxic potentials.

Most clinical reports on polymyxin B pharmacokinetics are derived from patient populations are focused mainly on the serum concentration-time profile. However, the serum concentration alone may not provide comprehensive insights on the overall drug pharmacokinetics, particularly if the drug exhibits an atypical biodistribution pattern. It has been previously reported that organ distribution of polymyxin B was non-uniform, with greater accumulation in kidneys, liver and muscle tissues (Kunin, 1970). Similarly, Jacobson et al. investigated the *in vivo* distribution and binding of tritiated polymyxin B in a mouse model and results were in agreement with the previous report. The distribution pattern of polymyxin B was non-uniform, and the drug was rapidly accumulated in the kidney (Jacobson, Koch, Kuntzman, & Burchall, 1972).

Dose-limiting nephrotoxicity remains at the crux of the unresolved problems associated with clinical use of polymyxin B. A previous study from our lab provided circumstantial evidence that the renal tissue concentration of polymyxin B was associated with the onset and severity of drug-induced nephrotoxicity (Abdelraouf, Braggs, et al., 2012). The same total daily dose of polymyxin B administered subcutaneously every 6 h was associated with an earlier nephrotoxicity onset as compared to the once daily dosing. Interestingly, these findings insinuated that renal tissue concentration of polymyxin B could be

considered as a major determinant while investigating a potential correlation between polymyxin B daily dose and the onset of nephrotoxicity. Therefore, it is crucial to evaluate in-depth renal exposure of polymyxin B in addition to its serum pharmacokinetic profile.

Until now the underlying mechanism(s) of polymyxin B-induced nephrotoxicity and intrarenal uptake has not been well established. Several aspects of preferential intrarenal accumulation of polymyxin B still remain unanswered. The mechanistic factors driving the uptake of polymyxin B into renal cells remain unexplored. Despite a previous report investigating the involvement of transporters in renal uptake of colistin using isolated perfused rat kidney, there is lack of published literature available on the renal uptake of polymyxin B. Ma et al, proposed that renal reabsorption of colistin could potentially be mediated by organic cation transporter (OCT) and peptide transporter (PEPT-2) inhibited by tetraethylammonium and glycine-glycine, respectively (Ma et al., 2009). However, no direct evidence was further provided to support this hypothesis in an cellular/animal model.

To date, we have sparse information on the impact of renal accumulation of polymyxin B and its contribution towards drug-induced nephrotoxicity. Additionally, few studies have reported that daily dosing is one of the primary independent risk factors associated with polymyxin B-induced nephrotoxicity (Dubrovskaya et al., 2015; Mendes, Cordeiro, & Burdmann, 2009; Phe et al., 2014). A recent study reported that high concentration and prolonged residence of polymyxin B triggered events causing cell death. Several notable morphological changes in mitochondria, including loss of membrane potential, were observed, leading to cellular apoptosis in the rat (NRK-2E) and human (HK-2) kidney proximal tubular cells lines (Azad et al., 2013). However, these reports do not provide a concrete mechanistic framework correlating renal drug exposure and the onset of polymyxin B nephrotoxicity. Therefore, there remains a critical need to elucidate the precise mechanism of polymyxin B-induced nephrotoxicity to ensure safe clinical use that will attenuate toxicity concerns. It is pivotal to delineate the mechanism of intrarenal uptake of polymyxin B in order to identify the pharmacological target responsible for intracellular uptake. The outcome of this mechanistic study can be further translated to designing novel polymyxin B analogues with little or no affinity towards the identified pharmacological target. This would further minimize the intrarenal accumulation and diminish the incidence of nephrotoxicity.

1.3 Research Objectives

The **long-term goal** of our research is to design safe and effective treatment strategies against infections caused by MDR Gram-negative bacteria. Over the past few decades, polymyxin B has re-emerged in clinical settings as a last treatment resort against challenging Gram-negative infections. It is crucial to ensure its safe clinical use until new and effective therapeutic options are available.

Our **central hypothesis** is that polymyxin B is non-uniformly distributed *in vivo* and accumulates predominantly in the kidneys. We hypothesize that preferential accumulation of polymyxin B in renal tissues is correlated to the onset of dose-dependent nephrotoxicity. Therefore, the objectives of the proposed research are first, to provide additional insights into the overall distribution and disposition characteristics of polymyxin B using an animal model. Secondly, we aim to establish a correlation between renal drug exposure and the onset of nephrotoxicity, in conjunction with delineating the role of underlying uptake transport system in the renal accumulation of polymyxin B.

The outcome of this research could be used in identifying the pharmacological target and designing future interventions to alleviate polymyxin B-induced nephrotoxicity. It is anticipated that the results of this investigation will elucidate the details of polymyxin B pharmacokinetics. This would guide future

studies to facilitate the optimization of appropriate dosing strategies, which maximize efficacy and minimize the incidence of nephrotoxicity. In the long run, the optimization of polymyxin B dosing strategies based on the sound knowledge of drug pharmacokinetics/ toxicodynamics to ensure greater safety and efficacy in clinical settings is warranted. Figure 1.3 represents the advantages of the innovative approaches to dosing polymyxin B as compared to the currently used paradigm.

Figure 1.3: Advantages of Proposed Approach over Conventional Approach

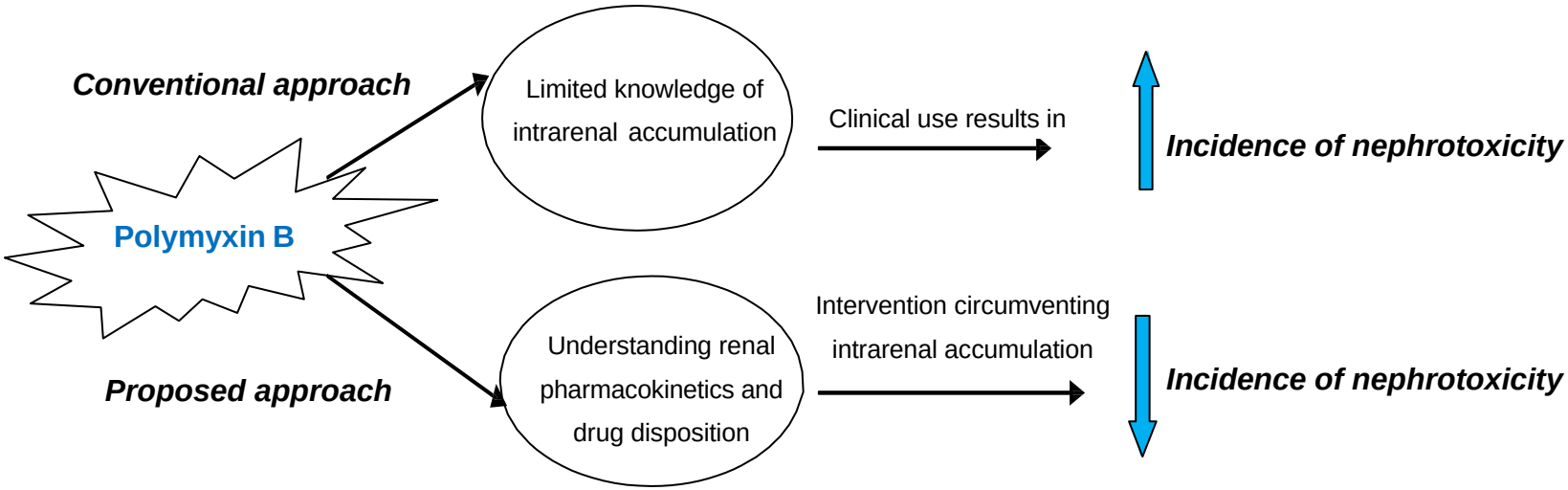

1.4 Research Design

The proposed research design was implemented as depicted in the Figure 1.4.

Figure 1.4: Flowchart Depicting the Implementation of Research Design

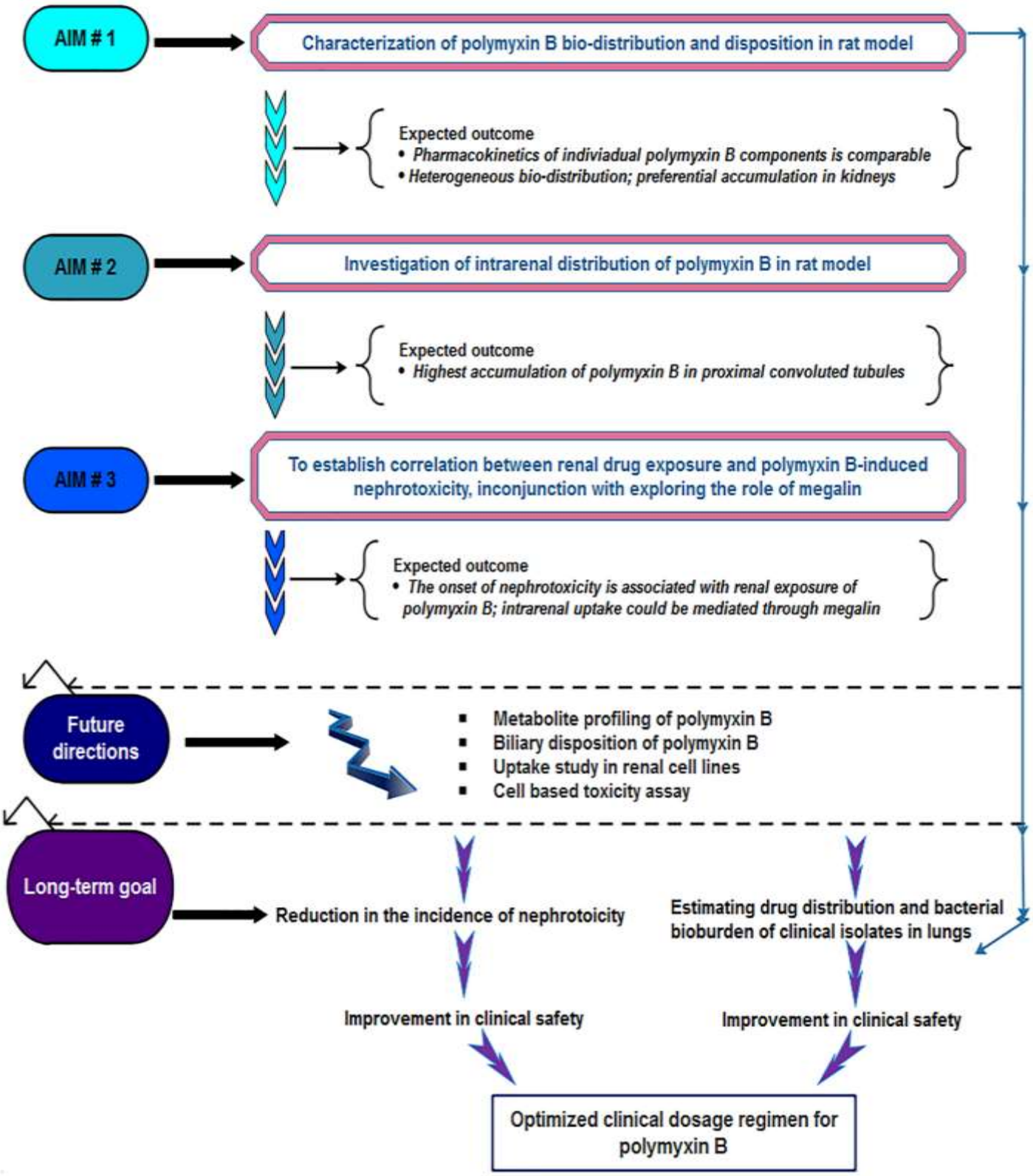

1.5 Research Plan

The overall research plan is designed to be conducted using three specific aims, which are intended to be performed sequentially. The step-wise execution of these aims will provide insights into the intricacies of polymyxin B pharmacokinetics by explaining the biodistribution, disposition, and cellular transport mechanism(s) within the kidneys.

- **Specific Aim 1: To investigate the organ biodistribution and disposition of polymyxin B using a rat model.**

  Working hypothesis: Commercially available polymyxin B is a mixture of closely related structural analogs (Orwa et al., 2001). Preliminary studies from our lab have demonstrated that the *in vitro* potencies of the different polymyxin B components were comparable (Tam et al., 2005). Therefore, we hypothesized those various components of polymyxin B exhibit similar pharmacokinetic characteristics. Clinically, nephrotoxicity is the most prevalent dose-limiting adverse effect of polymyxin B (Falagas, Kasiakou, Kofteridis, Roditakis, & Samonis, 2006; Mendes, Cordeiro, & Burdmann, 2009). It has been previously reported that organ distribution of polymyxin B was non-uniform with greater accumulation in kidneys, liver and muscle tissues (Kunin, 1970). Therefore, we hypothesize that

polymyxin B exhibits heterogeneous distribution and preferentially accumulates in the kidneys, which contribute to its nephrotoxic potentials.

- **Specific Aim 2: To investigate the intrarenal distribution of polymyxin B in a rat model.**

  Working hypothesis: In a previous study, polymyxin B was observed to be significantly accumulated in the renal proximal tubular cells in a mouse model (Yun, Azad, Nowell, et al., 2015). Our lab has demonstrated that polymyxin B-induced renal injuries were mainly confined to the proximal tubules (Abdelraouf, Braggs, et al., 2012). Therefore, based on these relevant facts we hypothesize that proximal tubules are the primary renal cell type with the highest accumulation of polymyxin B.

- **Specific Aim 3: To elucidate the mechanism(s) that leads to intracellular accumulation of polymyxin B within the kidneys**

  Working hypothesis: Several studies have earlier reported polymyxin B daily dose as one of the primary independent risk factors closely associated with its nephrotoxicity (Dubrovskaya et al., 2015;

Mendes et al., 2009). Moreover, megalin, a renal endocytic receptor playing a critical role in the renal uptake of endogenous compounds and xenobiotics, is reported to have a high binding affinity for polybasic drugs such as polymyxin B (Moestrup et al., 1995). Therefore, we hypothesized that the onset of polymyxin B nephrotoxicity was dose dependent: the higher the daily dose, the greater the renal drug exposure. Moreover, we hypothesized that the intrarenal uptake of polymyxin was mediated by megalin.

1.6 Intrarenal accumulation of Polymyxin B: The Role of Megalin

Some recent reports have demonstrated that polybasic drugs such as polymyxin B, colistin, gentamicin and amikacin have a high binding affinity towards megalin, a renal endocytic receptor. It has been speculated that the binding of these drugs to megalin leads to their internalization within the kidneys as depicted in Figure 1.5 (Dagil, O'Shea, Nykjaer, Bonvin, & Kragelund, 2013; Moestrup et al., 1995; Schmitz et al., 2002). Megalin is one of the members of the low-density lipoprotein protein-2 (LRP-2) receptor gene family, with a molecular weight of approximately 600 kDa (Christensen & Nielsen, 2007; Marzolo & Farfan, 2011) as represented in Figure 1.5.

Figure 1.5: Schematic Representation of Megalin Localization in Renal Proximal Tubular Epithelium (Christensen, Wagner, & Kaissling, 2012; Weyer et al., 2013)

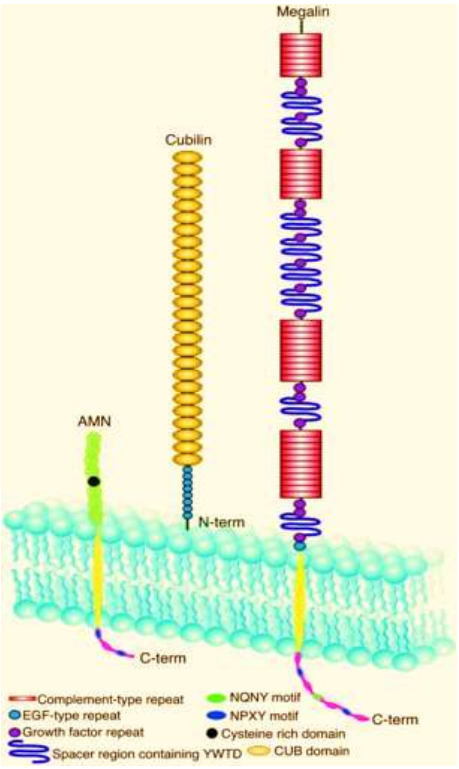

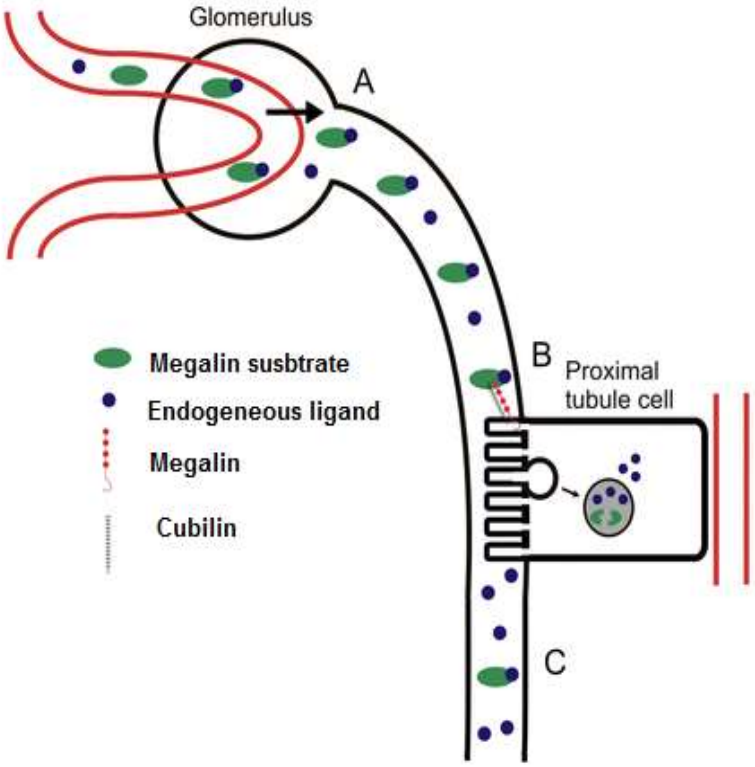

Megalin is predominantly expressed in the renal proximal tubular epithelium, labyrinth membrane of the inner ear and retinal epithelium (Lundgren et al., 1997). It is reported to function as an endocytic receptor and is responsible for the internalization/uptake of a large variety of endogenous molecules as well as xenobiotics (De, Kuwahara, & Saito, 2014). Several endogenous molecules such as vitamin D, calcium, lipoprotein lipases, plasminogen activator inhibitor type-1 complex and receptor-associated protein (RAP) are known ligands of megalin (Ternes & Rowling, 2013; Zheng, Marino, Zhao, & McCluskey, 1998). Based on these relevant literature findings, we hypothesized that polymyxin B renal uptake could be mediated through megalin.

REFERENCES

Abdelraouf, K., Braggs, K. H., Yin, T., Truong, L. D., Hu, M., & Tam, V. H. (2012). Characterization of polymyxin b-induced nephrotoxicity: Implications for dosing regimen design. *Antimicrob Agents Chemother, 56*(9), 4625-4629. doi:10.1128/AAC.00280-12

Abdelraouf, K., He, J., Ledesma, K. R., Hu, M., & Tam, V. H. (2012). Pharmacokinetics and renal disposition of polymyxin b in an animal model. *Antimicrob Agents Chemother, 56*(11), 5724-5727. doi:10.1128/AAC.01333-12

Abdul Rahim, N., Cheah, S. E., Johnson, M. D., Yu, H., Sidjabat, H. E., Boyce, J., . . . Li, J. (2015). Synergistic killing of NDM-producing MDR klebsiella pneumoniae by two 'old' antibiotics-polymyxin b and chloramphenicol. *J Antimicrob Chemother, 70*(9), 2589-2597. doi:10.1093/jac/dkv135

Bergen, P. J., Bulitta, J. B., Forrest, A., Tsuji, B. T., Li, J., & Nation, R. L. (2010). Pharmacokinetic/pharmacodynamic investigation of colistin against pseudomonas aeruginosa using an in vitro model. *Antimicrob Agents Chemother, 54*(9), 3783-3789. doi:10.1128/AAC.00903-09

Bergen, P. J., Landersdorfer, C. B., Zhang, J., Zhao, M., Lee, H. J., Nation, R. L., & Li, J. (2012). Pharmacokinetics and pharmacodynamics of 'old'

polymyxins: What is new? *Diagn Microbiol Infect Dis, 74*(3), 213-223. doi:10.1016/j.diagmicrobio.2012.07.010

Bergen, P. J., Li, J., Rayner, C. R., & Nation, R. L. (2006). Colistin methanesulfonate is an inactive prodrug of colistin against pseudomonas aeruginosa. *Antimicrob Agents Chemother, 50*(6), 1953-1958. doi:10.1128/AAC.00035-06

Christensen, E. I., & Nielsen, R. (2007). Role of megalin and cubilin in renal physiology and pathophysiology. *Rev Physiol Biochem Pharmacol, 158*, 1-22.

Christensen, E. I., Wagner, C. A., & Kaissling, B. (2012). Uriniferous tubule: Structural and functional organization. *Compr Physiol, 2*(2), 805-861. doi:10.1002/cphy.c100073

Dagil, R., O'Shea, C., Nykjaer, A., Bonvin, A. M., & Kragelund, B. B. (2013). Gentamicin binds to the megalin receptor as a competitive inhibitor using the common ligand binding motif of complement type repeats: Insight from the NMR structure of the 10th complement type repeat domain alone and in complex with gentamicin. *J Biol Chem, 288*(6), 4424-4435. doi:10.1074/jbc.M112.434159

De, S., Kuwahara, S., & Saito, A. (2014). The endocytic receptor megalin and its associated proteins in proximal tubule epithelial cells. *Membranes (Basel), 4*(3), 333-355. doi:10.3390/membranes4030333

Dubrovskaya, Y., Prasad, N., Lee, Y., Esaian, D., Figueroa, D. A., & Tam, V. H. (2015). Risk factors for nephrotoxicity onset associated with polymyxin b therapy. *J Antimicrob Chemother, 70*(6), 1903-1907. doi:10.1093/jac/dkv014

Dudhani, R. V., Turnidge, J. D., Coulthard, K., Milne, R. W., Rayner, C. R., Li, J., & Nation, R. L. (2010). Elucidation of the pharmacokinetic/pharmacodynamic determinant of colistin activity against pseudomonas aeruginosa in murine thigh and lung infection models. *Antimicrob Agents Chemother, 54*(3), 1117-1124. doi:10.1128/AAC.01114-09

Dudhani, R. V., Turnidge, J. D., Nation, R. L., & Li, J. (2010). FAUC/MIC is the most predictive pharmacokinetic/pharmacodynamic index of colistin against acinetobacter baumannii in murine thigh and lung infection models. *J Antimicrob Chemother, 65*(9), 1984-1990. doi:10.1093/jac/dkq226

Falagas, M. E., Kasiakou, S. K., Kofteridis, D. P., Roditakis, G., & Samonis, G. (2006). Effectiveness and nephrotoxicity of intravenous colistin for treatment of patients with infections due to polymyxin-only-susceptible (pos) gram-negative bacteria. *Eur J Clin Microbiol Infect Dis, 25*(9), 596-599. doi:10.1007/s10096-006-0191-2

Gales, A. C., Jones, R. N., & Sader, H. S. (2011). Contemporary activity of colistin and polymyxin b against a worldwide collection of gram-negative pathogens: Results from the sentry antimicrobial surveillance program (2006-09). *J Antimicrob Chemother, 66*(9), 2070-2074. doi:10.1093/jac/dkr239

He, J., Ledesma, K. R., Lam, W. Y., Figueroa, D. A., Lim, T. P., Chow, D. S., & Tam, V. H. (2010). Variability of polymyxin b major components in commercial formulations. *Int J Antimicrob Agents, 35*(3), 308-310. doi:10.1016/j.ijantimicag.2009.11.005

Jacobson, M., Koch, A., Kuntzman, R., & Burchall, J. (1972). The distribution and binding of tritiated polymyxin b in the mouse. *J Pharmacol Exp Ther, 183*(2), 433-439.

Keirstead, N. D., Wagoner, M. P., Bentley, P., Blais, M., Brown, C., Cheatham, L., Kern, G. (2014). Early prediction of polymyxin-induced nephrotoxicity with next-generation urinary kidney injury biomarkers. *Toxicol Sci, 137*(2), 278-291. doi:10.1093/toxsci/kft247

Kunin, C. M. (1970). Binding of antibiotics to tissue homogenates. *J Infect Dis, 121*(1), 55-64.

Kwa, A., Kasiakou, S. K., Tam, V. H., & Falagas, M. E. (2007). Polymyxin b: Similarities to and differences from colistin (polymyxin e). *Expert Rev Anti Infect Ther, 5*(5), 811-821. doi:10.1586/14787210.5.5.811

Kwa, A. L., Lim, T. P., Low, J. G., Hou, J., Kurup, A., Prince, R. A., & Tam, V. H. (2008). Pharmacokinetics of polymyxin b1 in patients with multidrug-resistant gram-negative bacterial infections. *Diagn Microbiol Infect Dis, 60*(2), 163-167. doi:10.1016/j.diagmicrobio.2007.08.008

Kwa, A. L., Tam, V. H., & Falagas, M. E. (2008). Polymyxins: A review of the current status including recent developments. *Ann Acad Med Singapore, 37*(10), 870-883.

Landman, D., Georgescu, C., Martin, D. A., & Quale, J. (2008). Polymyxins revisited. *Clin Microbiol Rev, 21*(3), 449-465. doi:10.1128/CMR.00006-08

Lundgren, S., Carling, T., Hjalm, G., Juhlin, C., Rastad, J., Pihlgren, U., . . . Hellman, P. (1997). Tissue distribution of human gp330/megalin, a putative ca(2+)-sensing protein. *J Histochem Cytochem, 45*(3), 383-392.

Ma, Z., Wang, J., Nation, R. L., Li, J., Turnidge, J. D., Coulthard, K., & Milne, R. W. (2009). Renal disposition of colistin in the isolated perfused rat kidney. *Antimicrob Agents Chemother, 53*(7), 2857-2864. doi:10.1128/AAC.00030-09

Marzolo, M. P., & Farfan, P. (2011). New insights into the roles of megalin/lrp2 and the regulation of its functional expression. *Biol Res, 44*(1), 89-105. doi:10.4067/S0716-97602011000100012/S0716-97602011000100012

Mendes, C. A., Cordeiro, J. A., & Burdmann, E. A. (2009). Prevalence and risk factors for acute kidney injury associated with parenteral polymyxin b use. *Ann Pharmacother, 43*(12), 1948-1955. doi:10.1345/aph.1M277

Moestrup, S. K., Cui, S., Vorum, H., Bregengard, C., Bjorn, S. E., Norris, K., . . . Christensen, E. I. (1995). Evidence that epithelial glycoprotein 330/megalin mediates uptake of polybasic drugs. *J Clin Invest, 96*(3), 1404-1413. doi:10.1172/JCI118176

Nandha, R., Sekhri, K., & Mandal, A. K. (2013). To study the clinical efficacy and nephrotoxicity along with the risk factors for acute kidney injury associated with parenteral polymyxin b. *Indian J Crit Care Med, 17*(5), 283-287. doi:10.4103/0972-5229.120319

Orwa, J. A., Govaerts, C., Busson, R., Roets, E., Van Schepdael, A., & Hoogmartens, J. (2001). Isolation and structural characterization of polymyxin b components. *J Chromatogr A, 912*(2), 369-373.

Ouderkirk, J. P., Nord, J. A., Turett, G. S., & Kislak, J. W. (2003). Polymyxin b nephrotoxicity and efficacy against nosocomial infections caused by multiresistant gram-negative bacteria. *Antimicrob Agents Chemother, 47*(8), 2659-2662.

Owen, R. J., Li, J., Nation, R. L., & Spelman, D. (2007). In vitro pharmacodynamics of colistin against acinetobacter baumannii clinical isolates. *J Antimicrob Chemother, 59*(3), 473-477. doi:10.1093/jac/dkl512

Phe, K., Lee, Y., McDaneld, P. M., Prasad, N., Yin, T., Figueroa, D. A., . . . Tam, V. H. (2014). In vitro assessment and multicenter cohort study of comparative nephrotoxicity rates associated with colistimethate versus polymyxin b therapy. *Antimicrob Agents Chemother, 58*(5), 2740-2746. doi:10.1128/AAC.02476-13

Poudyal, A., Howden, B. P., Bell, J. M., Gao, W., Owen, R. J., Turnidge, J. D., . . . Li, J. (2008). In vitro pharmacodynamics of colistin against multidrug-resistant klebsiella pneumoniae. *J Antimicrob Chemother, 62*(6), 1311-1318. doi:10.1093/jac/dkn425

Schmitz, C., Hilpert, J., Jacobsen, C., Boensch, C., Christensen, E. I., Luft, F. C., & Willnow, T. E. (2002). Megalin deficiency offers protection from renal aminoglycoside accumulation. *J Biol Chem, 277*(1), 618-622. doi:10.1074/jbc.M109959200

Tam, V. H., Cao, H., Ledesma, K. R., & Hu, M. (2011). In vitro potency of various polymyxin b components. *Antimicrob Agents Chemother, 55*(9), 4490-4491. doi:10.1128/AAC.00119-11

Tam, V. H., Schilling, A. N., Vo, G., Kabbara, S., Kwa, A. L., Wiederhold, N. P., & Lewis, R. E. (2005). Pharmacodynamics of polymyxin b against pseudomonas aeruginosa. *Antimicrob Agents Chemother, 49*(9), 3624-3630. doi:10.1128/AAC.49.9.3624-3630.2005

Ternes, S. B., & Rowling, M. J. (2013). Vitamin d transport proteins megalin and disabled-2 are expressed in prostate and colon epithelial cells and are induced and activated by all-trans-retinoic acid. *Nutr Cancer, 65*(6), 900-907. doi:10.1080/01635581.2013.805422

Tran, T. B., Cheah, S. E., Yu, H. H., Bergen, P. J., Nation, R. L., Creek, D. J., . . . Li, J. (2016). Anthelmintic closantel enhances bacterial killing of polymyxin b against multidrug-resistant acinetobacter baumannii. *J Antibiot (Tokyo), 69*(6), 415-421. doi:10.1038/ja.2015.127

Weyer, K., Nielsen, R., Petersen, S. V., Christensen, E. I., Rehling, M., & Birn, H. (2013). Renal uptake of 99mtc-dimercaptosuccinic acid is dependent on normal proximal tubule receptor-mediated endocytosis. *J Nucl Med, 54*(1), 159-165. doi:10.2967/jnumed.112.110528

Yuan, Z., & Tam, V. H. (2008). Polymyxin B: A new strategy for multidrug-resistant gram-negative organisms. *Expert Opin Investig Drugs, 17*(5), 661-668. doi:10.1517/13543784.17.5.661

Yun, B., Azad, M. A., Nowell, C. J., Nation, R. L., Thompson, P. E., Roberts, K. D., . . . Li, J. (2015). Cellular uptake and localization of polymyxins in renal tubular cells using rationally designed fluorescent probes. *Antimicrob Agents Chemother, 59*(12), 7489-7496. doi:10.1128/AAC.01216-15

Zavascki, A. P., Goldani, L. Z., Cao, G., Superti, S. V., Lutz, L., Barth, A. L., . . . Li, J. (2008). Pharmacokinetics of intravenous polymyxin B in critically ill patients. *Clin Infect Dis, 47*(10), 1298-1304. doi:10.1086/592577

Zavascki, A. P., Goldani, L. Z., Li, J., & Nation, R. L. (2007). Polymyxin B for the treatment of multidrug-resistant pathogens: A critical review. *J Antimicrob Chemother, 60*(6), 1206-1215. doi:10.1093/jac/dkm357

Zheng, G., Marino, M., Zhao, J., & McCluskey, R. T. (1998). Megalin (gp330): A putative endocytic receptor for thyroglobulin (tg). *Endocrinology, 139*(3), 1462-1465. doi:10.1210/endo.139.3.5978

CHAPTER 2

GENERAL METHODOLOGY AND EXPERIMENTATION

2.1 Polymyxin B Assay

2.1.1 Ultra Performance Liquid Chromatography-Tandem Mass Spectrometry Assay (UPLC-MS/MS)

A validated UPLC-MS/MS method for simultaneous detection as well as quantification of major components of polymyxin B was developed. The UPLC conditions were: system, Waters Acquity^{TM}; column, Acquity UPLC BEH C_{18} column (50 mm X 2.1 mm internal diameter, 1.7 μm, Waters, Milford, MA, USA); mobile phase A, 0.1% formic acid; mobile phase B, 100% acetonitrile; gradient, 0-0.5 min, 5% B, 3.2-4.2 min, 15% B, 4.2-4.6 min, 20% B, 4.6-5 min, 80% B, 5-7 min, 5% B; flow rate, 0.5 ml/min; column temperature, 60 ºC; and injection volume, 10 μl. Carbutamide (5 μg/ml) was used as an internal standard.

An API 3200 Qtrap triple quadrupole mass spectrometer (Applied Biosystem/MDS SCIEX, Foster City, CA, USA) was used to determine polymyxin B concentration in samples by Multiple Reaction Monitoring method (MRM) in the

positive ion mode with the transition of m/z 402 → m/z 101 for polymyxin B1, m/z 397 → m/z 101 for polymyxin B2, m/z 397 → m/z 101 for polymyxin B3, m/z 402 → m/z 101 for isoleucine polymyxin B1 and m/z 272 → m/z 74 for carbutamide. The main instrument parameters for mass spectrometer were set as follows: ion spray voltage, 5.5 kV; ion source temperature, 650 ºC; gas1, 40 psi; gas2, 40 psi; curtain gas, 20 psi. The compound-dependent parameters for polymyxin B components (analyte) and carbutamide (internal standard) are represented in Table 2.1. The quantification was carried out using software analyst 1.5.2.

The concentrations of various polymyxin B components were quantified by constructing a calibration curve using at least eight concentrations of reference standards (with known purity of content) (EvoPure®, Bellingham, WA), in different matrices. The standard stock solution of polymyxin B1, B2, B3, and Ile-B1 were prepared by dissolving a known amount of the reference standards in LCMS grade water. The working solutions were obtained by serial dilution of the prepared mixture stock solution in 0.1% formic acid to achieve the final concentration range of 0.00625 - 32 µl/ml. To establish a calibration curve, blank serum (100 µl) was spiked with 40 µl of the above working solutions of the standard mixture and 10 µl of the internal standard (carbutamide) solution. To precipitate proteins, 5% trichloroacetic acid (150 µl) was added to the mixture, to yield a final concentration range of 0.025 - 12.8 µl/ml.

Table 2.1: Compound-Dependent Parameters for Simultaneous Estimation of Polymyxin B Components and Carbutamide using UPLC-MS/MS

Compound	MRM Transitions [(Q1 → Q3) Da]	Time (msec)	Declustering Potential (volts)	Entrance Potential (volts)	Collision Energy (volts)	Collision Cell Exit Potential (volts)
Polymyxin B1	m/z 402 → m/z 101	100	34	10	32	21.39
Polymyxin B2	m/z 397 → m/z 101	100	39	10	27	21.26
Polymyxin B3	m/z 397 → m/z 101	100	39	10	27	21.26
Isoleucine-Polymyxin B1	m/z 402 → m/z 101	100	34	10	32	21.39
Carbutamide	m/z 272 → m/z 74	100	47	10	20	17.76

The linearity of calibration curves for each component was determined by the best fit of peak area ratios (analyte area/ internal standard area) versus concentration and fitted using a linear regression ($1/x^2$ weighing) method. The slope, intercept and correlation coefficient of the linear regression equation for each polymyxin B component in various matrices were derived. The lower limit of quantification (LLOQ) was determined based on a signal-to-noise ratio 10:1. The assay was validated based on accuracy, precision, and inter- and intra-day variability, which were well within 15% of the coefficient of variation (CV) and did not exceed 20% of the CV for the LLOQ. Figure 2.1 represents a typical UPLC chromatogram of spiked major polymyxin B purified standards in rat serum.

Figure 2.1: Typical UPLC-MS/MS chromatogram of Major Polymyxin B Components and Carbutamide (Internal Standard) in Rat Serum

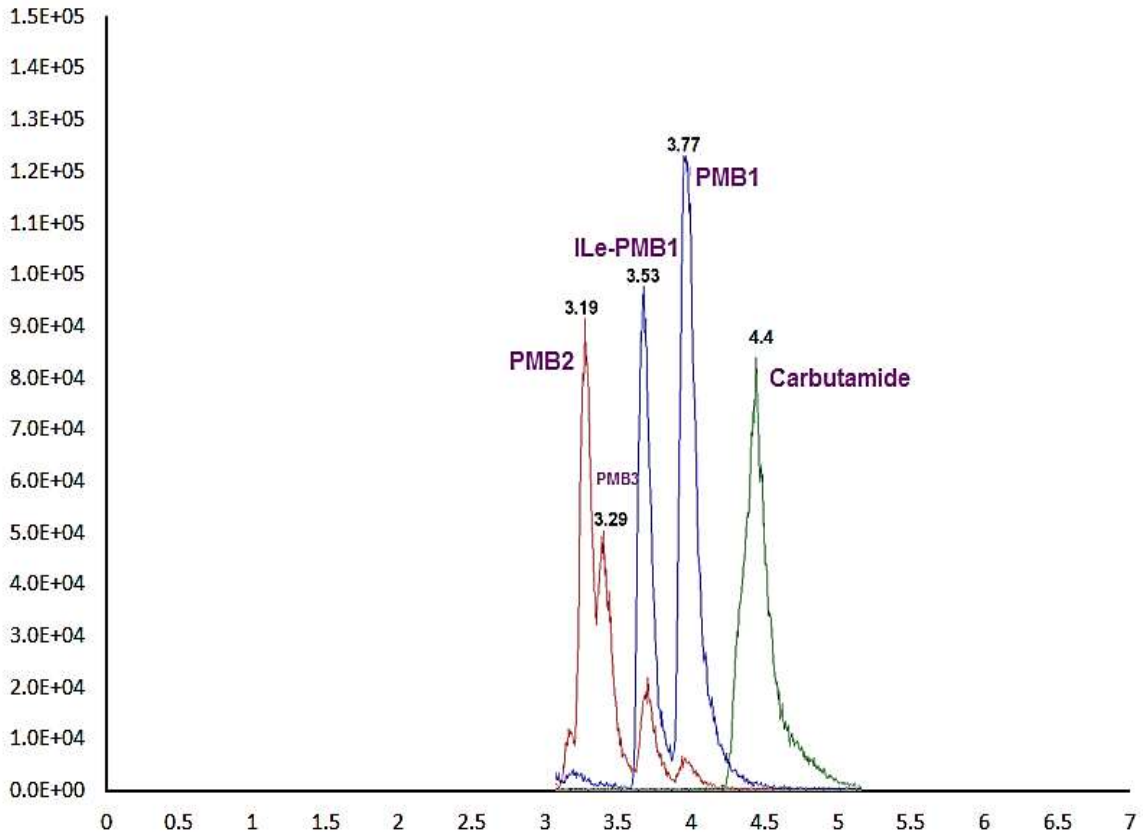

2.1.2 UPLC-MS/MS Assay of Polymyxin B in Rat Serum/Tissue Homogenate

The UPLC/MS/MS method was modified to determine the concentrations of polymyxin B in rat serum, brain, heart, lungs, liver, spleen, kidneys, and skeletal muscle tissues (He, Gao, Hu, Chow, & Tam, 2013). The tissue samples were homogenized in deionized water (1:2). Briefly, 100 µl **of** serum or tissue homogenate samples were spiked with 10 µl of an internal standard (carbutamide 5 µg/ml) and then extracted with 150 µl of 5% trichloroacetic acid. The samples were vortexed for 1 min, followed by centrifugation at 18,000 x g for 20 min at 4ºC as previously described. The supernatant was transferred to a new tube and evaporated to dryness under a stream of ambient air. The residue was then reconstituted with 100 µl of a mixture of acetonitrile and 0.1% formic acid (1:1 v/v). The samples were again centrifuged at 18,000 × g for 20 min at 4°C, and 10 µl of the supernatant was injected into the UPLC-MS/MS system for quantitative analysis.

The calibration curves of major components of polymyxin B [polymyxin B1 (PMB1), polymyxin B2 (PMB2), polymyxin B3 (PMB3) and isoleucine polymyxin B1 (Ile-PMB1)] in 0.1% formic acid, rat serum, brain, heart, lungs, liver, spleen, kidneys and skeletal muscle tissues are represented in Figures 2.2 - 2.10,

respectively. The linearity of calibration curves for each component was determined by the best fit of peak area ratios (analyte area/ internal standard area) versus concentration and fitted using a linear regression ($1/x^2$ weighing) method. The linear concentration ranges for PMB1 in 0.1% formic acid, rat serum, brain, heart, lungs, liver, spleen, kidneys and muscle tissue homogenate were 0.00625- 32 µg/ml, 0.1-12.8 µg/ml, 0.05-12.8 µg/ml, 0.05-12.8 µg/ml, 0.05-12.8 µg/ml, 0.0125-12.8 µg/ml, 0.05-12.8 µg/ml, 0.05-12.8 µg/ml, and 0.1-6.4 µg/ml, respectively. The linear regression coefficients were ≥ 0.99 in all the calibration curves.

The assay was validated based on precision, inter and intraday variability within 15% of the coefficient of variation and accuracy within 85% -115% for lower limit of quantification (LLOQ). With regards to the matrix effect and recovery in the serum matrix, the assay method was previously validated in lab (He et al., 2013). The matrix effect and recovery in various other rat tissue homogenate (brain, heart, lungs, liver, spleen, kidneys and skeletal muscle tissues) were estimated by partial validation using 1-2 concentration from their linear range. The mean matrix effect and extraction recovery in brain, heart, lungs, liver, spleen, kidneys and skeletal muscle tissues homogenate were roughly within 90 % - 115% and 89% - 119% range.

Figure 2.2: PMB1 Calibration Curve in 0.1% Formic Acid

Y = 2.3786 x - 0.2275 (r^2 = 0.9981)

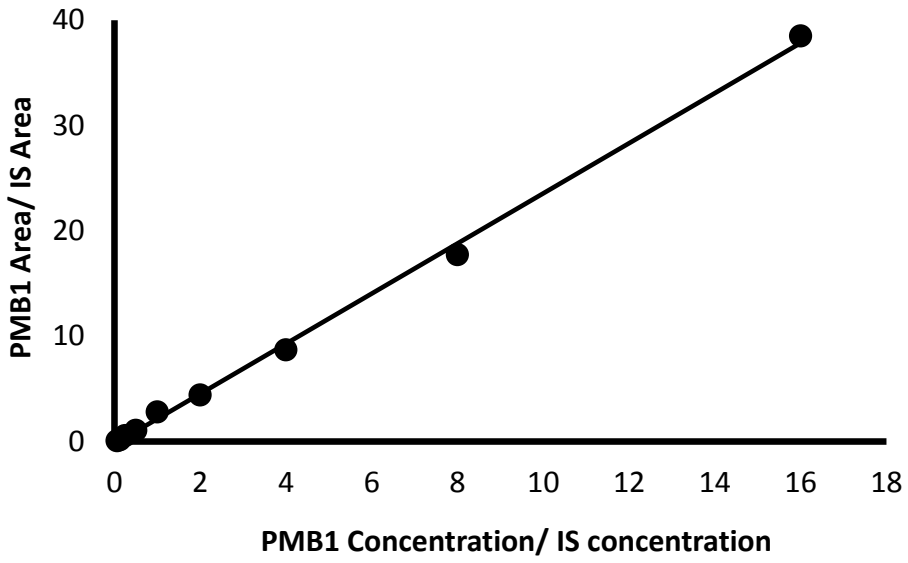

Figure 2.3: PMB1 Calibration Curve in Rat Serum

Y = 0.2507 x + 0.0035 (r^2 = 0.9963)

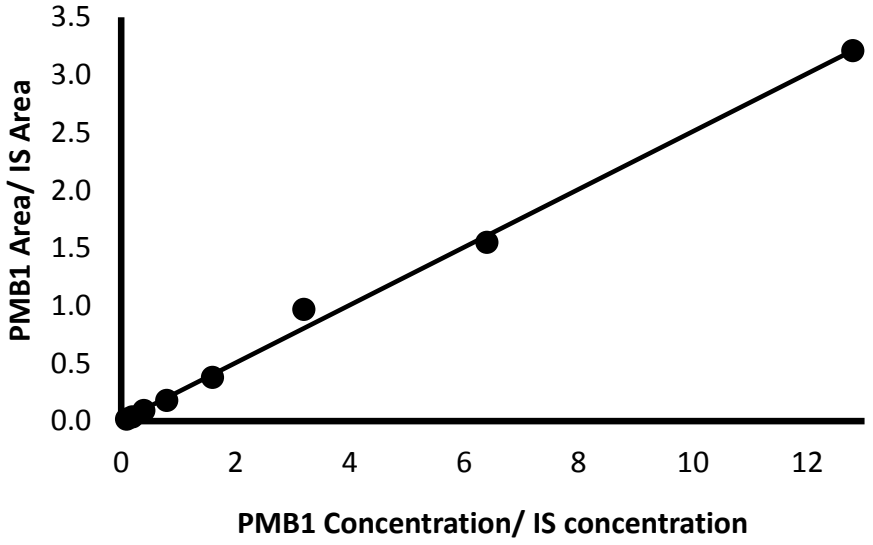

Figure 2.4: PMB1 Calibration Curve in Brain Tissue Homogenate

Y = 0.1036 x + 0.0254 (r^2 = 0.9935)

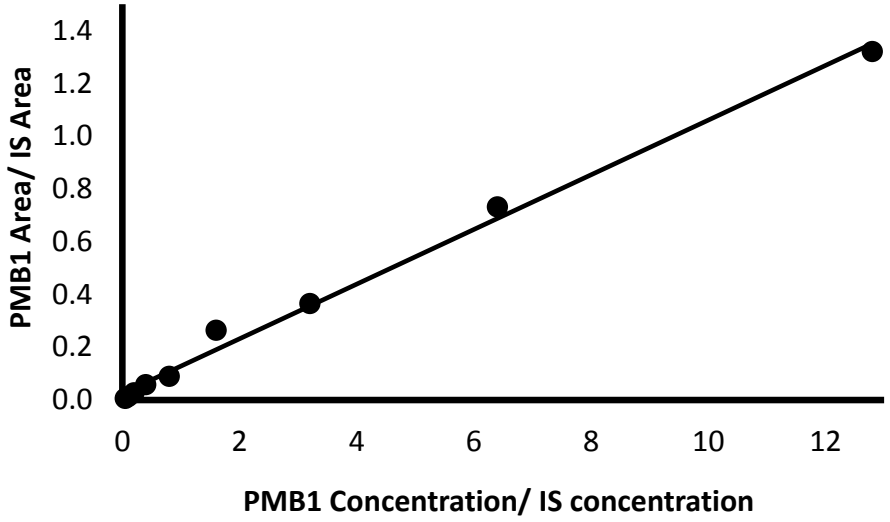

Figure 2.5: PMB1 Calibration Curve in Heart Tissue Homogenate

Y = 0.0963 x + 0.0042 (r^2 = 0.9989)

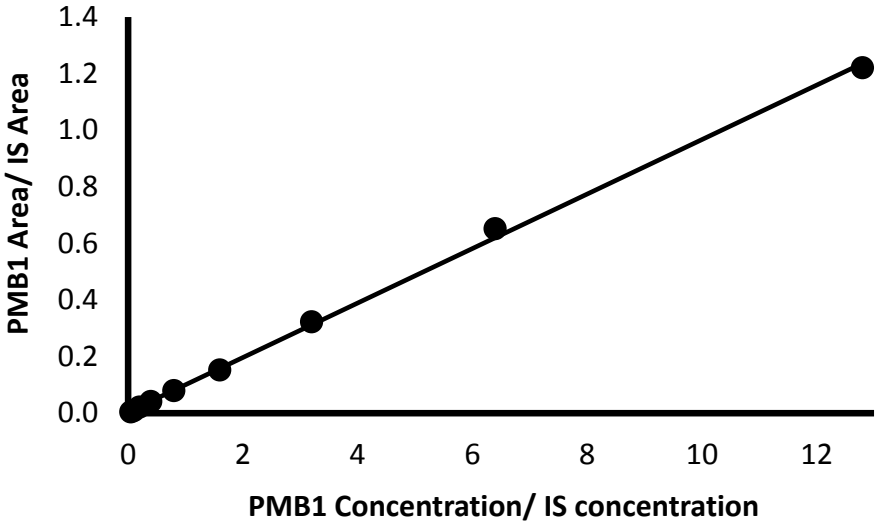

Figure 2.6: PMB1 Calibration Curve in Lung Tissue Homogenate

Y = 0.1077 x - 0.003 (r^2 = 0.9945)

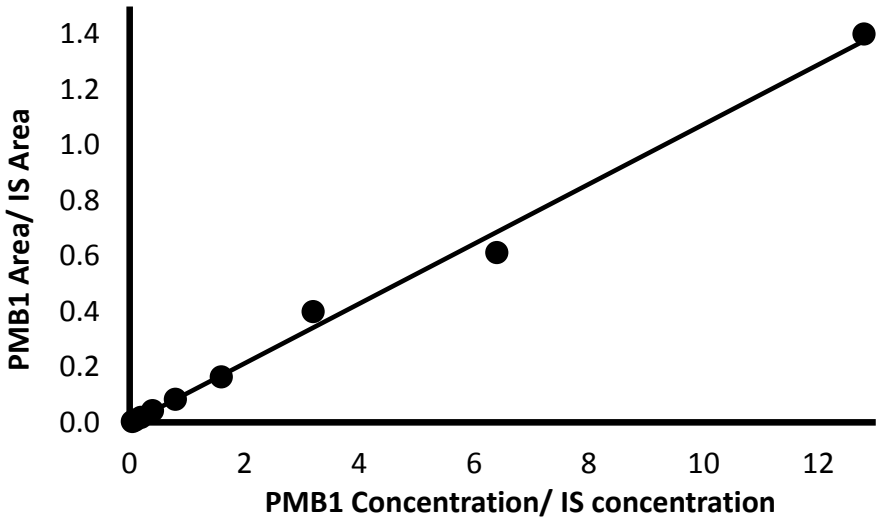

Figure 2.7: PMB1 Calibration Curve in Liver Tissue Homogenate

Y = 0.0453 x + 0.0135 (r^2 = 0.9864)

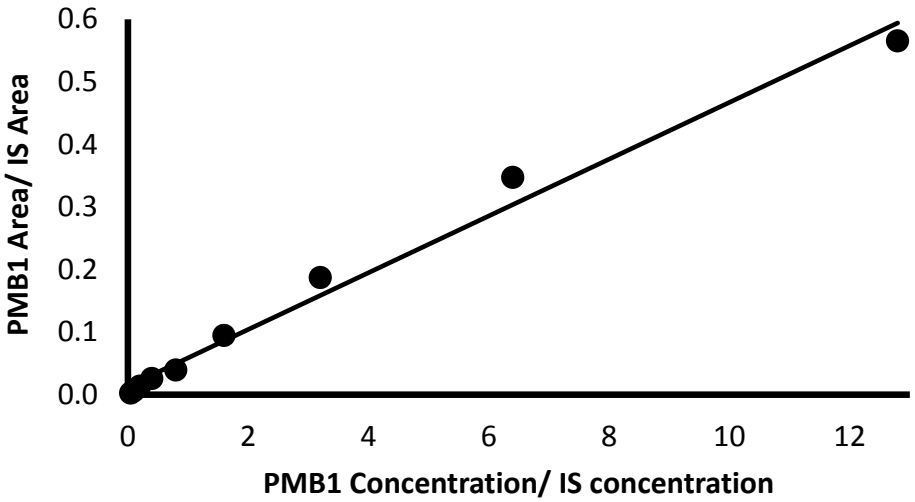

Figure 2.8: PMB1 Calibration Curve in Spleen Tissue Homogenate

Y = 1.93 x + 0.2865 (r^2 = 0.9982)

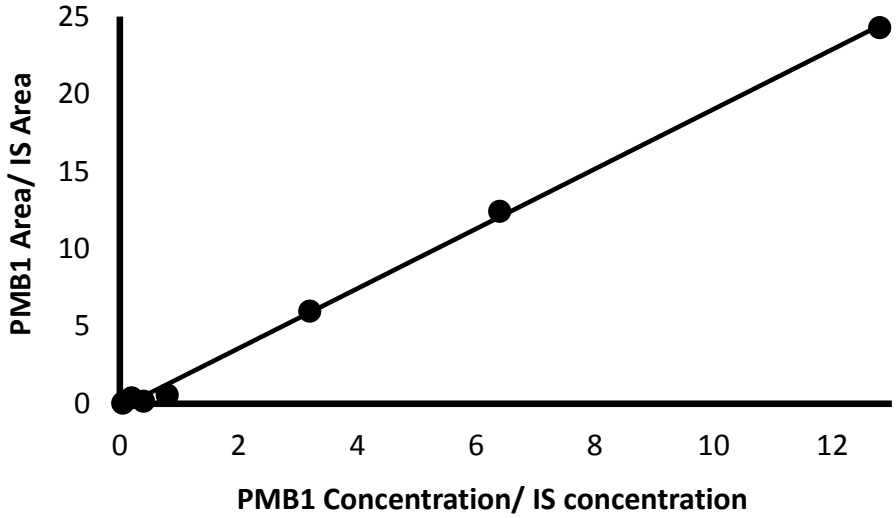

Figure 2.9: PMB1 Calibration Curve in Kidney Tissue Homogenate

Y = 0.099 x + 0.0011 (r^2 = 0.9924)

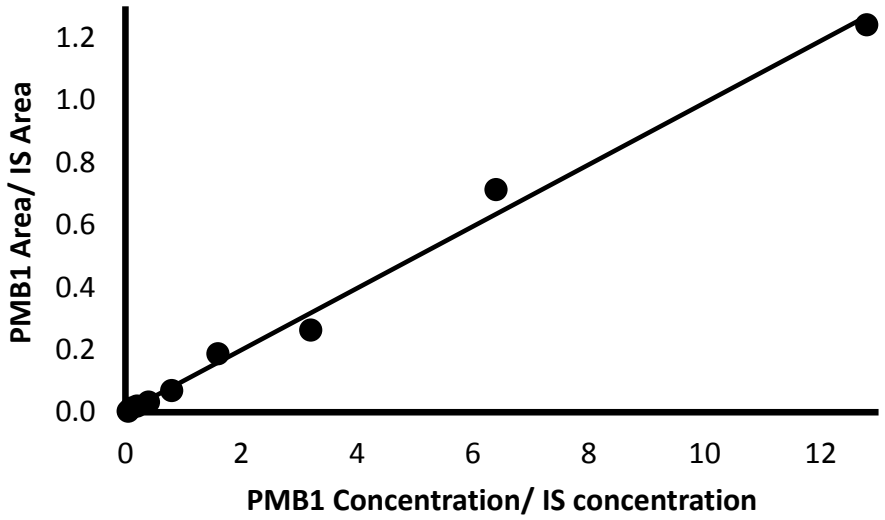

Figure 2.10: PMB1 Calibration Curve in Muscle Tissue Homogenate

Y = 0.075 x + 0.005 (r^2 = 0.9979)

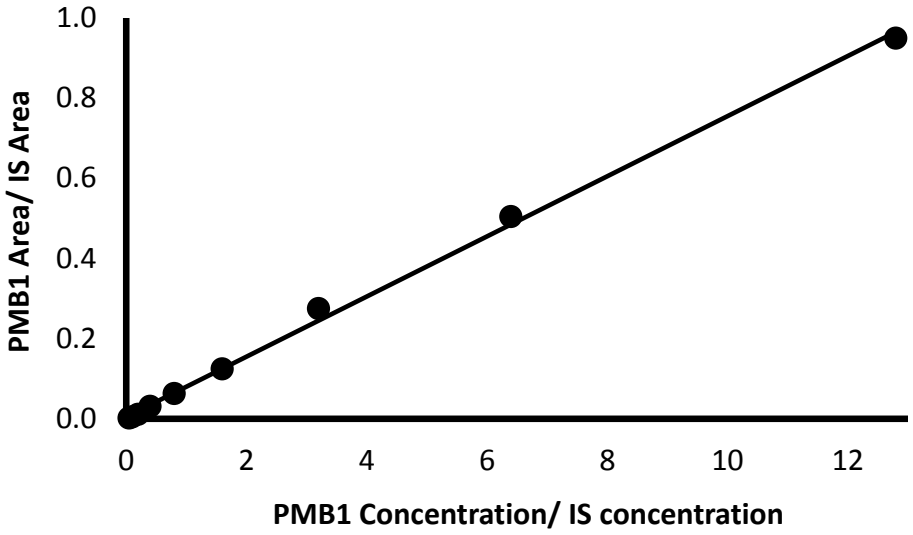

2.1.3 UPLC-MS/MS Assay of Polymyxin B in Rat Urine

A standard stock solution of polymyxin B1, B2, B3, and Ile-B1 were prepared by dissolving a known amount of the reference standards in LCMS grade water. The working solutions were obtained by serial dilution of the prepared mixture stock solution in 0.1% formic acid to achieve the final concentration range of 0.125 - 32 µl/ml. Briefly, to prepared the standard curve samples in rat urine matrix, 200 µl of drug-free (blank) urine supplemented with 100 µl of blank serum to avoid adsorption of polymyxin B to the polypropylene tubes and minimize the matrix effect due to urinary salts. Subsequently, the

mixture was spiked with 40 µl of the above working solutions of the standard mixture and 20 µl of the internal standard (carbutamide, 5 µg/ml) solution. To precipitate proteins, 5% trichloroacetic acid (640 µl) was added to the mixture, vortexed for 1 min and then centrifuged at 18,000 x g for 20 min at 4ºC as previously described. The supernatant was transferred to a new tube and loaded onto Oasis HLB solid-phase extraction (SPE) cartridges (30 mg, 1ml, Waters, Milford, MA). The SPE cartridges were preconditioned with 1ml methanol followed by 2 x 1ml de-ionized water on a vacuum suction manifold (Supelco, Bellefonte, PA). Salts and other impurities were removed by washing with 1ml of water. Polymyxin B was eluted with 2 x 1ml of 0.1% formic acid and acetonitrile (1:1 v/v) mixture the eluent was evaporated to dryness under a stream of ambient air. The residue was then reconstituted with 100 µl of a mixture of 0.1% formic acid and acetonitrile (1:1 v/v). The 10 µl of the resultant solution was then injected to UPLC-MS/MS. Figure 2.11 represents a typical UPLC chromatogram of spiked major polymyxin B purified standards in rat urine samples. The linear concentration ranges for PMB1 in urine samples was 0.025 – 12.8 µg/ml. The linear regression coefficients were ≥ 0.99 in all the calibration curves as shown in Figure 2.12.

Figure 2.11: Typical UPLC-MS/MS Chromatogram of Major Polymyxin B Components and Carbutamide in Rat Urine

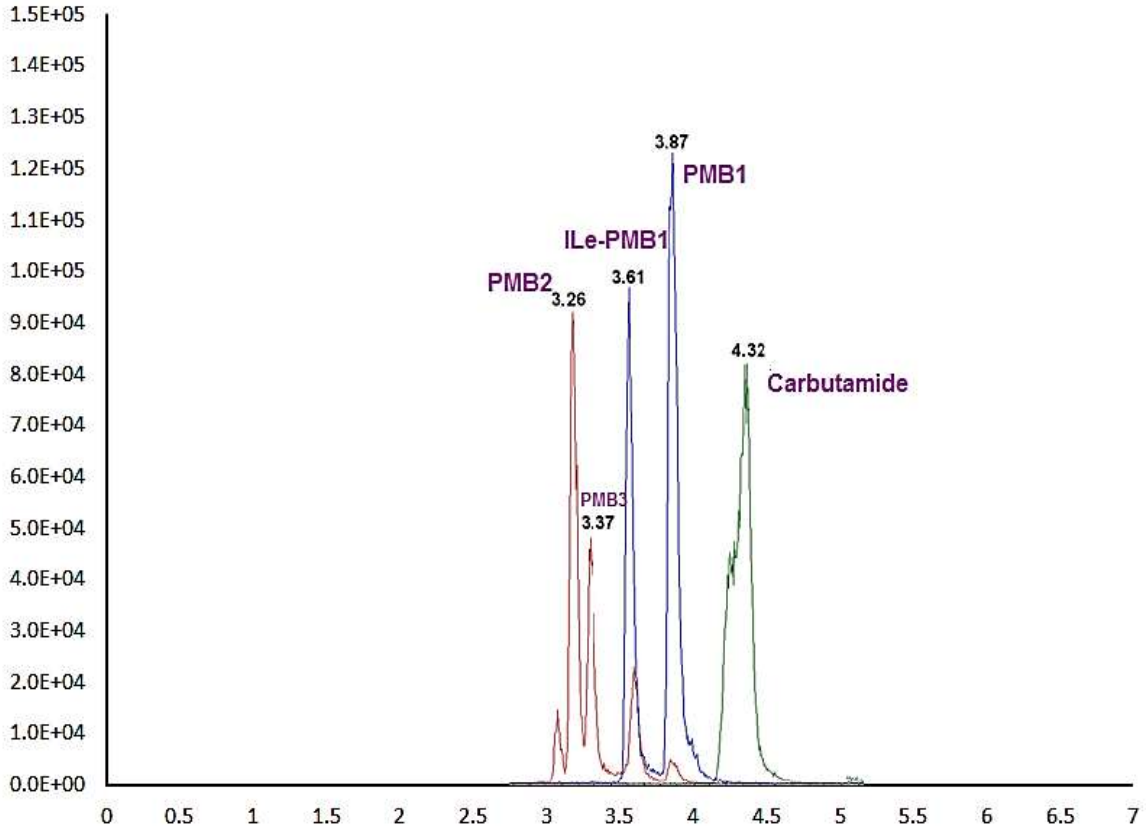

Figure 2.12: PMB1 Calibration Curve in Rat Urine

$Y = 0.1161 x + 0.0077 (r^2 = 0.9954)$

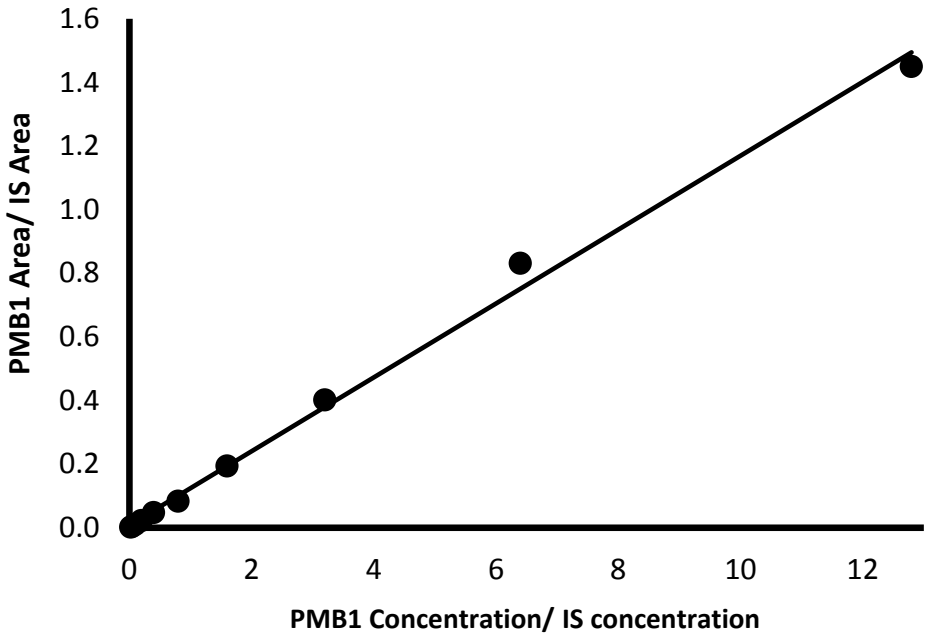

2.1.4 UPLC-MS/MS Assay of Polymyxin B in Rat Bile

The UPLC/MS/MS method was modified to determine the concentrations of polymyxin B in rat bile. Briefly, 20 μl of bile was first spiked with 50 μl blank serum (> 2 times the volume of bile) as an attempt to minimize matrix effect caused due to bile components. Then, 10 μl internal standard (carbutamide 5 μg/ml) added to it followed by 130 μl of 5% trichloroacetic acid to precipitate proteins. The samples were vortexed for 1 min, followed by centrifugation at 18,000 x g for 20 min at 4ºC as previously described. The supernatant was transferred to a new tube and loaded onto Oasis HLB solid-phase extraction (SPE) cartridges (30 mg, 1ml, Waters, Milford, MA). The SPE cartridges were preconditioned with 1ml methanol followed by 2 x 1ml de-ionized water on a vacuum suction manifold (Supelco, Bellefonte, PA). Salts and other impurities were removed by washing with 1ml of water. Polymyxin B was eluted with 2 x 1ml of 0.1% formic acid and acetonitrile (1:1 v/v) mixture and the eluent was evaporated to dryness under a stream of ambient air. The residue was then reconstituted with 100 μl of a mixture of 0.1% formic acid and acetonitrile (1:1 v/v). The 10 μl of the resultant solution was then injected to UPLC-MS/MS. Figure 2.13 represents a typical UPLC chromatogram of spiked major polymyxin B purified standards in rat bile samples. The linear concentration ranges for PMB1 in bile samples was 0.05 – 12.8 μg/ml. The linear regression coefficients were ≥ 0.99 in all the calibration curves as shown in Figure 2.14.

Figure 2.13: Typical UPLC-MS/MS Chromatogram of Major Polymyxin B Components and Carbutamide in Rat Bile

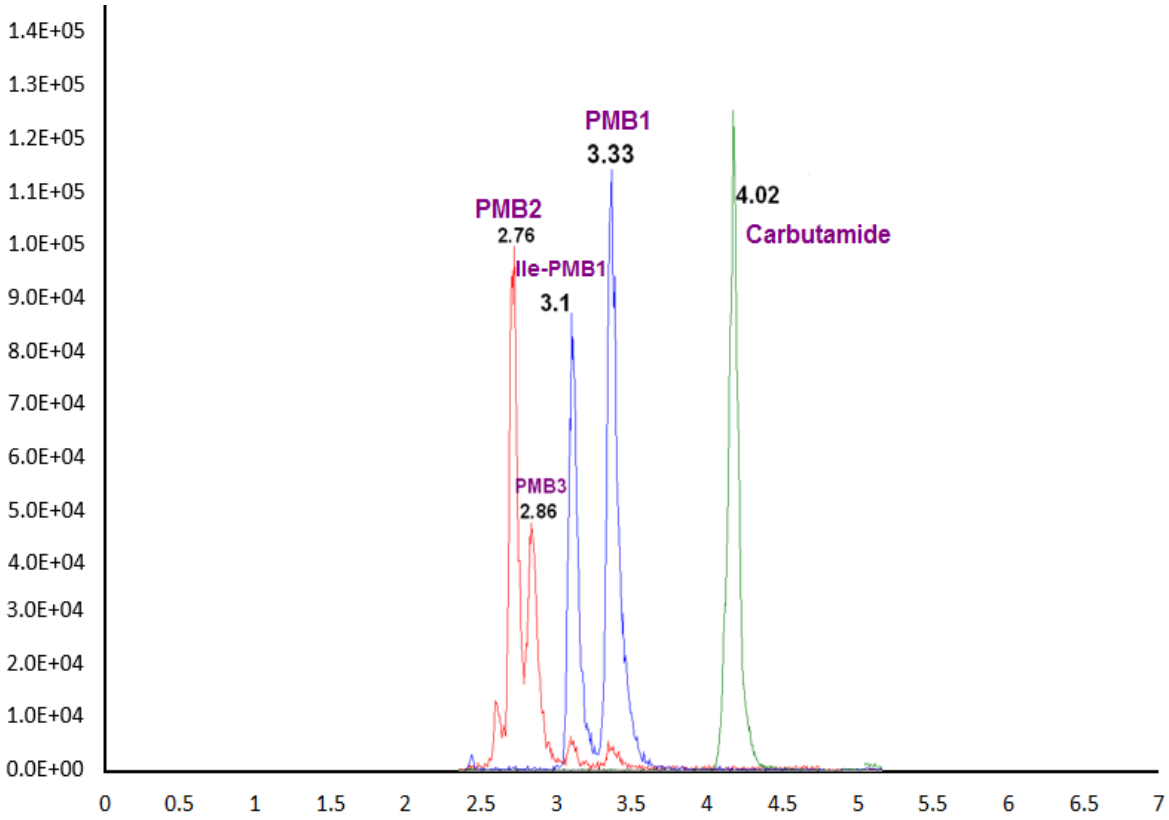

Figure 2.14: PMB1 Calibration Curve in Rat Bile

Y = 0.0716 x - 0.0096 (r^2 = 0.9869)

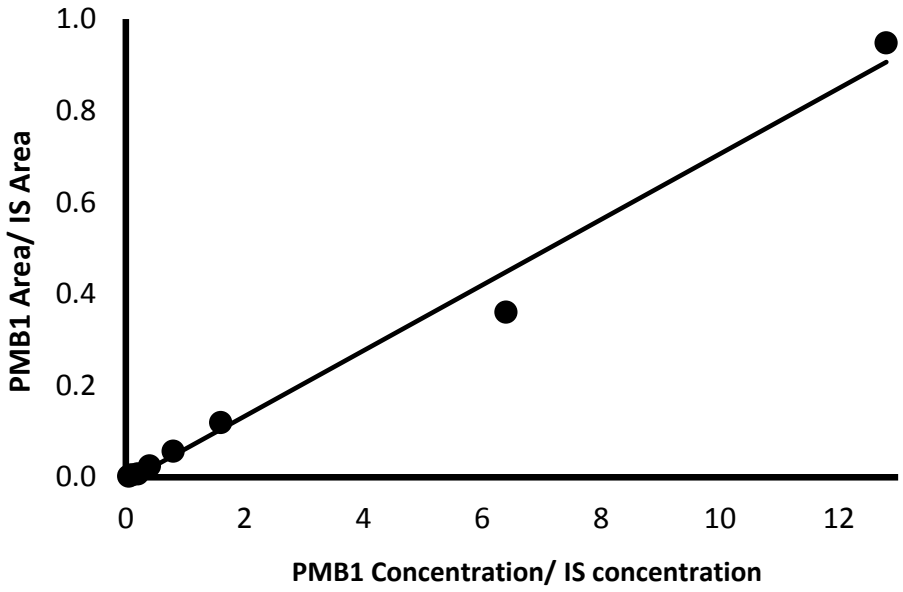

2.2 Microbiological Assay of Polymyxin B in Rat Urine

A validated microbiological assay method was also modified to determine the concentrations of pharmacologically active polymyxin B in the rat urine samples, as previously described (He, Figueroa, Lim, Chow, & Tam, 2010). *Bordetella bronchiseptica* ATCC 10580, obtained from American Type Culture Collection (Manassas, VA), was used as the reference organism. Bacteria in logarithmic-phase growth were incorporated into 30 ml of molten cation-adjusted Muller Hilton II Agar at 50 ºC to achieve a final concentration of approximately 1000,000 CFU/ml. The agar was allowed to solidify in 150-mm medium plates. A size 3 cork bore was used to puncture nine wells in the agar plate. Five polymyxin B standards (4, 8, 16, 32 and 64 µl), blank and urine sample from three rat (40 µl each) were placed on each plate. The plates were prepared in duplicates and were then incubated at 35 ºC for 24 hours. Further, the elimination of polymyxin B in urine was estimated by plotting the calibration curves between inhibition zone diameters (mm) versus the logarithmic standard polymyxin B drug concentrations in urine from each plate. The assay was previously validated based on accuracy, precision, inter and intraday variability (He et al., 2013). The LLOQ was determined to be 2 µg/ml.

REFERENCES

He, J., Figueroa, D. A., Lim, T. P., Chow, D. S., & Tam, V. H. (2010). Stability of polymyxin b sulfate diluted in 0.9% sodium chloride injection and stored at 4 or 25 degrees c. *Am J Health Syst Pharm, 67*(14), 1191-1194. doi:10.2146/ajhp090472

He, J., Gao, S., Hu, M., Chow, D. S., & Tam, V. H. (2013). A validated ultra-performance liquid chromatography-tandem mass spectrometry method for the quantification of polymyxin b in mouse serum and epithelial lining fluid: Application to pharmacokinetic studies. *J Antimicrob Chemother, 68*(5), 1104-1110. doi:10.1093/jac/dks536

CHAPTER 3

CHARACTERIZATION OF POLYMYXIN B BIODISTRIBUTION AND DISPOSITION

3.1 Materials and Method

3.1.1 Antimicrobial Agent

Polymyxin B (USP) was purchased from Sigma-Aldrich (St. Louis, MO) and X-GEN Pharmaceuticals, Inc. (Northport, NY). Prior to each animal experiment, polymyxin B (USP) was reconstituted and diluted to the desired concentrations with normal saline. The reconstituted drug solutions were stored at -80ºC until analysis.

3.1.2 Animals

Female Sprague-Dawley rats (225-250g) (Harlan, Indianapolis, IN, USA) were used. The rats received food and water *ad libitum*. In selected experiments, jugular veins of selected animals were cannulated to facilitate intravenous drug administration. The rats were maintained in a 12hr dark/light cycle and in a temperature-and-humidity-controlled environment. All animals were cared for in

accordance with the highest humane and ethical standards, as approved by Institutional Animal Care and Use Committee (IACUC) of the University of Houston.

3.1.3 Chemicals and Reagents

Blank human and rat sera were obtained from Equitech-Bio Inc (Kerrville, TX). Carbutamide was purchased from Aldrich (Milwaukee, WI). LC-MS grade acetonitrile and water were obtained from Mallinckrodt Baker (Philipsburg, NJ). LC-MS grade formic acid was purchased from Fluka Analytical (St. Louis, MO). Trichloroacetic acid, phosphate buffer saline with 0.01% were purchased from Sigma-Aldrich (St. Louis, MO). Carbutamide was purchased from Aldrich (Milwaukee, WI). LC-MS grade acetonitrile and water were obtained from Mallinckrodt Baker (Philipsburg, NJ). LC-MS grade formic acid was purchased from Fluka Analytical (St. Louis, MO).

3.1.4 Pharmacokinetics of Polymyxin B in Rats

A total of 17 female Sprague-Dawley rats (225-250g) (Harlan, Indianapolis, IN) were used. The rats were administered a single intravenous dose of polymyxin B (3 mg/kg). Blood samples were obtained at 1, 1.5, 3, 4.5, 6 and 7.5 h post-dose and allowed to clot on the ice. Serum samples were

obtained by centrifugation (6000x g for 15 minutes at 4ºC) and stored at -80 °C until drug analysis. A median of 4 samples (range: 2-8) were obtained at each time point, the average concentration of each time point was used for pharmacokinetic analysis.

A validated liquid chromatography tandem mass spectrometry (UPLC-MS/MS) method was used to determine the concentrations of polymyxin B in rat and human sera (He et al., 2013). The serum concentrations of each component were quantified individually and subsequently reported collectively as the total polymyxin B concentration.

3.1.5 Pharmacokinetic Modeling

The pharmacokinetics of polymyxin B was derived using two different approaches. In the first approach, we used the total polymyxin B concentrations in serum**.** In contrast, the concentration-time profiles of individual polymyxin B components were used in the second approach. The dose fractions of the individual components were based on their relative abundance in the USP mixture (previously estimated to be 0.612, 0.254, 0.056 and 0.077 for polymyxin B1, B2, B3 and isoleucine B1, respectively). In both scenarios, a **o**ne-compartment linear model with a zero order input was used to fit the

concentration-time profiles using ADAPT 5 (University of Southern California, Los Angeles, CA).

3.1.6 Polymyxin B Assay

A validated liquid chromatography tandem mass spectrometry (UPLC/MS/MS) method was modified to determine the concentrations of polymyxin B in rat serum, brain, heart, lungs, liver, spleen, kidneys and skeletal muscle tissues (He et al., 2013). Briefly, serum, bile or tissue homogenate was spiked with 10 µl of an internal standard (carbutamide 5 µg/ml) and extracted with 150 µl of 5% trichloroacetic acid. The samples were vortexed for 1 min, followed by centrifugation as previously described (He et al., 2013). The supernatant was transferred to a new tube and evaporated to dryness under a stream of ambient air. The residue was then reconstituted with 100 µl of a mixture of acetonitrile and 0.1% formic acid (1:1 v/v). The samples were again centrifuged at 18,000 $\times$ g for 20 min at 4°C, and 10 µl of the supernatant was injected into the UPLC-MS/MS system for quantitative analysis.

The calibration curves in serum/urine/tissue samples were constructed using at least eight concentration standards. The linearity of the calibration curves was determined by the best fit of peak-area ratios (analyte/internal

standard) versus concentrations and fitted using a linear regression ($1/x^2$ weighing) method. The lower limit of quantification (LLOQ) was determined based on the signal to noise ratio of 10:1. The assay was validated based on accuracy, precision, inter and intraday variability, which was well within 15% of the coefficient of variation (CV) and did not exceed 20% of the CV for the LLOQ (He et al., 2013).

A validated microbiological assay method was also modified to determine the concentrations of polymyxin B in the rat urine samples, as previously described (18). *Bordetella bronchiseptica* ATCC 10580, obtained from American Type Culture Collection (Manassas, VA), was used as the reference organism. Bacteria in logarithmic-phase growth were incorporated into 30 ml of molten cation-adjusted Muller Hilton II Agar at 50 ºC to achieve a final concentration of approximately 1000,000 CFU/ml. The agar was allowed to solidify in 150-mm medium plates. A size 3 cork bore was used to puncture nine wells in the agar plate. Five polymyxin B standards (4, 8, 16, 32 and 64 µl), blank and urine sample from three rats (40 µl each) were placed on each plate. The plates were prepared in duplicates and were then incubated at 35 ºC for 24 hours. Further, the elimination of polymyxin B in urine was estimated by plotting the calibration curves between inhibition zone diameter (mm) versus the logarithmic standard

polymyxin B drug concentration in urine from each plate. The assay was previously validated based on accuracy, precision, inter and intraday variability; LLOQ was determined to be 2 µg/ml.

3.1.7 Biodistribution of Polymyxin B

Prior to each experiment, polymyxin B powder was dissolved in sterile water for injection and diluted to the desired concentration. The rats were given a single intravenous dose of polymyxin B (3 mg/kg) and sacrificed after 3 h (n=3), 6 h (n=6) and 24 h (n=3), respectively. The harvested tissues were weighed and homogenized in deionized water (1:2). The mean tissue/serum drug concentration ratios were estimated for each tissue matrix. The groups were compared using one-way ANOVA, followed by Tukey's posthoc test. P-values <0.05 were considered significant.

3.1.8 Pre- and Post-Dose Urine Sampling

The rats (n=3) were housed individually in separate metabolic cages to facilitate urine collection. Blank urine was collected from each rat, prior to the administration of a single intravenous dose of polymyxin B (3 mg/kg). The cumulative urine of each rat was collected daily from day -1 to 2 following drug

administration. The urine samples were spun down to remove the particulate matter, and volumes were recorded. Subsequently, the urine samples were aliquoted and stored at -80 ºC prior to analysis.

3.1.9 Elimination of Polymyxin B in Urine

Prior to analysis, samples were thawed and loaded into the solid-phase extraction cartridges (Oasis HLB 1cc cartridges, 30 µm) preconditioned with 1m of methanol and 1 x 2 ml of water. After loading the urine samples, the cartridges were washed twice with water followed by eluting solvent (0.1% formic acid in water: acetonitrile, 50:50) mixture. Subsequently, the eluent was injected UPLC/MS-MS for quantification of polymyxin B in urine samples. To quantify the active metabolite of polymyxin B using microbiological assay, the urine sample were thawed and concentrated 2X by evaporation to reduce the lower limit of detection. The urine samples were then placed in wells of the agar plate incorporated with bacteria (*Bordetella bronchiseptica* ATCC 10580) along with the polymyxin B standards in urine as shown in figure 3.3. Subsequently, the inhibition zone diameter (mm) of the urine samples were measured for the quantification of pharmacologically active form (metabolite if any) of polymyxin B eliminated in the urine.

3.2 Results

3.2.1 Pharmacokinetics of Polymyxin B in Rats

The overall model fit to the rat data was satisfactory, as shown in Figure 3.1. In addition, best-fit pharmacokinetic parameters are shown in Table 3.1. Strictly speaking, the pharmacokinetic parameters (e.g., clearance and volume of distribution) of the individual components were not identical, but most the differences were within a 2-fold range.

The weighted average pharmacokinetic parameters using individual components were in reasonably close agreement with those derived directly from the total polymyxin B concentrations. The $AUC_{(0-\infty)}$ observed for total polymyxin B was 10.7 $mg.h.L^{-1}$, which was comparable to that derived from adding $AUC_{(0-\infty)}$ of individual polymyxin B components in the mixture (10.9 $mg.h.L^{-1}$). A similar trend was also observed in the patient samples, as shown in Table 1.

Table 3.1: Comparison of the Best-Fit Pharmacokinetic Parameters in Rats

	CL (L/kg/h)	V (L/kg)	$T_{1/2}$ (h)	Ke (h^{-1})	$AUC_{(0-\infty)}$ ($mg.h.L^{-1}$)	R^2
Total PMB	0.28	1.00	2.47	0.28	10.71	0.90
PMB1	0.30	0.95	2.21	0.31	6.17	0.91
PMB2	0.32	1.16	2.50	0.28	2.37	0.93
PMB3	0.15	0.75	3.59	0.19	1.16	0.63
Ile-PMB1	0.19	1.02	3.76	0.18	1.23	0.71
Weighted average*	0.29	1.00	2.48	0.29		
Sum of individual components					10.93	

NOTE. $AUC_{(0-\infty)}$, area under the concentration curve from zero to infinity; CL, clearance; V, volume of distribution; Ke, elimination rate constant; $T_{1/2}$, elimination half-life.

* Weighted average based on the relative abundance of different polymyxin B component

Figure 3.1: Model Fitting of Total Polymyxin B and Individual Components

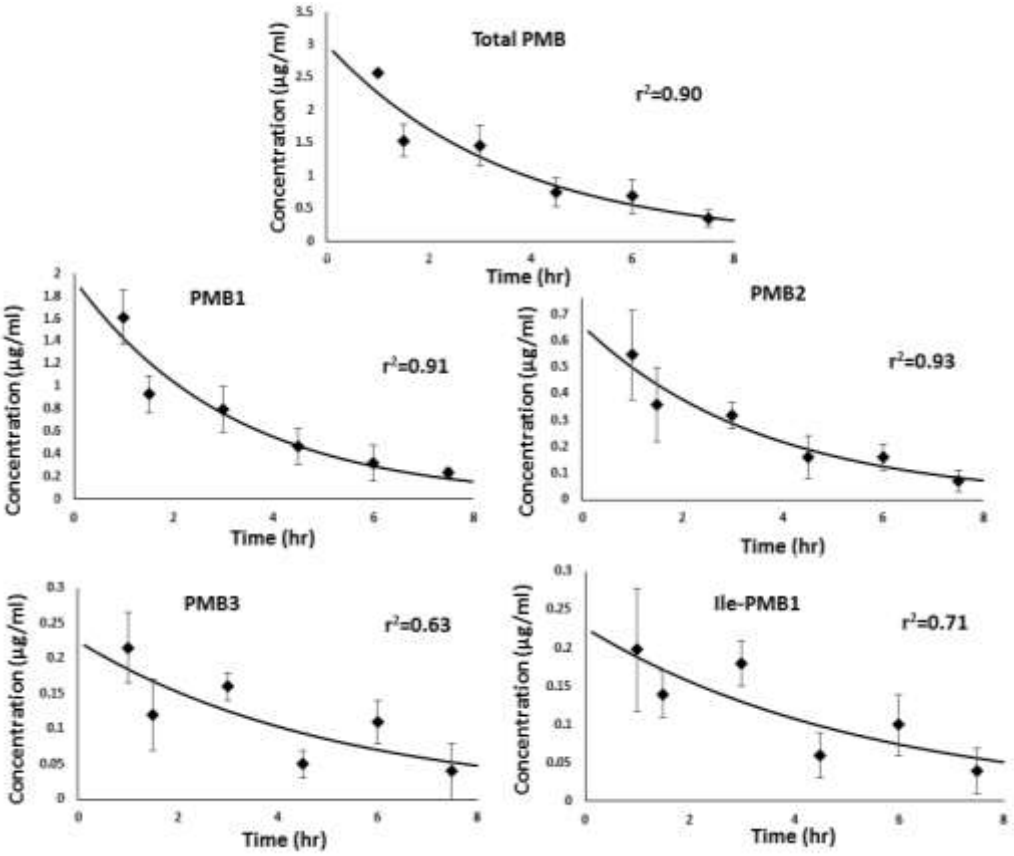

The data points represent the average serum concentrations of each time point; error bars depict the standard deviations, and solid lines represent the best-fit lines

3.2.2 Polymyxin B Assay

The linear concentration ranges for polymyxin B in serum, bile, brain, heart, lungs, liver, spleen, kidneys and muscle tissue homogenate were 0.1-12.8 µg/ml, 0.05-12.8 µg/ml, 0.05-12.8 µg/ml, 0.05-12.8 µg/ml, 0.05-12.8 µg/ml, 0.0125-12.8 µg/ml, 0.05-12.8 µg/ml, 0.05-12.8 µg/ml, and 0.1-6.4 µg/ml, respectively. The linear concentration range for polymyxin B in urine samples was 0.025-12.8 µg/ml. The linear regression coefficients were ≥ 0.99 in all the calibration curves. For the microbial assay of polymyxin B in urine, the linear concentration range was 2-64 µg/ml respectively.

3.2.3 Biodistribution of Polymyxin B

Among all the organs evaluated, polymyxin B distribution was the highest in the kidneys. The mean renal tissue/serum polymyxin B concentration ratios were 7.45 (95 % CI, 4.63-10.27) at 3 h and 19.62 (95 % CI, 5.02-34.22) at 6 h post-dose, respectively as shown in Figure 3.2. As shown in Table 3.2, all tissue concentrations at 24 h were lower than those observed at 6 h, but the mean tissue/serum ratio at 24 h could not be calculated because the polymyxin B concentration in the serum was below the limit of detection. The kidney concentration at 24 h was roughly 1.4-5.8 times those observed in organs other than the brain. Polymyxin B levels in the brain remained consistently lower than

that observed in serum. All other organs exhibited a similar distribution profile as serum (Figure 3.2).

3.2.4 Elimination of Polymyxin B in Urine

We observed that less than 1% of dose of polymyxin B was eliminated in the urine in unchanged form whereas less than 5% of the dose of polymyxin B was eliminated in pharmacologically active form.

Figure 3.2: Tissue/Serum Concentration Ratio of Polymyxin B in Various Tissues; (A) 3 h Post-Dose, (B) 6 h Post-Dose

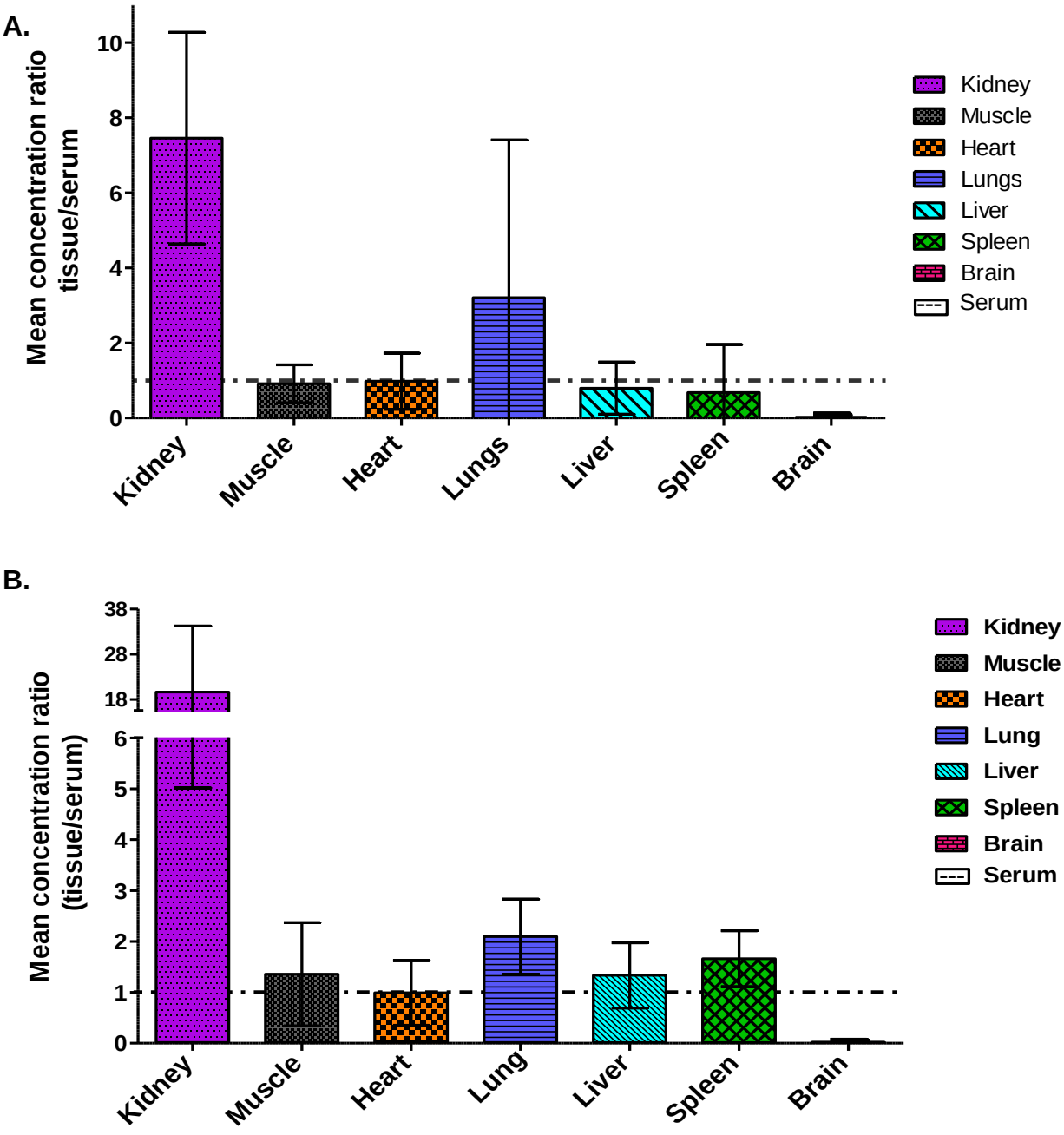

Vertical error bars represent the 95% confidence intervals

Table 3.2: Biodistribution of Polymyxin B in Rat Serum and Tissue Homogenates

Time (h)	Polymyxin B concentrations (mean ± SD)							
	Serum (µg/ml)	**Kidney (µg/g)**	**Muscle (µg/g)**	**Liver (µg/g)**	**Heart (µg/g)**	**Lung (µg/g)**	**Spleen (µg/g)**	**Brain (µg/g)**
3	1.46 ± 0.38	10.57 ± 1.21	1.31 ± 0.41	1.10 ± 0.29	1.50 ± 0.78	4.93 ± 3.71	0.86 ± 0.43	0.04 ± 0.04
6	0.69 ± 0.29	11.32 ± 5.06	0.77 ± 0.34	0.82 ± 0.24	0.57 ± 0.18	1.33 ± 0.41	1.11 ± 0.50	0.02 ± 0.02
24	< LLOQ	0.76 ± 0.41	0.53 ± 0.18	0.13 ± 0.04	0.28 ± 0.06	0.25 ± 0.04	0.50 ± 0.07	0.01 ± 0.02

Figure 3.3: Microbiological Assay of Polymyxin B in Rat Urine

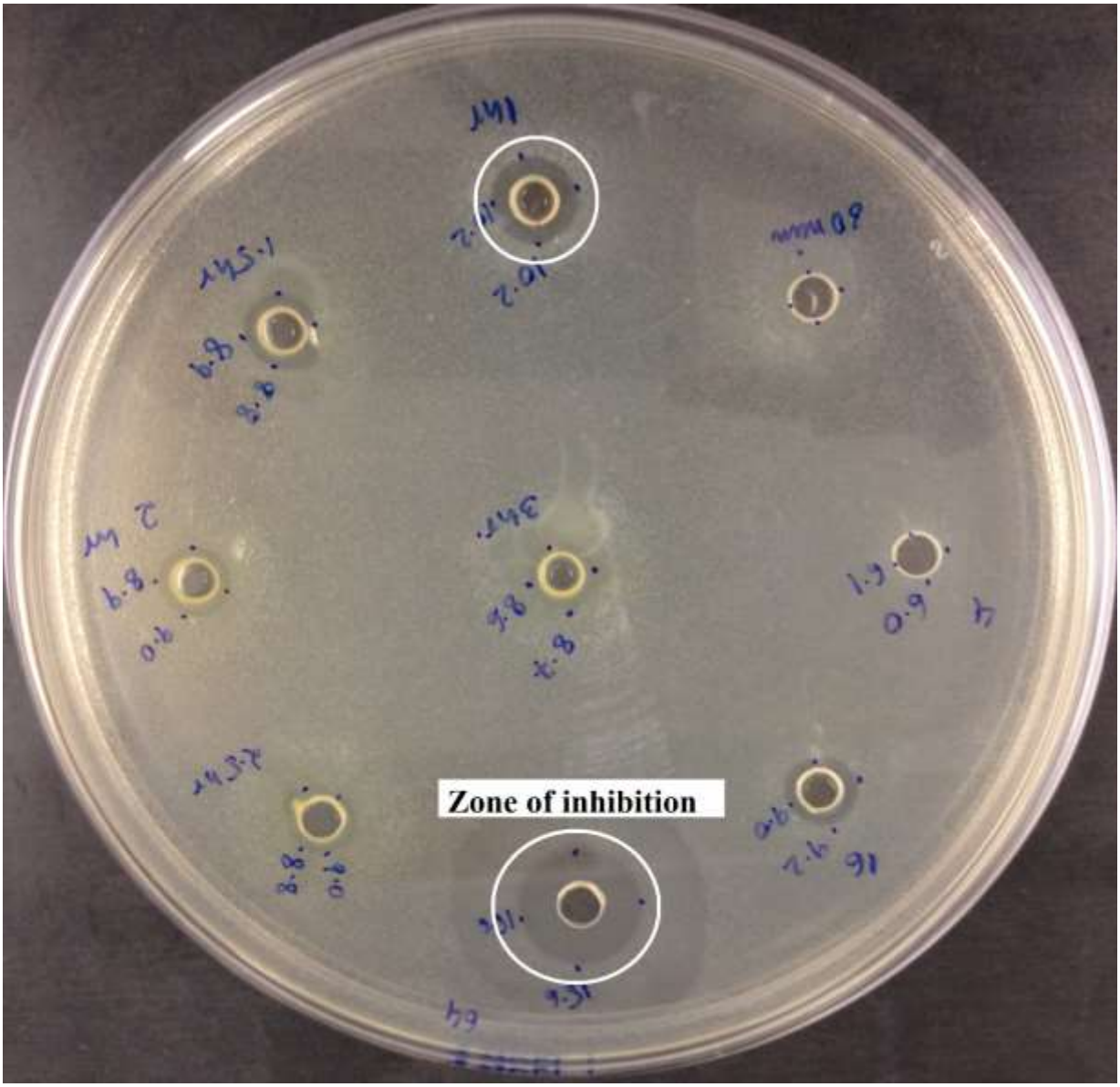

REFERENCE

He, J., Gao, S., Hu, M., Chow, D. S., & Tam, V. H. (2013). A validated ultra-performance liquid chromatography-tandem mass spectrometry method for the quantification of polymyxin b in mouse serum and epithelial lining fluid: Application to pharmacokinetic studies. *J Antimicrob Chemother, 68*(5), 1104-1110. doi:10.1093/jac/dks536

CHAPTER 4

INTRARENAL DISTRIBUTION OF POLYMYXIN B

4.1 Materials and Method

4.1.1 Antimicrobial Agent

Polymyxin B sulfate (USP) powder was purchased from Sigma-Aldrich (St. Louis, MO). Prior to each experiment, the drug was reconstituted and diluted to the desired concentrations with normal saline. The reconstituted drug solutions were stored at -80ºC until analysis.

4.1.2 Animals

Female Sprague-Dawley rats (225-250g) (Harlan, Indianapolis, IN, USA) were used. The rats received food and water *ad libitum*. In selected experiments, jugular veins of selected animals were cannulated to facilitate intravenous drug administration. The rats were maintained in a 12hr dark/light cycle and a temperature-and-humidity-controlled environment. All animals were cared for in accordance with the highest humane and ethical standards, as approved by Institutional Animal Care and Use Committee (IACUC) of the University of Houston.

4.1.3 Chemicals and Reagents

Polymyxin B sulfate (USP) powder, trichloroacetic acid, phosphate buffer saline with 0.01% Tween 80 (PBST), 4% paraformaldehyde (PFA), 30% sucrose solution in phosphate buffer saline (PBS) were purchased from Sigma-Aldrich (St. Louis, MO).Normal goat serum, streptavidin DyLight 488 (green) and 649 (red), fluorogel-II with DAPI (blue) were obtained from Jackson ImmunoResearch Laboratories (West Grove, PA). Anti-mouse IgG secondary antibody, avidin-biotin blocking kits and biotinylated lectins were purchased from Vector Laboratories (Burlingame, CA). The natural sources, targeted nephron regions and optimal dilutions of various lectins are listed in Table 4.1.

4.1.4 Harvesting and Processing of Rat Kidney

The rats (n=3) were given a single intravenous dose of polymyxin B (4 mg/kg) and sacrificed at 6 h post-dose. The kidneys were perfusion-fixed with 4% paraformaldehyde and stored overnight. Subsequently, the kidneys were cryoprotected in 30% sucrose solution in PBS and finally cryosectioned at 20 µm intervals into thin tissue cross-sections.

4.1.5 Identification of Renal Cell Type and Immunostaining for Polymyxin B

Different anatomical regions of the nephron were identified by staining with specific lectin markers. The fresh frozen kidney tissue sections were placed in PBST maintained at pH 7.4 for 5-10 min before staining. Briefly, the sections were pre-incubated in avidin-biotin blocking solution, followed by incubation with biotinylated lectins diluted with PBST to the concentrations specified in Table 4.1, each for 30 min at room temperature. After washing 3 times in PBST, the sections were incubated for 30 min at room temperature with streptavidin DyLight 649 (10 µg/ml diluted in PBST). Subsequently, the sections were washed in PBST followed by washing 3 times with distilled water. The sections were then mounted using the fluorogel-II mounting agent with DAPI. Controls were prepared by the same staining procedure, except that the lectins were replaced by PBST.

The double immunostaining of renal tissue section was carried out using polymyxin B antibody and lectins. The sections were incubated with 5% normal goat serum followed by incubation with an avidin-biotin blocking solution for 30 min at room temperature. Subsequently, the sections were treated with polymyxin B antibody (1:20 dilution in 5% normal goat in PBS) for 1 h at 4°C, and later incubated with biotinylated mouse anti-polymyxin B antibody (1:150 dilution in 5% normal goat serum). After washing 3 times with PBST, the sections were

incubated with streptavidin DyLight 488 (10 µg/ml, diluted in PBST) for 30 min each at room temperature. Subsequently, staining with a specific lectin marker was performed on the same tissue section, as described above. Controls were prepared by same staining procedure except primary antibody and lectins were replaced by PBST.

4.1.6 Co-localization of Polymyxin B Antibody with Lectin

Images were captured using an Olympus IX61 DSU. Several region of interest (ROI) were randomly selected from individual overlay/co-localized image for each cell type. Selected ROI(s) from each overlay image were further analyzed using a computer-assisted software Image J (version 1.47); the Mander's overlap coefficient (R_{colo}), which signifies the percentage of overlap of two signal intensities, was calculated using Just Another Co-localization Plug-in (JACoP). The coefficient value above 0.7 was deemed to be a good degree of co-localization.

4.2 Results

4.2.1 Identification of Renal Cell Type and Immunostaining for Polymyxin B

A gross cross-section of the kidney revealed that the intrarenal distribution of polymyxin B was heterogeneous, as shown in Figure 4.1. Polymyxin B accumulated mainly in the renal cortex and outer stripe of the outer medulla.

The differential staining pattern was satisfactory with each lectin marker, as shown in Figure 4.2. Strong, focal staining of the brush border epithelium of proximal tubular cells was seen with Phaseolus vulgaris erythroagglutinin (PHA-E) lectin. Soybean agglutinin (SBA) lectin predominantly stained the distal convoluted tubular cells. The staining pattern of SBA lectin was reasonably distinct; cytoplasmic staining of distal cells was observed. For glomeruli, a strong, global and diffused staining pattern was seen with Wheat germ agglutinin (WGA) lectin.

Figure 4.1: Confocal Images of a Kidney Cross-Section

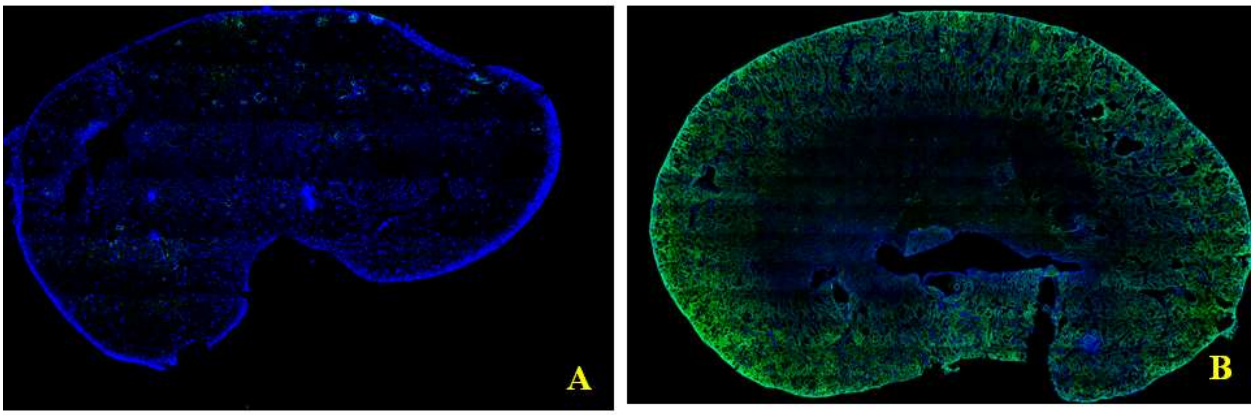

Panel A represents a kidney cross-section from control rat whereas panel B represents a cross-section from polymyxin B-treated rat. Blue color represents counterstaining with nuclear stain (DAPI) whereas green color represents staining with anti-polymyxin B antibody.

Table 4.1: Lectins Used for the Staining of Rat Kidney Cross-Section

Lectin	Source	Target	Final dilution of lectin in PBST (µg/ml)
Phaseolus vulgaris erythroagglutinin (PHA-E)	Red kidney bean	Proximal convoluted tubules (PCT)	10
Glycine max/ Soybean agglutinin (SBA)	Soybean	Distal convoluted tubules (DCT)	20
Wheat germ agglutinin (WGA)	Wheat germ	Glomerulus	20

Figure 4.2: Lectin Staining Pattern in Cortical Region of a Rat Kidney Cross-Section

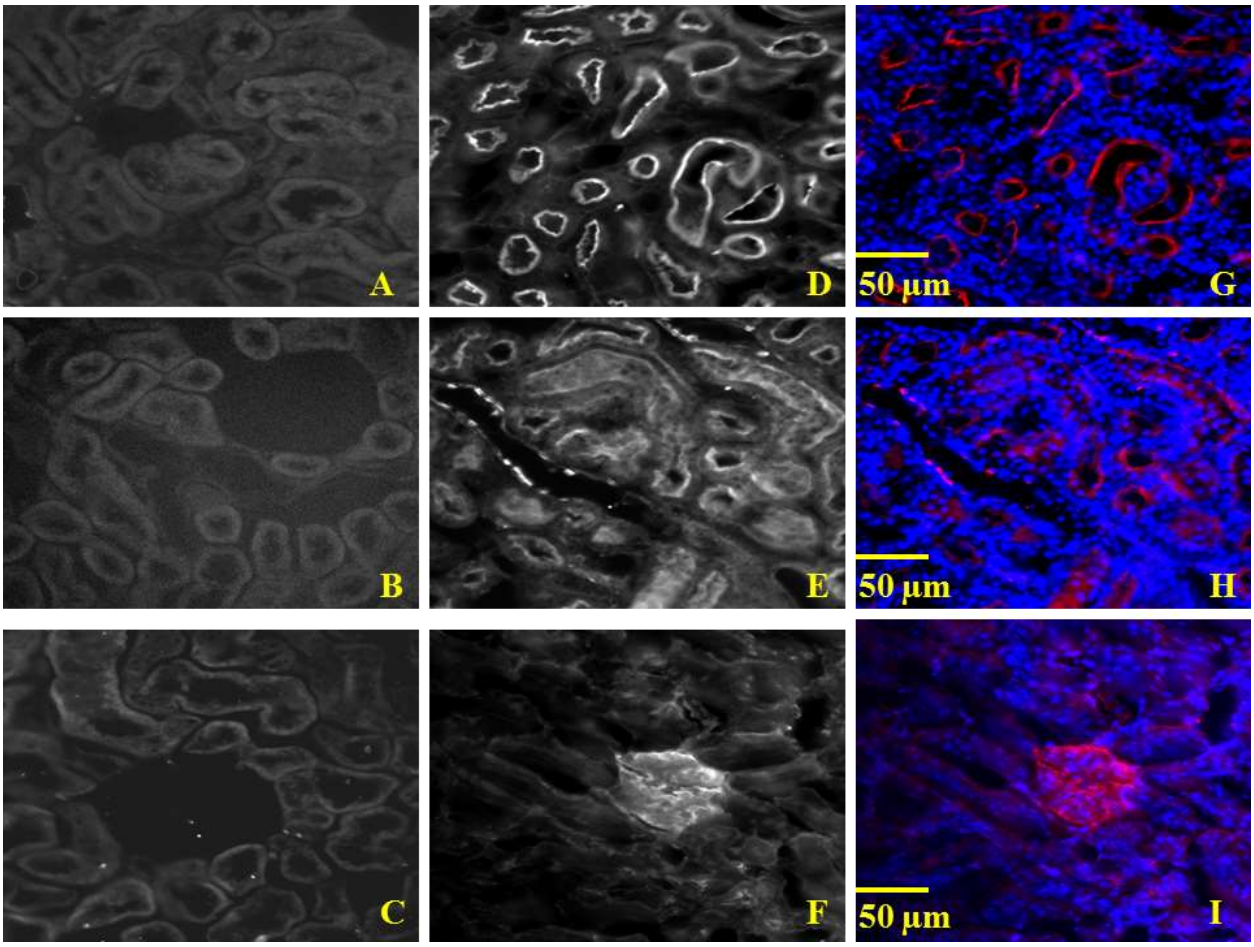

Panel A-C represent the control section; D-F represents the staining with lectins; I-K represents multichannel images of lectin stained kidney sections. Blue color represents counterstaining with nuclear stain (DAPI) whereas red color represents staining with specific lectins targeted toward different regions of the nephron.

4.2.1 Co-localization of Polymyxin B Antibody with Lectin

The double staining with polymyxin B antibody and lectins is shown in Figure 4.3. Polymyxin B was found to be accumulated primarily in the proximal tubular cells, with Mander's overlap coefficient (R_{colo}) of 0.998 for proximal tubular cells, 0.366 for distal tubular cells and 0.097 for the glomerulus, respectively as shown in Table 4.2.

Figure 4.3: Double Staining with Polymyxin B Antibody and Lectins a Rat Kidney Cross-Section

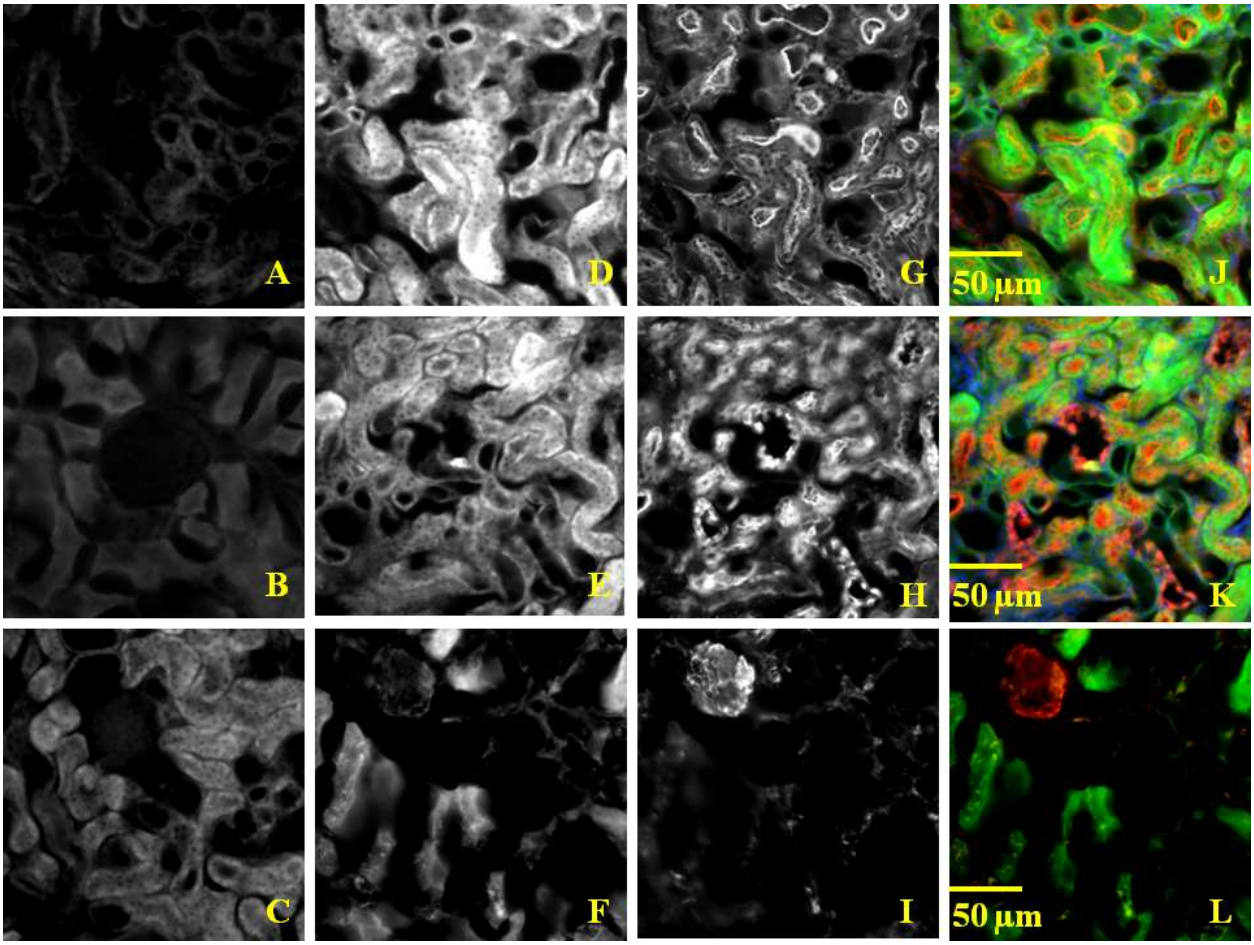

Panel A-C represent control section; D-F represents the staining with anti-polymyxin B antibody; G-I represent staining with lectin; J-L represents multichannel images of double staining with polymyxin B antibody and lectin.

Green color represents staining with anti-polymyxin B antibody and red color represents staining with specific lectin marker, respectively. The green-red co-localized signals produced a yellow signal in the overlay images

Table 4.2: Semi-Quantitative Analysis to Assess Degree of Co-Localization in Various Renal Cell Types

Renal cell type	Mander's overlap coefficient (R_{colo})	Degree of co-localization
Proximal convoluted tubules (PCT)	0.998	99.8 %
Distal convoluted tubules (DCT)	0.366	33.6 %
Glomerulus	0.097	9.7

CHAPTER 5

CORRELATION BETWEEN ONSET OF POLYMYXIN B NEPHROTOXICITY, RENAL DRUG EXPOSURE AND ROLE OF MEGALIN

5.1 Materials and Method

5.1.1 Antimicrobial Agent

Polymyxin B sulfate (USP) powder was purchased from APP Pharmaceuticals, LLC (lot number 6107834) (Schaumburg, IL, USA) and Sigma-Aldrich (St. Louis, MO, USA). Prior to each experiment, the drug was reconstituted and diluted to the desired concentrations with normal saline. The reconstituted drug solutions were stored at -80ºC until analysis.

5.1.2 Animals

Female Sprague-Dawley rats (225-250g) (Harlan, Indianapolis, IN, USA) were used. The rats received food and water *ad libitum*. All animals were cared for in accordance with the highest humane and ethical standards, as approved by Institutional Animal Care and Use Committee (IACUC) of the University of

Houston. Jugular veins of selected animals were cannulated to facilitate intravenous drug administration.

5.1.3 Chemicals and Reagents

Sodium maleate dibasic salt was obtained from Sigma-Aldrich. LC-MS grade acetonitrile and water were obtained from Mallinckrodt Baker (Philipsburg, NJ, USA); LC-MS grade formic acid was purchased from Fluka Analytical (St. Louis, MO, USA). The enzyme-linked immunosorbent assay (ELISA) kit for low-density lipoprotein receptor-related protein (Lrp2) / megalin was purchased from Cedarlane (Burlington, NC, USA).

5.1.4 Polymyxin B Assay

A validated liquid chromatography tandem mass spectrometry (UPLC/MS/MS) method was modified to determine the concentrations of polymyxin B in rat serum and renal tissues, as previously described (Manchandani, Zhou, et al., 2016). The LLOQ was 50 µg/ml for all the major components of polymyxin B in serum matrix as well as renal tissue homogenate.

5.1.5 Correlation between Onset of Nephrotoxicity and Renal Tissue Concentration of Polymyxin B

Prior to each experiment, polymyxin B for injection (USP) was reconstituted with sterile water for injection (USP) and diluted to achieve desired concentration. The reconstituted drug solution was stored at -80ºC in aliquots and thawed before dosing. Three groups of rats (n=13 each) were administered escalating dose levels of polymyxin B (5 mg/kg, 10 mg/kg and 20 mg/kg, respectively) once daily subcutaneously for up to 7 days. Blood samples (approximately 200 µl) were withdrawn via the tail vein at baseline and on a daily basis (pre-dosing when applicable). Blood was allowed to clot on the ice and serum was separated by centrifugation at 4,000× g for 10 minutes. Serum samples (100 µl) were further assayed for creatinine levels using a clinical chemistry analyzer (Piccolo Xpress, Abaxis, Inc., Union City, CA). A significant elevation in serum creatinine (≥ 2× baseline level) was set as the endpoint for nephrotoxicity. Kaplan-Meier survival analysis and log-rank (Mentel-Cox) test were used to compare the onset of nephrotoxicity among various groups. Right censoring was used if the nephrotoxicity endpoint was not observed by day 7.

To determine the renal tissue concentration of polymyxin B, three rats from each dosing group were randomly selected and sacrificed at 24 h after the

first dose; kidneys were harvested and homogenized. The major components of polymyxin B (polymyxin B1, polymyxin B2, polymyxin B3 and isoleucine polymyxin B1) were quantified in the renal tissue homogenate (as described above). The summed concentration of individual components was used to estimate the overall renal drug exposure (Manchandani, Dubrovskaya, Gao, & Tam, 2016). One-way ANOVA test followed by post hoc Tukey's test were used to compare the mean renal tissue concentrations among the dosing groups and *p*-values <0.05 were considered significant.

5.1.6 Effect of Maleate Administration on Urinary Excretion of Megalin

The rats (n=3) were housed individually in separate metabolic cages 24 h prior to maleate pre-treatment. A single dose of 400 mg/kg of sodium maleate was given intraperitoneally, and cumulative urine was collected daily from day -1 to 15. The urine samples were spun down to remove the particulate matter, and volumes were recorded. Subsequently, the urine samples were aliquoted and stored at -80 ºC prior to analysis. The samples were thawed, and urinary Lrp2 / megalin was quantitatively measured using a commercially available ELISA kit for megalin. For each animal, the daily megalin concentrations were expressed as a normalized ratio to its baseline value.

5.1.7 Electron Microscopy of Maleate-Treated Kidney Section

Two rats were administered a single dose of 400 mg/kg of sodium maleate intraperitoneally. One animal was sacrificed at 3 h; the other was sacrificed 14 days after maleate administration to collect the kidneys. The harvested kidneys were cut into thin traverse sections and processed for standard electron microscopy sample preparation. Briefly, tissue samples from both renal cortical and medullary regions were fixed in 2% glutaraldehyde at 4 ºC overnight, followed by additional fixation in osmium tetroxide. Tissue was dehydrated and embedded in epoxy resin. Approximately 1µm thick pilot sections were stained with toluidine for selecting the areas for further ultrastructural examination. Thin sections of these selected areas were cut and were subjected to examination under a Joel 300 electron microscope at 80 kV. The kidneys from two naïve rats were harvested, processed in a similar fashion and used as controls.

5.1.8 Polymyxin B Pharmacokinetics in Megalin-Shedding Rats

The rats were divided into two groups (n=13 each), to study the impact of sodium maleate pre-treatment on systemic/renal exposure of polymyxin B. Animals in both groups were administered a single intravenous dose of 3 mg/kg of polymyxin B sulfate (USP). In contrast, the animals in the treatment group were given 400 mg/kg of sodium maleate intraperitoneally 3-6 hours prior to

polymyxin B administration. Serum samples were obtained at 1.5, 3, 4.5, 6 and 7.5 h post polymyxin B dosing. In addition, the rats were sacrificed to harvest the kidneys at 3, 6 and 24 h (n=3 at each time point) post-dosing. Polymyxin B concentrations in serum and renal tissue samples were assayed by the validated UPLC-MS/MS method detailed above. The mean concentrations of polymyxin B in serum, as well as renal tissue samples at each time point, were used. A modified two-compartment model (Figure 5.5) was used to co-fit the serum / renal tissue concentration-time profiles using ADAPT 5. Using the best-fit parameters, the area under the curve from 0 to infinity was estimated by integrating the instantaneous concentrations over time. The $AUC_{(0-\infty)\ renal\ tissue}$/ $AUC_{(0-\infty)\ serum}$ ratio, was used as an index to quantitatively assess the preferential accumulation of polymyxin B in renal tissue.

To further examine if the effect of sodium maleate on the renal accumulation of polymyxin B is transient, three additional rats were given 400 mg/kg of sodium maleate intraperitoneally. After two weeks of pre-treatment, the animals were given with a single dose of 3 mg/kg of polymyxin B intravenously. The rats were sacrificed at 3 h post dosing; kidneys were harvested and homogenized. Polymyxin B concentrations in renal tissue samples were assayed by the validated UPLC-MS/MS method.

5.1.9 Absolute Quantification of Polymyxin B Components in Renal Tissues and Serum

To further assess whether any component of polymyxin B demonstrated greater affinity towards megalin transporter, we performed absolute quantification of each component of polymyxin B (PMB1, Ile-PMB1, PMB2, and PMB3) individually in serum as well as renal tissues. Fractions of each component were firstly compared between control and sodium maleate treatment group in renal tissues to ascertain if any one component was exhibited preferential renal uptake due to higher affinity towards megalin. Subsequently, unpaired two-tailed student's t-test was used to analyze the significant difference in the mean concentrations of the individual components between control and treatment group, both in the serum and renal tissues, respectively.

5.2 Results

5.2.1 Correlation between Onset of Nephrotoxicity and Renal Tissue Concentration of Polymyxin B

All the animals (10 out of 10) that received 20 mg/kg of polymyxin B reached the pre-defined endpoint. In contrast, none of the animals given 5 mg/kg of polymyxin B reached the endpoint by day 7. Furthermore, we observed a more gradual onset of nephrotoxicity in the 10 mg/kg group as compared to 20 mg/kg dosing group, as shown in Figure 5.1. More specifically, 80% (8 out of 10) of the animals that received 20 mg/kg reached the endpoint within first 48 h of treatment. On the contrary, only 10 % (1 out of 10) animals that received 10 mg/kg reached pre-defined endpoint within first 48 h of treatment ($p < 0.001$). These findings suggested that a higher daily dose of polymyxin B was associated with a more rapid onset of nephrotoxicity.

There was also a similar trend observed in the renal tissue concentration of polymyxin B among various dosing groups, as shown in Figure 5.2. The renal tissue concentrations of polymyxin B observed were 3.6 ± 0.4 μg/g, 9.9 ± 1.5 μg/g and 21.7 ± 4.8 μg/g of renal tissue in the 5 mg/kg, 10 mg/kg and 20 mg/kg dosing groups, respectively ($p = 0.0008$). These data implied that drug concentration observed in renal tissues was correlated to the daily dose given.

Figure 5.1: Comparison of Onset of Nephrotoxicity among Different Polymyxin B Dosing Groups

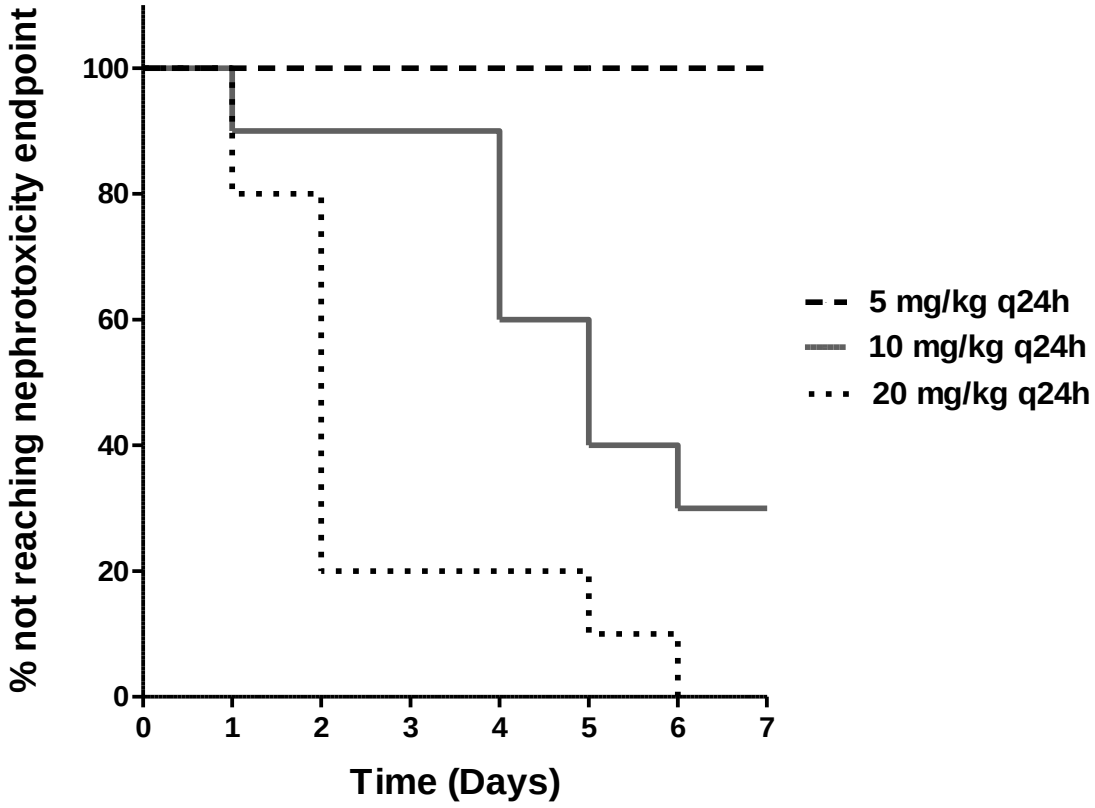

P < 0.001

Figure 5.2: Renal Tissue Concentration at Escalating Dose Levels of Polymyxin B

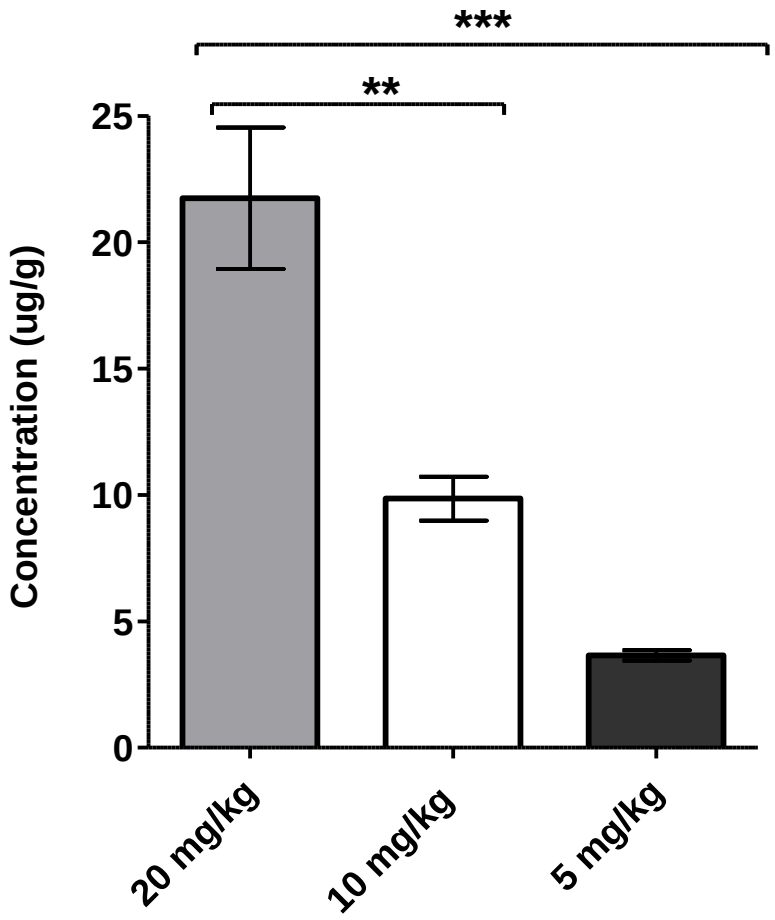

Vertical error bars represent the mean standard deviation within a group. The post hoc Tukey's test was used for multiple 2-way comparisons of mean among different groups (****P* < 0.001; ** *P* < 0.01).

5.2.2 Effect of Maleate Administration on Urinary Excretion of Megalin

There was a considerable elevation (approximately 20 times the baseline measurement) in the level of urinary megalin post maleate treatment. However, the urinary megalin levels reverted gradually to baseline approximately after 11 days of treatment as represented in Figure 5.3.

Figure 5.3: Mean Urinary Megalin Profile Post-Maleate Administration

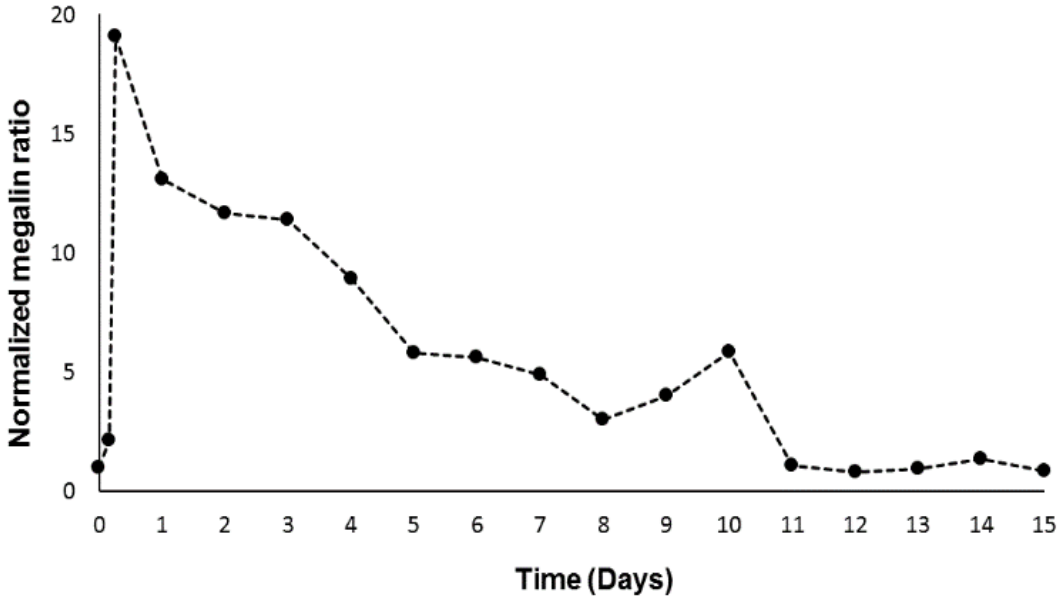

5.2.3 Electron Microscopy of Maleate-Treated Kidney Section

The electron microscopic images of control and maleate-treated kidneys depicted dramatic differences, as shown in Figure 5.4. No significant ultrastructural changes were noticed in the ultrathin sections of the control kidney. Specifically, the proximal tubules in control sections revealed intact microvilli, mitochondria of normal size, shape, and density, and the presence of few microvesicles and lysosomes (Figure 5.4 -A). Of note, there were also no noticeable changes seen in glomeruli, blood vessels or any other type of renal tubules. In contrast, within 3 h, maleate pre-treatment resulted in the appearance of morphological and ultrastructural changes in the proximal tubules which included multifocal disruption of microvilli, variation in the sizes and shapes of mitochondria. The presence of multiple dilated microvesicles and abundantly enlarged lysosomes were few other notable changes seen in the ultrathin sections of the maleate-treated kidney, as represented in Figure 5.4-B.

Two weeks after maleate administration, the electron microscopic images of ultrathin sections of maleate-treated kidney revealed no significant changes as compared to the control kidney sections (Figure 5.4-C). This suggested that the maleate-induced ultrastructural alterations in proximal renal tubules were not long-lasting.

Figure 5.4: Electron Microscopic Images of Control and Maleate-Treated Ultrathin Kidney Sections

A. Control – 3h **B. Treatment – 3h** **C. Treatment – 14 days**

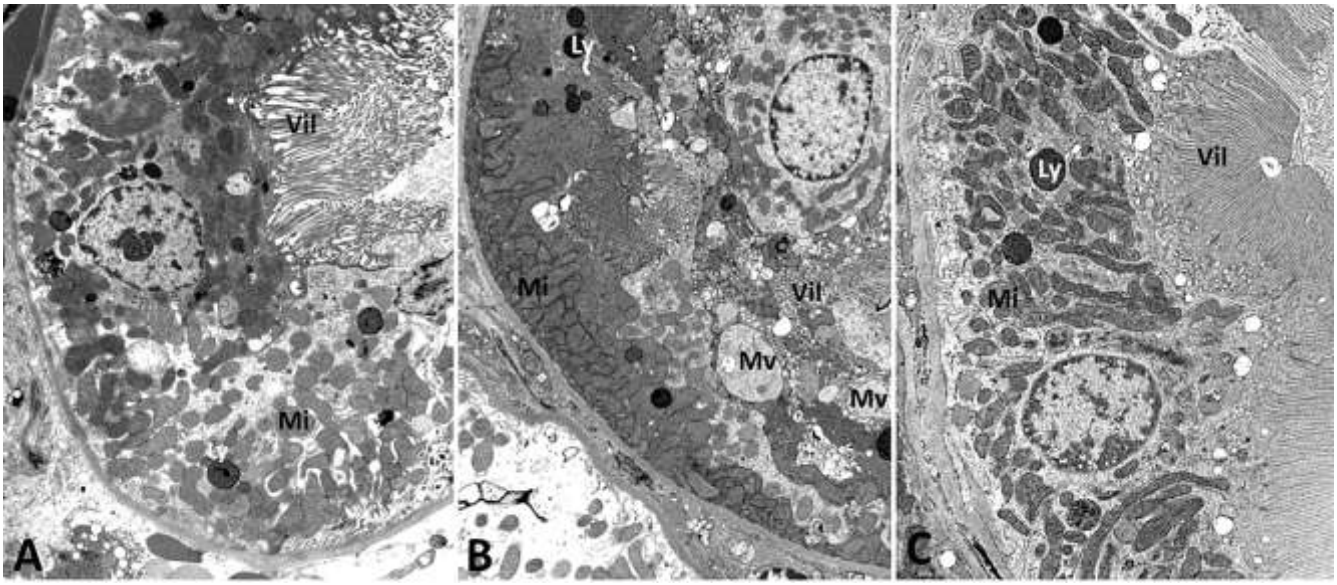

Panel A: No significant changes were noted in control kidney. Specifically, the proximal tubular cells displayed intact microvilli (Vil), mitochondria (Mi) of normal sizes, shapes, and density. A few microvesicles/ lysosomes (Ly) are noted. Panel B: Marked changes were noted in proximal tubular cells of the experimental animal, including degenerative changes of individual tubular cells (lower right), multifocal disruption or loss of microvilli (Vil), abundant mitochondria (Mi) of variable sizes and shapes, and multiple dilated microvesicles (Mv). There were no significant changes in glomeruli, blood vessels or other types of renal tubules. Panel C: Proximal tubular cells are displaying normal features including intact microvilli (Vil), normal mitochondria (Mi), and few lysosomes (Ly). [Original magnification x 10,000 for all panels]

5.2.4 *Polymyxin B Pharmacokinetics in Megalin-Shedding Rats*

We built a two-compartment (serum-renal tissue) pharmacokinetic model with slight modification as represented in Figure 5.5. In both groups (with or without maleate pre-treatment), the overall model fits to the data were satisfactory. The coefficients of determination for serum concentration-time profiles were > 0.94 and for renal concentration-time profiles were > 0.87. The $AUC_{(0-\infty)\ serum}$ in both groups were comparable; (11.1 $mg.h.L^{-1}$ versus 10.4 $mg.h.L^{-1}$, respectively). In contrast, the $AUC_{(0-\infty)\ renal\ tissue}$ were considerably different (211.9 $mg.h.L^{-1}$ and 121.0 $mg.h.L^{-1}$) in control and treatment group, respectively, as represented in Figure 5.6. The $AUC_{(0-\infty)\ renal\ tissue}$ / $AUC_{(0-\infty)\ serum}$ ratios were 19.1 in control and 11.6 in the treatment group, respectively. These findings suggested that in megalin-shedding rats, the systemic exposure of polymyxin B remained unaltered, but the renal exposure was reduced considerably after maleate administration.

After 2 weeks of treatment with maleate, our results showed that renal tissue polymyxin B concentrations in the sodium maleate pre-treated rats were comparable to those of the control rats (11.08 µg/g vs. 11.45 µg/g, $p = 0.61$). This finding suggested that the effect of sodium maleate on the renal accumulation of polymyxin B was also reversible in nature.

Figure 5.5: Structure of Serum-Renal Tissue Pharmacokinetic Co-Model

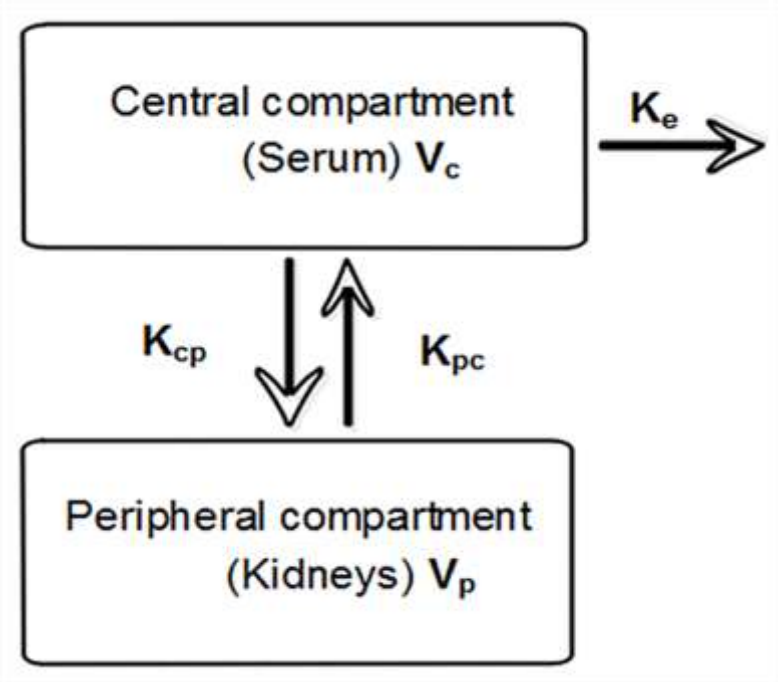

Differential equations:

$$dC_{serum} / dt = K_{pc} \times C_{renal\ tissue} / D - (K_{cp} + K_e) \times C_{serum} + R$$

$$dC_{renal\ tissue} / dt = K_{cp} \times C_{serum} - K_{pc} \times C_{renal\ tissue} / D$$

Where,

C_{serum} and $C_{renal\ tissue}$: Polymyxin B concentrations in serum and renal tissue;

K_{cp}: Inter-compartmental transfer rate constant from central to peripheral compartment;

$K_{pc:}$ Inter-compartmental transfer rate constant from peripheral to central compartment;

K_e: Elimination rate constant;

D: Polymyxin B distribution ratio between serum and renal tissue.

Figure 5.6: Mean Polymyxin B Concentrations in Serum and Renal Tissues

A. Serum

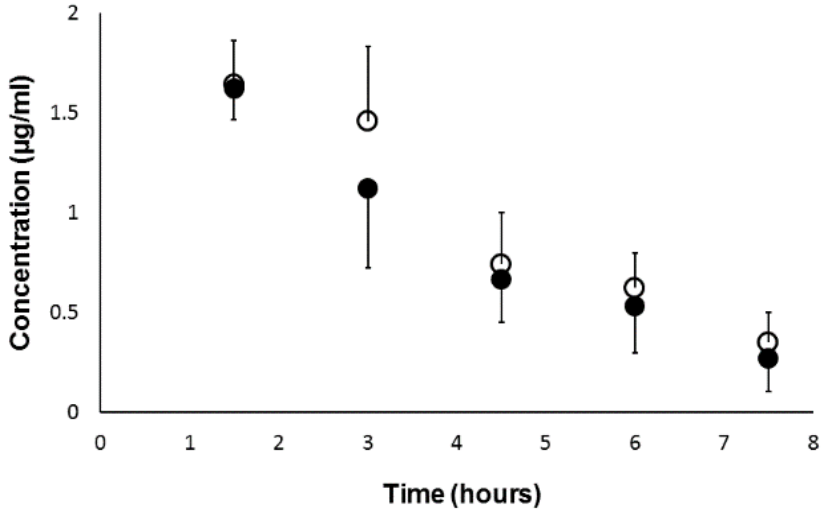

B. Renal tissues

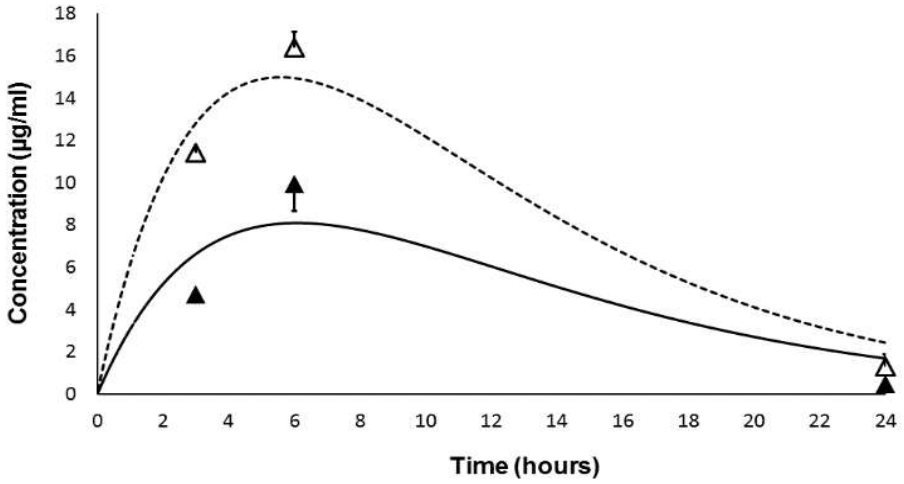

Solid and open circles indicate mean serum concentrations of polymyxin B in the treatment and control group, respectively; solid and open triangles indicate mean renal tissue concentrations of polymyxin B for in the treatment and control group, respectively. Dotted line is the best-fit line for the renal concentration-time profile in the control group whereas the solid line is the best-fit line for renal tissue concentration-time profile in the treatment group, respectively. Vertical error bars represent the standard deviation at each time point.

5.2.5 *Absolute Quantification of Polymyxin B Components in Renal Tissues and Serum*

The absolute quantification of individual components of polymyxin B in the renal tissues was represented in Table 5.1 (A & B). The results indicated that PMB1 was significantly different between control and treatment group at 3 h ($p=0.003$) and 24 h ($p=0.005$), respectively. However, the renal concentration of PMB2 and Ile-PB1 between two group was observed to be significant different only at 3 h ($p=0.045$) and 24 h ($p=0.006$), respectively. Our results revealed that the renal concentration between both the groups did not remain significantly different at all the time points (3, 6 and 24 h) throughout the study. Therefore, the overall consistent pattern suggesting the preferential uptake of any particular polymyxin B components was not observed in both the groups. This indicated that all the polymyxin B components possess fairly similar affinity towards megalin. We further compared the quantification of polymyxin B components obtained from renal tissue with those derived from serum samples as shown in Table 5.1 (B). The absolute quantification in serum samples demonstrated a similar trend, and the fractions of individual components were in reasonable agreement with those obtained from renal tissues. These results indicated that uptake process was not specific for any particular component of polymyxin B; individual components exhibited comparable affinity towards megalin transporter.

Table 5.1: Absolute Quantification of Polymyxin B Components in Renal Tissues, (A) Control and (B) Treatment Group

A. Control group

Time (h)	Mean serum concentration (μg/ml)				
	PMB1	Ile-PMB1	PMB2	PMB3	Total PMB
3	7.13	0.62	2.02	1.62	11.39
6	8.76	1.13	4.25	2.25	16.39
24	0.89	ND	0.23	0.18	1.30

B. Sodium maleate treatment group

Time (h)	Mean serum concentration (μg/ml)				
	PMB1	Ile-PMB1	PMB2	PMB3	Total PMB
3	2.16	0.35	1.24	0.96	4.70
6	4.95	1.01	2.66	1.30	9.92
24	0.26	ND	0.12	0.09	0.47

Table 5.2: Absolute Quantification of Polymyxin B Components in Serum, (A) Control and (B) Treatment Group

A. Control group

Time (h)	Mean serum concentration (μg/ml)				
	PMB1	Ile-PMB1	PMB2	PMB3	Total PMB
1.5	1.03	0.15	0.36	0.11	1.64
3.0	0.96	0.14	0.27	0.09	1.42
4.5	0.47	0.06	0.16	0.05	0.74
6.0	0.40	0.05	0.15	0.03	0.62
7.5	0.24	0.02	0.07	0.02	0.32

B. Sodium maleate treatment group

Time (h)	Mean serum concentration (μg/ml)				
	PMB1	Ile-PMB1	PMB2	PMB3	Total PMB
1.5	1.05	0.15	0.30	0.12	1.62
3.0	0.65	0.12	0.27	0.08	1.12
4.5	0.41	0.06	0.15	0.05	0.66
6.0	0.32	0.05	0.11	0.05	0.53
7.5	0.18	0.02	0.06	0.01	0.27

5.2.6 Proposed mechanism of Megalin-Mediated Polymyxin B Endocytosis

Based on these results we hypothesized that megalin, a renal endocytic receptor plays a pivotal role in the renal uptake of polymyxin B through microvesicle recycling apparatus. Figure 5.7 demonstrate the diagrammatic proposed mechanism of megalin-mediated cellular endocytosis in the proximal renal tubules. Sodium maleate inhibits the formation of recycling apparatus which is required for the endocytosis of polymyxin B. Consequently, this leads to the inhibition of polymyxin B uptake in the proximal renal tubules.

Figure 5.7: Diagrammatic Representation of Proposed Mechanism of Megalin-Mediated Endocytosis of Polymyxin B in Renal Proximal Tubules

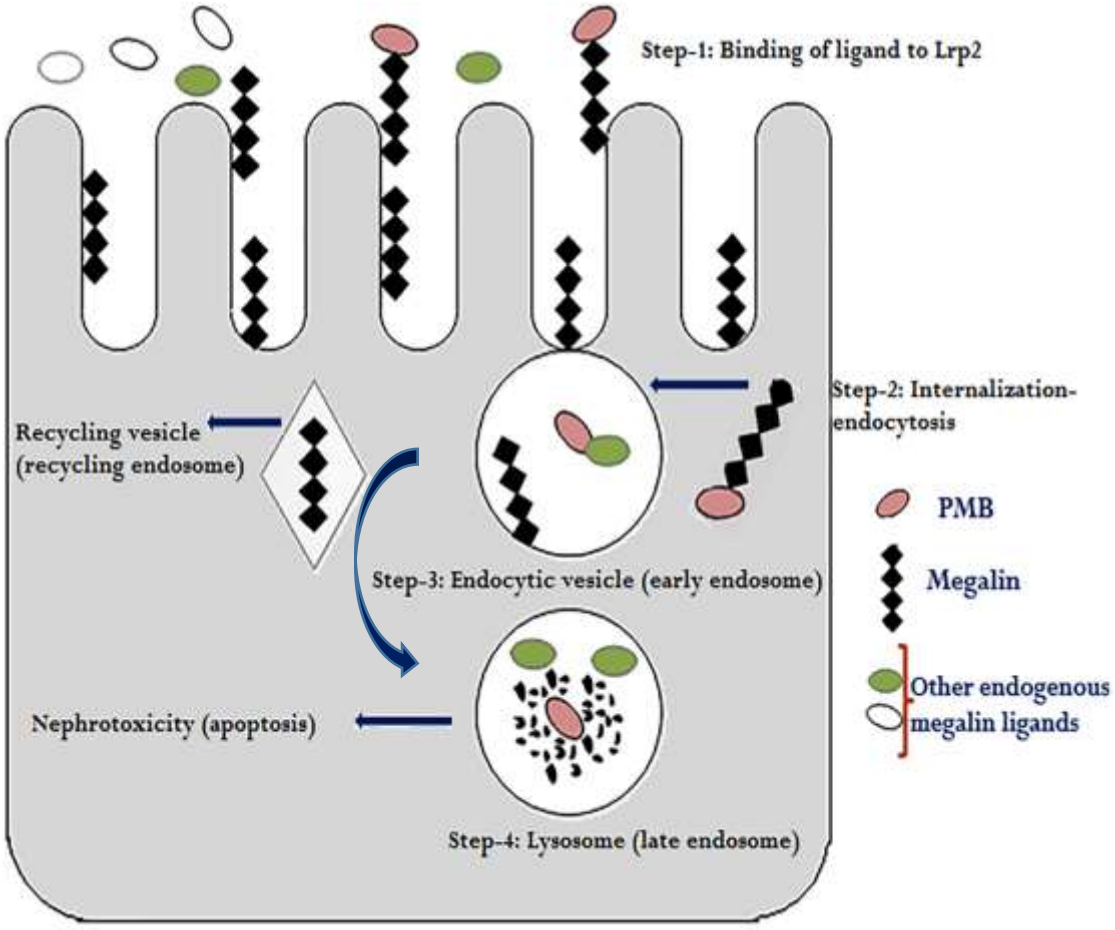

REFERENCES

Manchandani, P., Dubrovskaya, Y., Gao, S., & Tam, V. H. (2016). Comparative pharmacokinetic profiling of different polymyxin b components. *Antimicrob Agents Chemother*. doi:10.1128/AAC.00702-16

Manchandani, P., Zhou, J., Ledesma, K. R., Truong, L. D., Chow, D. S., Eriksen, J. L., & Tam, V. H. (2016). Characterization of polymyxin b biodistribution and disposition in an animal model. *Antimicrob Agents Chemother, 60*(2), 1029-1034. doi:10.1128/AAC.02445-15

CHAPTER 6

DISCUSSION

We are currently facing a shortage of viable treatment options against nosocomial/hospital-acquired infections caused by multidrug-resistant Gram-negative pathogens. Due to prevailing multidrug-resistance among Gram-negative bacteria, the persistent reliance on polymyxin B as a last viable treatment option is expected to accelerate worldwide. The clinical utility of polymyxin B is hindered mainly by its dose-limiting nephrotoxicity, which could be attributed to poor understanding of its pharmacokinetics, toxicodynamic profile, and underlying mechanisms of nephrotoxicity. Nonetheless, over the past decade, few noteworthy attempts have been made to characterize the pharmacokinetics, pharmacodynamic and nephrotoxicity of polymyxin B (Kwa et al., 2008; Tam, Cao, Ledesma, & Hu, 2011; Zavascki et al., 2008). Despite being available as a mixture of closely related analogs, the pharmacokinetic, pharmacodynamic and toxicological properties of polymyxin B are commonly reported as an aggregate of the individual components (Abdelraouf, He, Ledesma, Hu, & Tam, 2012; Sandri et al., 2013). Most pharmacokinetic studies reported so far have used total polymyxin B concentrations (sum of the chromatographic peak area of individual components) for drug quantification in

biological matrices. In these reports, the pharmacokinetic properties of individual aggregates were presumed to be the same as those of total polymyxin B, an assumption that is yet to be validated. Therefore, it remains critical to investigate whether individual components of polymyxin B exhibit similar pharmacokinetic characteristics (Tam, Hou, Kwa, & Prince, 2009).

In our investigation, we compared the pharmacokinetic profiles of the major components of polymyxin B in a rat model. We observed that the weighted average pharmacokinetic parameters (clearance and volume of distribution) derived using serum concentration for individual components were in reasonably close agreement (within two-fold range) with those derived directly from the total polymyxin B concentration. Furthermore, to compare systemic exposure in rats, area under the curve from 0 h to infinity $AUC_{(0-\infty)}$ observed from total polymyxin B was 10.7 mg. h. L^{-1} which was akin to that derived from adding the $AUC_{(0-\infty)}$ of individual polymyxin B components in the mixture which was 10.9 $mg.h.L^{-1}$ (Manchandani, Dubrovskaya, et al., 2016). Collectively, these findings suggest that the pharmacokinetics of various individual polymyxin B components were comparable. Furthermore, it appeared reasonable to use the summed concentrations of individual components (i.e. total polymyxin B concentrations) in pharmacokinetic studies to estimate overall drug exposure. Therefore; we used

summed concentration of polymyxin B components in our subsequent biodistribution and disposition studies.

To date, several attempts have been made to characterize the biodistribution and disposition profile of polymyxin B. Kunin et al*.* examined the biodistribution of polymyxin B in rabbits and observed that the distribution was non-uniform with higher accumulation in kidneys, liver, and muscles (Kunin & Bugg, 1971a, 1971b). Jacobson et al. investigated the distribution and binding of tritiated polymyxin B in a mouse model and observed higher accumulation in the kidneys (Jacobson et al., 1972). Our group also reported that polymyxin B was preferentially accumulated in rat kidneys with a prolonged residence time (Abdelraouf, He, et al., 2012).

In the present investigation, we provided additional insights into the overall biodistribution characteristics of polymyxin B. Despite using different animal species, methods for sample preparation and analysis, our biodistribution results were concordant with previously reported biodistribution results by Kunin et al. This suggested that polymyxin B distribution to different organs is not homogenous and the drug is preferentially accumulated in the kidneys. However, in contrast to previous studies by Kunin et al. (Kunin & Bugg, 1971a, 1971b), we

observed consistently low drug concentrations in the brain. The earlier studies by Kunin et al. used a non-specific microbiological assay to quantify the polymyxin B in various tissue homogenate rather than a sensitive, specific UPLC-MS/MS assay. Moreover, in these previous studies, a liquid-liquid extraction method was used for sample preparation; the drug was estimated separately in the organic and aqueous extraction layers in the bound and free form, respectively (Kunin & Bugg, 1971b). This procedure may have over-estimated the drug concentration as the final drug recovered from serum and tissue homogenate was found to be greater than the dose administered. Our brain tissue biodistribution results were in accordance with a recent review of clinical findings (Falagas, Bliziotis, & Tam, 2007). Interestingly, we observed a higher concentration of polymyxin B in lung tissues as compared to serum at 6 h (but not at 3 h). This finding is in contrast to our previously reported low polymyxin B levels in the epithelial lining fluid (ELF) in mice (He, Gao, Hu, Chow, & Tam, 2013). Since lungs consist of several sub-compartments (lung parenchyma, alveolar epithelium, macrophages, ELF and blood-alveolar barrier, etc.), assaying drug concentrations in the whole organ could be subjected to a high degree of variability. In summary, the present investigation provided valuable insights to the overall *in vivo* distribution properties of polymyxin B. We concluded that among all the organs evaluated; polymyxin B was highly accumulated in the kidneys, which may contribute to its nephrotoxic potentials.

We further aimed at elucidating the intrarenal distribution pattern of polymyxin B. We have previously shown histological evidence that the polymyxin B-induced injury was mainly confined to the proximal tubular cells of the rat kidneys (Abdelraouf, Braggs, et al., 2012). In a mouse model, polymyxin B was found to be substantially accumulated in the renal proximal tubular cells (Yun, Azad, Wang, et al., 2015). Yun et al. also provided circumstantial evidence linking polymyxin B distribution to the site of renal injury.

In the present investigation, the sites of polymyxin B accumulation within the kidneys were identified at the cellular level using the same rat model. We evaluated drug accumulation in the multiple renal cell types (proximal convoluted tubules, distal convoluted tubules, and glomerulus) in a semi-quantitative fashion, establishing a more concrete association between site of drug accumulation and the site of renal injury. Among the different renal cell types evaluated, proximal tubular cells demonstrated the highest accumulation of polymyxin B. Collectively; these findings suggest that polymyxin B accumulation within the kidneys is heterogeneous, and is primarily confined to the proximal tubular cells. In conjunction with previous findings, it is likely that there is a direct link between the site of drug accumulation and injury at the cellular level within the kidneys.

These findings are expected to guide future investigations focusing on identifying/ elucidating the cellular apoptotic pathways as well as toxic mechanisms linked with polymyxin B-induced nephrotoxicity.

To delineate polymyxin B disposition characteristics in-depth, we explored various routes of elimination of polymyxin B. In contrast to an earlier study which reported that approximately 60% of the polymyxin B dose was recovered (Hoeprich, 1970), polymyxin B recovery from urine was reported to be very low in several recent studies. Abdelraouf et al. reported that less than 1% of polymyxin B was recovered in an unchanged form in the urine over 48 h after single intravenous dose (Abdelraouf, Braggs, et al., 2012; Abdelraouf, He, et al., 2012). Based on the urinary excretion data of polymyxin B available from 17 critically ill patients, Sandri et al. also reported the median urinary recovery to be 4.0% (range 1.0% - 17.4%) of the administered dose (Sandri et al., 2013). In line with previous findings, Zavascki et al. reported that less than 1% of the dose was recovered unchanged in urine samples following intravenous administration of polymyxin B in critically ill patients (Zavascki et al., 2008).

In the present investigation, we observed that urine recovery of polymyxin B was substantially low. Our results from validated UPLC-MS/MS assay of the

urine samples after a single dose administration of polymyxin B indicated that less than 1% of the administered dose was recovered over 48 h in its parent form. Although these results corroborated previous findings on a low recovery of the drug in urine, the urinary disposition of any active metabolite remained unknown. We further confirmed that less than 5% of the administered dose (or pharmacologically active metabolites, if any) was recovered from urine over 48 h using a validated microbiological assay method. In addition to demonstrating a low urine recovery of polymyxin B, the use of a microbiological assay in this study provided additional evidence that renal excretion of the active metabolite(s) are unlikely. A recent report by Nilsson et al. demonstrated the formation of amide hydrolytic adducts of polymyxin B in the renal tissue using high-resolution mass spectrometry imaging (Nilsson et al., 2015). This suggests that proteolytic degradation could be one of the potential pathways of *in vivo* biotransformation of polymyxin B. This could be one of the underlying factor for low urine recovery of polymyxin B in its parent form. However, further investigations are warranted to substantiate this finding.

Over the past decades, several noteworthy attempts have been made to advance our understanding of the nephrotoxicity associated with renal accumulation of polymyxins. A recent study by Azad et al. investigated the underlying mechanism of polymyxin B nephrotoxicity in the rat (NRK-52E) as well

as human (HK-2) kidney proximal tubular cell lines. Cellular apoptosis was identified to be a potential mechanism of polymyxin B-induced nephrotoxicity. It was reported that apoptosis was triggered via activation of the caspase pathway in a time and concentration-dependent fashion. The onset of polymyxin B-nephrotoxicity was observed to be highly correlated to the renal drug concentration (Azad et al., 2013).

In the present investigation, we observed that polymyxin B dose was correlated to the renal drug concentration, which was further correlated to the onset of nephrotoxicity. The higher daily dose of polymyxin B was associated with a greater degree of drug accumulation in the renal tissues and subsequently manifested as a more rapid onset of nephrotoxicity. These findings were consistent with the previous results from our laboratory demonstrating the preferential renal accumulation and prolonged residence of polymyxin B in an animal model, and thereby predisposing the kidneys to the toxic effect of polymyxin B (Abdelraouf, Braggs, et al., 2012; Abdelraouf, He, et al., 2012; Manchandani, Zhou, et al., 2016).

The preferential intrarenal accumulation of polymyxin B could be one of the key factors attributed to its nephrotoxicity. Therefore, delineating the mechanism

of intrarenal drug uptake is fundamental to bridging the knowledge gap in current understanding of polymyxin B nephrotoxicity. Recently, few significant published literature investigating the involvement of transporters in renal uptake of polymyxin B have been reported. Suzuki et al. reported a significant decrease in the renal concentration of colistin in megalin-shedding rats which suggested the involvement of megalin in the renal drug accumulation (Suzuki et al., 2013). Although, the renal accumulation of polymyxin B was markedly reduced (nearly one-third as compared to control rats) in megalin-shedding rats but could not be completely abolished. This insinuated that transporters other than megalin could be involved in renal uptake of polymyxin B. Lu et al. also demonstrated the role of oligopeptide transporter-2 (PEPT-2) in the renal uptake of polymyxins in human embryonic kidney cell line (HEK-293). Furthermore, both polymyxin B and colistin were used as competitive inhibitors to block the renal uptake of radiolabeled glycine-sarcosine, a potential substrate of PEPT-2 transporter overexpressed in HEK-293 cell line (Lu et al., 2016).

The other promising feature of the our study involves delineating the possible role of an endocytic receptor [megalin or low-density lipoprotein-2 (Lrp2)] in the renal accumulation of polymyxin B. Maleate was reported to disrupt the membrane association of megalin with the brush border epithelium in the

renal proximal tubular cells, which was earlier shown to induce shedding of megalin in rats (Suzuki et al., 2013). Additionally, we verified megalin-shedding by the quantitative recovery of megalin in urine and imaging of maleate-treated kidney sections. Electron microscopic examination of kidney sections revealed marked ultrastructural changes in the proximal tubules post maleate treatment. These results were consistent with those reported by Bergeron et al. (Bergeron, Mayers, & Brown, 1996). Maleate is also known to induce apical membrane-associated transport defects in the renal proximal epithelial cells similar to those observed in Fanconi syndrome. Maleate-induced ultrastructural changes transiently disrupt the apical endocytic and recycling apparatus leading to accumulation of microvesicles in the proximal tubules (Norden et al., 2002). Therefore, the abundance of apical microvesicles in our microscopic images suggests that maleate might be involved in the inhibition of membrane recycling process, thereby inducing generalized transport defects similar to those observed in Fanconi syndrome. This finding corroborated the conclusions of Christensen et al., who previously demonstrated that maleate induces inhibition of lysozyme transport from the endocytic vacuoles to the lysosomes (Christensen, Gliemann, & Moestrup, 1992). Collectively based on these findings, we hypothesize that megalin is involved in the internalization of polybasic drugs (such as polymyxin B) by playing a crucial role in drug transport through endocytic recycling apparatus.

Finally, we investigated the systemic/renal exposure of polymyxin B in megalin-shedding rats. Thematically, the tissue expression of megalin primarily corresponds to the renal proximal tubular epithelium in rats; we presumed that only renal exposure of polymyxin B would be affected and systemic exposure will remain unchanged upon induction of megalin-shedding in rats. Remarkably, our results indicated that polymyxin B concentration in renal tissue was attenuated by approximately 40% after maleate pre-treatment. However, the systemic drug exposure remained mostly unaltered in the megalin-shedding rats. This could primarily be attributed to the diminished availability of membrane-bound (i.e., functional) megalin in kidneys after pre-treatment with maleate. These findings suggested that preferential renal accumulation of polymyxin B could be reduced by disrupting relevant mechanism(s) of drug uptake, leading to possible delay in the onset of nephrotoxicity. We further performed the absolute quantification of individual components of polymyxin B in renal tissues for both control as well as maleate-treated rats. Our results indicated that the various polymyxin B components (PMB1, Ile-PMB1, PMB2, and PMB3) demonstrated comparable affinity towards renal megalin transporter. However, these results are further needed to be evaluated.

6.1 Potential Limitations of Present Research

There are several limitations to our investigation. The biodistribution and disposition properties of polymyxin B were investigated only after a single dose, further investigations to assess the steady-state pharmacokinetics, of polymyxin B after multiple doses are warranted.

With regards to intrarenal accumulation of polymyxin B, we successfully located the site of drug accumulation at the cellular level. However, for better resolution, future studies aimed at identifying the drug accumulation at subcellular/ organelle level are highly warranted. From the toxicity perspective, we could not delineate the polymyxin B-induced toxicity pathway that triggers cellular apoptosis in renal cells. In our future investigations, we need to evaluate the mechanisms of programmed cell death events in various cellular organelles induced as a result of prolonged residence of polymyxin B within renal cells.

Our investigation established a correlation between daily dose, renal drug exposure and the onset of polymyxin B-induced nephrotoxicity. We demonstrated that the higher daily dose of polymyxin B was associated with the greater drug accumulation in the renal tissues which further manifested as a more rapid onset of nephrotoxicity. Based on our results we projected that the same total daily

dose of polymyxin B, when administered on multiple days, would expedite the onset of drug-induced nephrotoxicity. We also observed that this preferential renal accumulation of polymyxin B could be attenuated by disrupting the megalin, a renal endocytic uptake transporter. Despite this evidence, we could not directly demonstrate the delay in onset of nephrotoxicity in megalin-shedding rats. This limitation was mainly attributed to the interference of megalin in the assessment of elevation in serum creatinine level which was an endpoint for nephrotoxicity onset. Owing to this limitation, the renal drug concentration was used as a surrogate marker for nephrotoxicity endpoint detection.

Furthermore, our preliminary results from the megalin-shedding rats established circumstantial evidence that megalin could be involved in the renal accumulation of polymyxin B. However, this conclusion was derived from an indirect and non-specific approach of disrupting the membrane-bound megalin using a chemical agent (sodium maleate). Therefore, there is a need to validate these findings using more direct methods. For future studies, we plan to use the specific molecular tools (such as siRNA-mediated gene silencing), use of the megalin knockout animal model to further corroborate the role of megalin in the renal accumulation of polymyxin B.

REFERENCES

Abdelraouf, K., Braggs, K. H., Yin, T., Truong, L. D., Hu, M., & Tam, V. H. (2012). Characterization of polymyxin b-induced nephrotoxicity: Implications for dosing regimen design. *Antimicrob Agents Chemother, 56*(9), 4625-4629. doi:10.1128/AAC.00280-12

Abdelraouf, K., He, J., Ledesma, K. R., Hu, M., & Tam, V. H. (2012). Pharmacokinetics and renal disposition of polymyxin b in an animal model. *Antimicrob Agents Chemother, 56*(11), 5724-5727. doi:10.1128/AAC.01333-12

Azad, M. A., Finnin, B. A., Poudyal, A., Davis, K., Li, J., Hill, P. A., Li, J. (2013). Polymyxin b induces apoptosis in kidney proximal tubular cells. *Antimicrob Agents Chemother*. doi:10.1128/AAC.02587-12

Bergeron, M., Mayers, P., & Brown, D. (1996). Specific effect of maleate on an apical membrane glycoprotein (gp330) in proximal tubule of rat kidneys. *Am J Physiol, 271*(4 Pt 2), F908-916.

Christensen, E. I., Gliemann, J., & Moestrup, S. K. (1992). Renal tubule gp330 is a calcium binding receptor for endocytic uptake of protein. *J Histochem Cytochem, 40*(10), 1481-1490.

Falagas, M. E., Bliziotis, I. A., & Tam, V. H. (2007). Intraventricular or intrathecal use of polymyxins in patients with gram-negative meningitis: A systematic review of the available evidence. Int J Antimicrob Agents, 29(1), 9-25. doi:S0924-8579(06)00381-5 [pii] 10.1016/j.ijantimicag.2006.08.024

He, J., Gao, S., Hu, M., Chow, D. S., & Tam, V. H. (2013). A validated ultra-performance liquid chromatography-tandem mass spectrometry method for the quantification of polymyxin b in mouse serum and epithelial lining fluid: Application to pharmacokinetic studies. J Antimicrob Chemother, 68(5), 1104-1110. doi:10.1093/jac/dks536dks536 [pii]

Hoeprich, P. D. (1970). The polymyxins. Med Clin North Am, 54(5), 1257-1265.

Kunin, C. M., & Bugg, A. (1971a). Binding of polymyxin antibiotics to tissues: The major determinant of distribution and persistence in the body. *J Infect Dis, 124*(4), 394-400.

Kunin, C. M., & Bugg, A. (1971b). Recovery of tissue bound polymyxin b and colistimethate. *Proc Soc Exp Biol Med, 137*(3), 786-790.

Kwa, A. L., Lim, T. P., Low, J. G., Hou, J., Kurup, A., Prince, R. A., & Tam, V. H. (2008). Pharmacokinetics of polymyxin b1 in patients with multidrug-resistant gram-negative bacterial infections. Diagn Microbiol Infect Dis, 60(2), 163-167. doi:10.1016/j.diagmicrobio.2007.08.008

Lu, X., Chan, T., Xu, C., Zhu, L., Zhou, Q. T., Roberts, K. D., Zhou, F. (2016). Human oligopeptide transporter 2 (pept2) mediates cellular uptake of polymyxins. *J Antimicrob Chemother, 71*(2), 403-412. doi:10.1093/jac/dkv340

Manchandani, P., Dubrovskaya, Y., Gao, S., & Tam, V. H. (2016). Comparative pharmacokinetic profiling of different polymyxin b components. *Antimicrob Agents Chemother*. doi:10.1128/AAC.00702-16

Manchandani, P., Zhou, J., Ledesma, K. R., Truong, L. D., Chow, D. S., Eriksen, J. L., & Tam, V. H. (2016). Characterization of polymyxin b biodistribution and disposition in an animal model. *Antimicrob Agents Chemother, 60*(2), 1029-1034. doi:10.1128/AAC.02445-15

Nilsson, A., Goodwin, R. J., Swales, J. G., Gallagher, R., Shankaran, H., Sathe, A., . . . Gupta, A. (2015). Investigating nephrotoxicity of polymyxin derivatives by mapping renal distribution using mass spectrometry imaging. *Chem Res Toxicol, 28*(9), 1823-1830. doi:10.1021/acs.chemrestox.5b00262

Norden, A. G., Lapsley, M., Igarashi, T., Kelleher, C. L., Lee, P. J., Matsuyama, T., . . . Moestrup, S. K. (2002). Urinary megalin deficiency implicates abnormal tubular endocytic function in fanconi syndrome. *J Am Soc Nephrol, 13*(1), 125-133.

Sandri, A. M., Landersdorfer, C. B., Jacob, J., Boniatti, M. M., Dalarosa, M. G., Falci, D. R., . . . Zavascki, A. P. (2013). Population pharmacokinetics of intravenous polymyxin b in critically ill patients: Implications for selection of dosage regimens. Clin Infect Dis, 57(4), 524-531. doi:10.1093/cid/cit334

Suzuki, T., Yamaguchi, H., Ogura, J., Kobayashi, M., Yamada, T., & Iseki, K. (2013). Megalin contributes to kidney accumulation and nephrotoxicity of colistin. *Antimicrob Agents Chemother, 57*(12), 6319-6324. doi:10.1128/AAC.00254-13

Tam, V. H., Cao, H., Ledesma, K. R., & Hu, M. (2011). In vitro potency of various polymyxin b components. Antimicrob Agents Chemother, 55(9), 4490-4491. doi:10.1128/AAC.00119-11

Tam, V. H., Hou, J., Kwa, A. L., & Prince, R. A. (2009). Comment on: Development and validation of a reversed-phase high-performance liquid chromatography assay for polymyxin b in human plasma. J Antimicrob Chemother, 63(3), 627-628; author reply 628-629. doi:10.1093/jac/dkn483

Tam, V. H., Schilling, A. N., Vo, G., Kabbara, S., Kwa, A. L., Wiederhold, N. P., & Lewis, R. E. (2005). Pharmacodynamics of polymyxin b against pseudomonas aeruginosa. Antimicrob Agents Chemother, 49(9), 3624-3630. doi:10.1128/AAC.49.9.3624-3630.2005

Yun, B., Azad, M. A., Wang, J., Nation, R. L., Thompson, P. E., Roberts, K. D., Li, J. (2015). Imaging the distribution of polymyxins in the kidney. *J Antimicrob Chemother, 70*(3), 827-829. doi:10.1093/jac/dku441

Zavascki, A. P., Goldani, L. Z., Cao, G., Superti, S. V., Lutz, L., Barth, A. L., Li, J. (2008). Pharmacokinetics of intravenous polymyxin b in critically ill patients. Clin Infect Dis, 47(10), 1298-1304. doi:10.1086/592577

CHAPTER 7

FUTURE DIRECTIONS

In summary, our results indicate that various individual components of polymyxin B exhibit comparable pharmacokinetic profiles. We have successfully established an overall biodistribution profile of polymyxin B *in vivo* using a rat model; polymyxin B demonstrated preferential accumulation and prolonged resistance in renal tissues. Furthermore, our results indicated that among various renal cell types (proximal tubules, distal tubules and glomerulus), proximal tubules are the primary anatomical sites with highest accumulation of polymyxin B. Concerning drug disposition, our urinary recovery data indicated that less than 1% of the administered dose was eliminated in the parent form. Furthermore, only less than 5% of the administered dose was eliminated in the pharmacologically active form (including metabolites, if any) through the urinary route.

Despite our efforts, we lack information about the comprehensive metabolic and biliary disposition profile of polymyxin B. We further aim to provide

insights into the mechanisms of cell uptake as well as cell toxicity. We intend to investigate the in-depth metabolic pathways of polymyxin B using *in vitro* as well as *in vivo* models. With regards to the drug disposition studies, we plan to assess the biliary disposition of polymyxin B after single as well as multiple dosing for longer duration in rats. Our research has successfully delineated that proximal convoluted tubules are the anatomical site of highest intrarenal drug accumulation and locus of polymyxin B-induced renal injuries. In the view of polymyxin B mechanistic studies pertaining to the investigation of intrarenal uptake and cellular toxicity, we propose to conduct series of uptake experiments and cytotoxicity assays using immortalized human proximal tubular (HK-2) cell line.

7.1 ***Aim 1*: To investigate *in vitro* and *in vivo* metabolism of polymyxin B**

7.1.1 Working Hypothesis

Our biodistribution and disposition study could not account for the majority of the administered dose *in vivo*. Moreover, the polymyxin B recovery was very low in urine (as a pharmacologically active form) and in bile (as parent form). Based on these findings, we hypothesize that polymyxin B might undergo hepatic drug metabolism.

7.1.2 Justification and Feasibility

7.1.2.1 Review of Relevant Literature

Nilsson *et al*., demonstrated the simultaneous distribution of polymyxin B and its metabolites in the rat kidney cross-section using mass spectrometry imaging and liquid extraction surface analysis (LESA). The study reported the biotransformation of polymyxin B into smaller peptide fragments formed as a by-product of amide hydrolysis. Moreover, biotransformation into demethylated and oxidative metabolites of parent polymyxin B was also reported (Nilsson et al., 2015). Since oxidation and demethylation are cytochromes P-450 mediated biotransformations, we performed an *in vitro* polymyxin B metabolism study using primary mouse hepatocytes. Midazolam was used as a control for the

experiment. We observed approximately 80% reduction in the parent drug concentration over 24 h of incubation with primary hepatocytes.

7.1.2.2 Preliminary Results

Our preliminary results obtained from LC-MS/MS analysis of rat urine after polymyxin B dosing using Qtrap 5500 UPLC-MS/MS (enabled with lightsight® and IDA wizard feature) system. Our results demonstrated the presence of oxidative, demethylated and glucuronide metabolites of polymyxin B. These results suggested the oxidation (at three different sites to form tri-oxidative metabolite); decarboxylation; demethylation and glucuronidation could be the most probable *in vivo* polymyxin B biotransformation pathways.

The preliminary results from an *in-vitro* metabolism study with primary mouse hepatocytes revealed that there was approximately 80% reduction in the intracellular concentration of parent polymyxin B2 as shown in Figure 7.1. The results of polymyxin B concentration estimated at regular time intervals after incubating with primary hepatocytes are summarized in Table 7.1. This insinuated the possibility of cytpchrome-450 mediated drug metabolism of polymyxin B.

Table 7.1: Intracellular Concentration of Polymyxin B in the Primary Hepatocyte Cells Culture

Incubation time (h)	Intracellular concentration (µg/ml)	
	Polymyxin B2	**Midazolam**
1	0.045	6.622
4	0.021	3.964
8	0.004	3.941
24	0.008	0.666

Figure 7.1: *In-vitro* Metabolism of Polymyxin B2 using Primary Hepatocyte Cell Culture

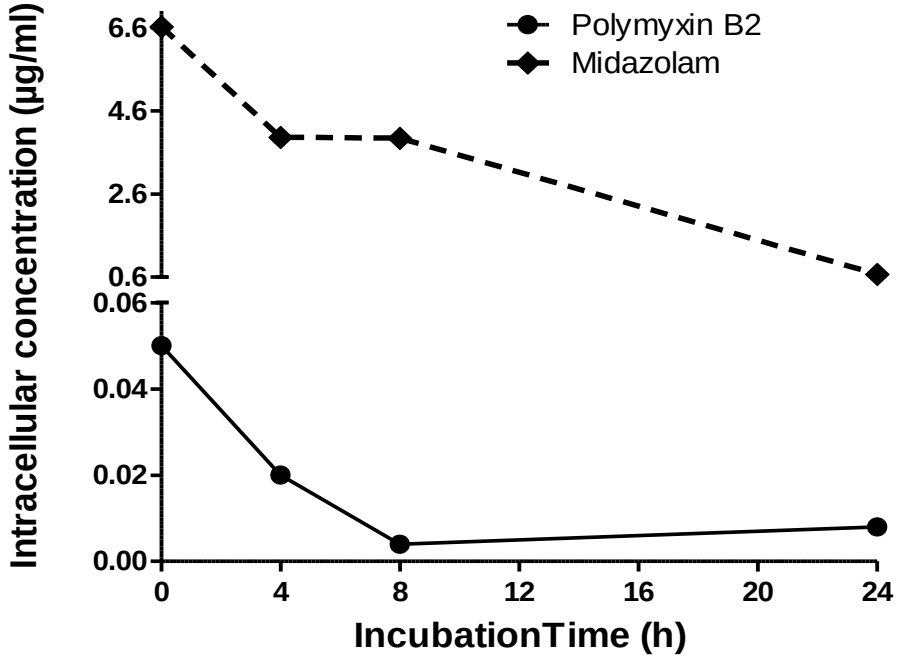

Figure 7.2: Metabolic Profiling of Polymyxin B in Rat Urine using IDA Wizard and Lightsight® Feature of Qtrap UPLC-MS/MS

A. Parent Polymyxin B Peak in Blank Rat Urine

B. Peak Representing Loss of Glucuronide and Decarboxylation in Rat Urine Dosed with Polymyxin B

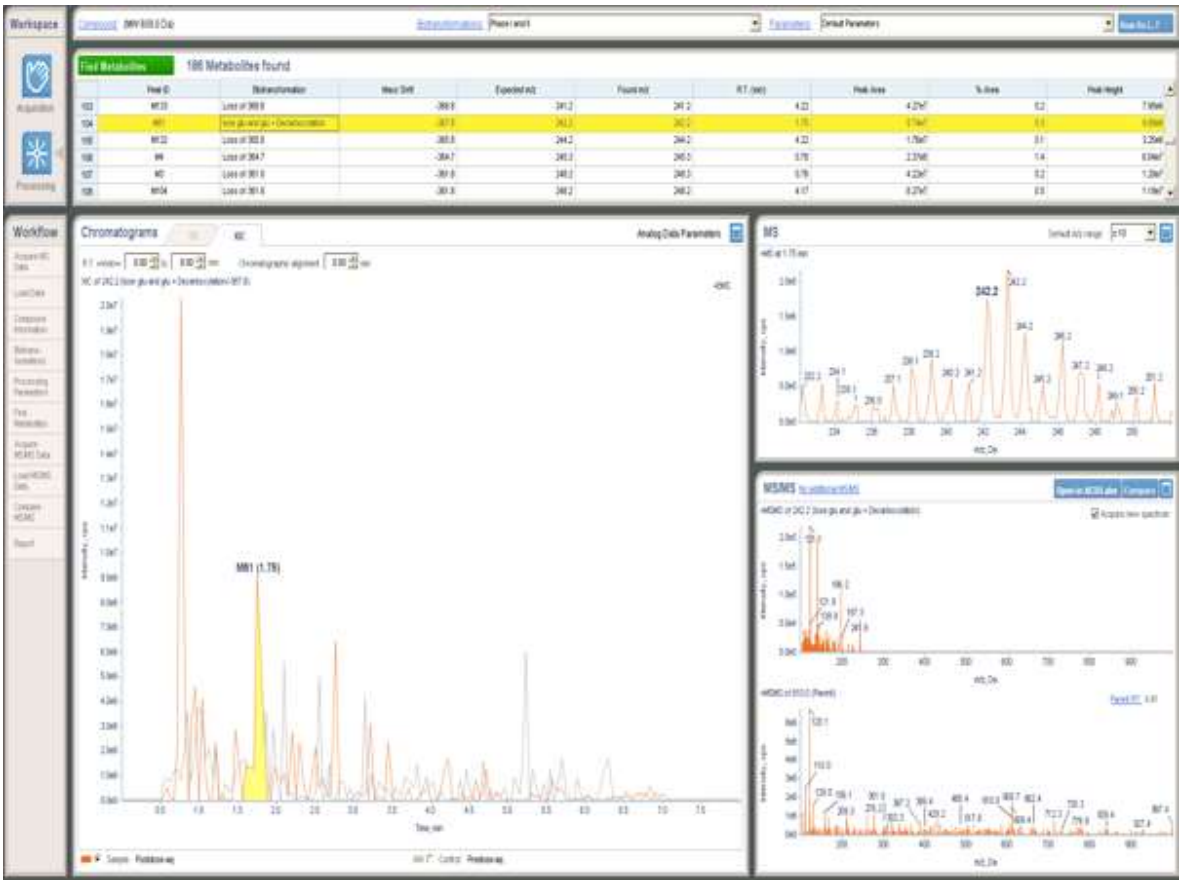

C. Peak Representing Tri-Oxidation in Rat Urine Dosed with Polymyxin B

D. Peak Representing Loss of Glucuronide and Demethylation in Rat Urine Dosed with Polymyxin B

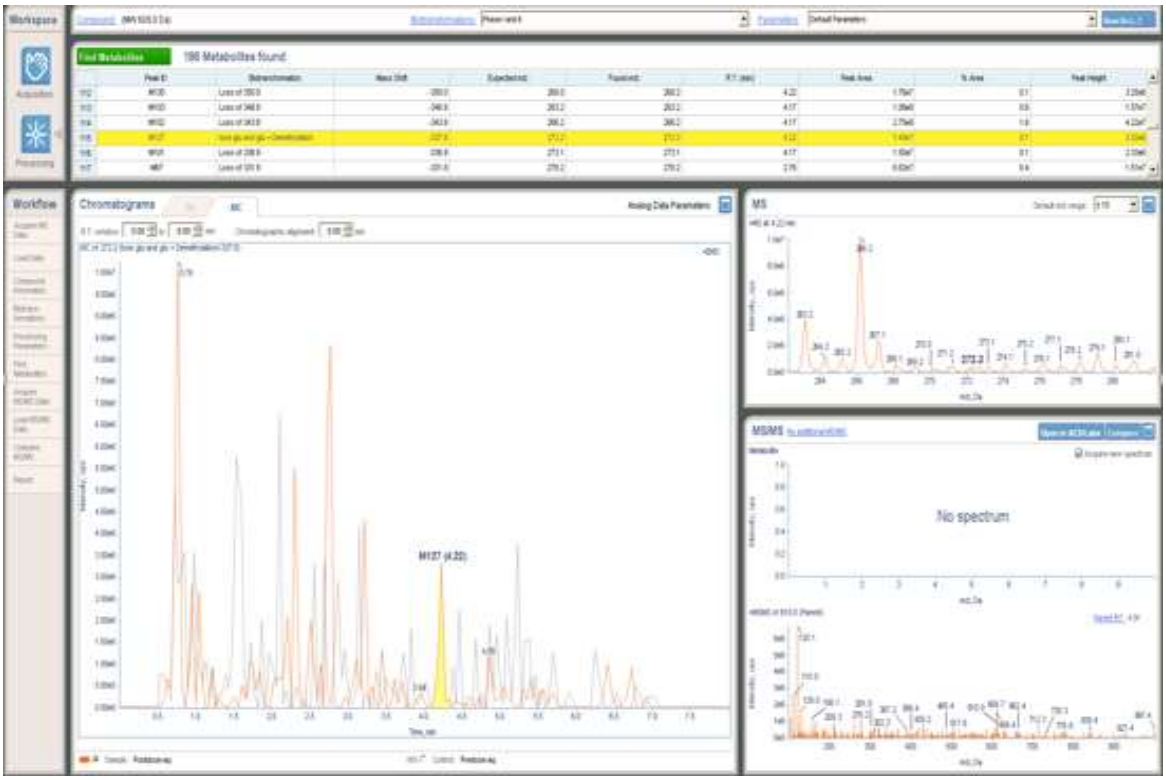

Figure 7.3: Chromatogram for Pre-and-Post Polymyxin B Dosed Rat Urine using MRM Feature of Qtrap UPLC-MS/MS

A. Pre-Dose Urine **B. Post-Dose Urine**

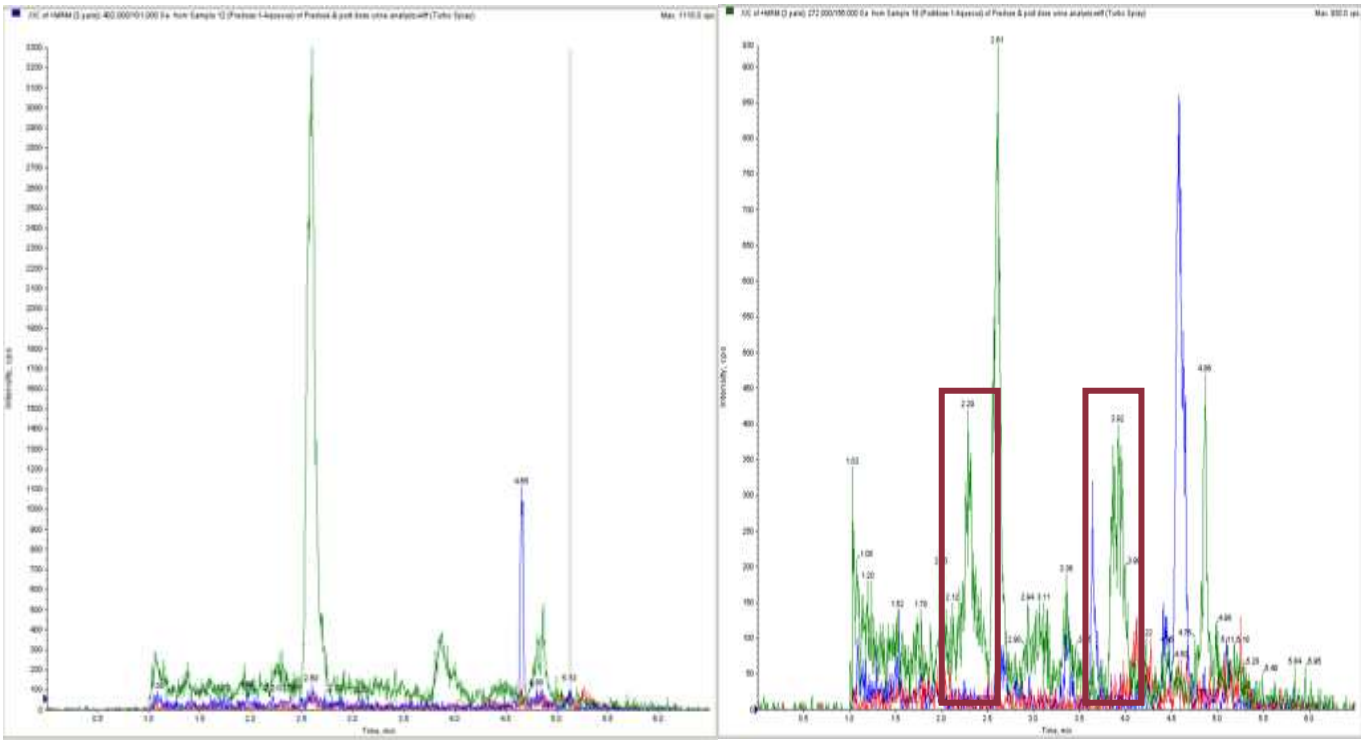

7.1.4 Research Design

7.1.4.1 *Antimicrobial Agent*

Polymyxin B sulfate (USP) powder will be purchased from Sigma-Aldrich (St. Louis, MO). Prior to each experiment, the drug will be reconstituted and diluted to the desired concentrations with normal saline. The reconstituted drug solutions will be stored at -80ºC until analysis.

7.1.4.2 *Animals*

Female Sprague-Dawley rats (225-250g) (Harlan, Indianapolis, IN, USA) will be used. The rats will receive food and water *ad libitum*. In selected experiments, jugular veins of selected animals will be cannulated to facilitate intravenous drug administration. Male C58BL/6 mice will be obtained from (Harlan Houston, TX). The mice will have access to regular rodent chow and water *ad libitum.* All animals will be maintained in a 12 h dark/light cycle and a temperature-and-humidity-controlled environment and cared for in accordance with the highest humane and ethical standards, as approved by Institutional Animal Care and Use Committee (IACUC) of the University of Houston.

7.1.4.3 *In vitro* Metabolism Studies

Primary mouse hepatocytes will be isolated from C57BL/6 mice using the two-step collagenase perfusion technique with slight modifications as described previously (Li et al., 2002; Ghose et al., 2004, 2008, 2009, 2011). Briefly, after digestion, the liver will be excised and transferred to a sterile 50 ml conical tube containing William's medium E supplemented with 1% streptomycin, glutamine, 0.1% gentamycin, glucagon and 10% fetal bovine serum. The hepatocytes will be then purified using a percoll gradient and washed twice; later screened for viability using the trypan blue exclusion technique. The cells with the viability of more than 90% will be further used for these studies. Cells will be plated at a density of 500,000 cells per well in six-well Primaria plates (BD Biosciences, San Diego, CA, U.S.A) and allowed to attach for 4h. Cells will be maintained for 48h with daily change of medium.

The cells will be incubated with serum-free William's medium E two hours prior to treatment. The cells will be incubated with polymyxin B (USP mixture) at varying final concentrations of 0.5, 1, 2, 4, 8 µg/ml in the culture well for 1, 2, 4, 8 and 24 h. After pretreatment with polymyxin mixture for a specific time, the reaction will be stopped with the solution (100 µl) of acetonitrile in phenacetin (1 µg/ml). Midazolam will be used as positive control and cells will be treated with 2

µM of midazolam in the similar fashion. The cells will further be lysed using lysis media and by passing through insulin syringe several times. The supernatants will be collected and stored in -80° until further analysis.

7.1.4.4 *UPLC-MS/MS Based Metabolic Profiling of Polymyxin B*

The rats (n=2) will be housed individually in separate metabolic cages to facilitate urine collection. Later, rats will be cannulated at jugular vein to facilitate drug administration. Blank urine will be collected from each rat prior to the administration of a single dose of polymyxin (3 mg/kg). The blood will be collected at 1, 2, 4, 8, 24 h time points through jugular vein catheter. Pre-dose and post-dose urine will be spun down to remove particulate matter and stored in aliquots at -80ºC until analysis. For metabolic profiling in bile, the rats will be cannulated at jugular vein as well as at bile duct. Pre-dose (blank) bile will be collected for 30 min followed by the collection of bile for 8 h post single dose (3 mg/kg) of polymyxin B dosing.

Prior to analysis, sample (serum, urine, and bile) will be thawed and processed for extraction with 5% TCA to precipitate protein as described in chapter 3. Additionally, for urine and bile samples, the supernatant after protein

precipitation will be loaded into the solid-phase extraction cartridges (Oasis HLB 1cc cartridges, 30 µm), preconditioned with 1m of methanol and 1 x 2 ml of water. After loading the urine samples, the cartridges will be washed with water followed by eluting solvent (0.1% formic acid in water: acetonitrile, 50:50) mixture. The eluent will be collected, diluted 10 times with water and then injected into UPLC/MS-MS for metabolic profiling.

ULPC-MS/MS Qtrap 5500 system equipped with lightsight® software functionality will be used for metabolite identification. The lightsight® software was designed to create compound-specific predicted multiple reactions monitoring-independent data acquisition for polymyxin B which will enable precise identification of metabolites.

7.1.5 Expected Outcome

We expect to see the oxidative, demethylated and glucuronide metabolites of polymyxin B. We anticipate that polymyxin B will also undergo amide hydrolysis to form smaller peptides.

7.1.6 Potential Problem and Alternate Strategy

Since we are using primary hepatocytes as our *in vitro* model to study metabolism, our metabolism information is only limited to the hepatic metabolism of polymyxin B. We might not be able to capture the information if polymyxin B undergoes renal metabolism. An alternative strategy would be to use S9 fractions/microsome derived from the rat kidney or the primary culture of isolated proximal convoluted tubules from rats as our future *in vitro* model. This would give us insights on the metabolic profile of polymyxin B via renal drug biotransformation.

7.2 ***Aim 2*: To investigate *the biliary disposition* of polymyxin B**

Finally, to the best of our knowledge, the present study is the first to examine the biliary excretion of polymyxin B. We detected all four major polymyxin B components in the bile over 4 h. To further substantiate this observation, we designed a multiple-dose (single dose of 3 mg/kg up to 10 consecutive days) biliary drug disposition study to further quantify polymyxin B in bile. Despite our efforts in quantifying all four major components of polymyxin B in bile, we could only account for the biliary excretion of the parent drug. Our results indicated a very low drug recovery; less than 1% of the parent drug was quantified over 24 h in bile. The major limitation of this study was that validated

UPLC-MS/MS assay in bile could only account for the parent form of the drug. Besides, the bile components and salts offered a high level of interference in the microbiological assay. Therefore, the drug cannot be accurately quantified. Nonetheless, we could not account for the majority of the administered dose in our biodistribution/disposition study.

Despite our efforts in quantifying all four major components of polymyxin B in bile, we could only account for the biliary excretion of the parent drug. Furthermore, many questions related to hepatic/renal drug metabolism and subsequent nonrenal excretion of its metabolites remain unanswered. Therefore, more rigorous studies are still needed to establish various facets such as *in vivo* metabolism profile and renal handling of polymyxin B. Future studies in our lab will aim at identifying as well as quantifying the major metabolites of polymyxin B. Currently, studies are ongoing in our lab to develop a validated UPLC-MS/MS assay which can reliably detect/quantify polymyxin B metabolites in bile. This will further delineate the disposition of drug metabolites in bile. Moreover, we also aim at investigating the renal uptake of polymyxin B using various mammalian cell lines. In conclusion, biliary excretion could be one of the possible routes of elimination for polymyxin B metabolites, which should be explored further.

7.2.1 Working Hypothesis

Our preliminary results on urine recovery of polymyxin B demonstrated that less than less than 1% of the administered dose was eliminated unchanged in the urine over 48 h (Abdelraouf, He, et al., 2012). Furthermore, we demonstrated that less than 5% of the administered dose was eliminated in the pharmacologically active form (metabolite, if any) through the urinary excretion route (Manchandani, Zhou, et al., 2016). These results insinuate that polymyxin B is most likely to be disposed via non-renal elimination pathways. Based on these findings, we hypothesize that polymyxin B could be eliminated via biliary route.

7.2.2 Justification and Feasibility

7.2.2.1 *Review of Relevant Literature*

We were able to successfully detect the four major components of polymyxin B in bile (Manchandani, Zhou, et al., 2016). Moreover, our preliminary metabolism studies predicted the presence of a glucuronide metabolite in the rat urine. Therefore, we further aim at developing a method to quantify a glucuronide metabolite in the bile.

7.2.2.2 *Preliminary Results*

Our results indicated that less than 1% of polymyxin B dose was excreted unchanged in bile 4 h after a single dose of polymyxin B as shown in Table 7.2. The bile could only be collected only until 4 h after drug administration due to limitation of our in-house surgical procedure as rats could not survive longer than 4 h. Initially, we suspected that survival of rats might be compromised due to lack of fluid replenishment after bile collection at every hour. To test this speculation we measured the volume of bile collected after every hour. Much to our surprise, the volume of bile collected every hour was roughly same (approximately 400 μl). However, to eradicate this limitation, we plan to further investigate biliary disposition of polymyxin B using surgically-modified rats which would facilitate bile collection for 24 h or longer duration.

Table 7.2: Biliary Disposition Profile of Parent Polymyxin B after Single Dosing

Rat ID	Amount of polymyxin B administered (µg)	Cumulative amount of polymyxin B in bile (µg)	% dose excreted unchanged in bile
1	745.92	2.74	0.37
2	716.70	3.60	0.50
3	716.70	3.34	0.47
4	744.50	1.94	0.26
5	744.50	2.18	0.29

Figure 7.4: Biliary Disposition Profile of Parent Polymyxin B after Single Dosing

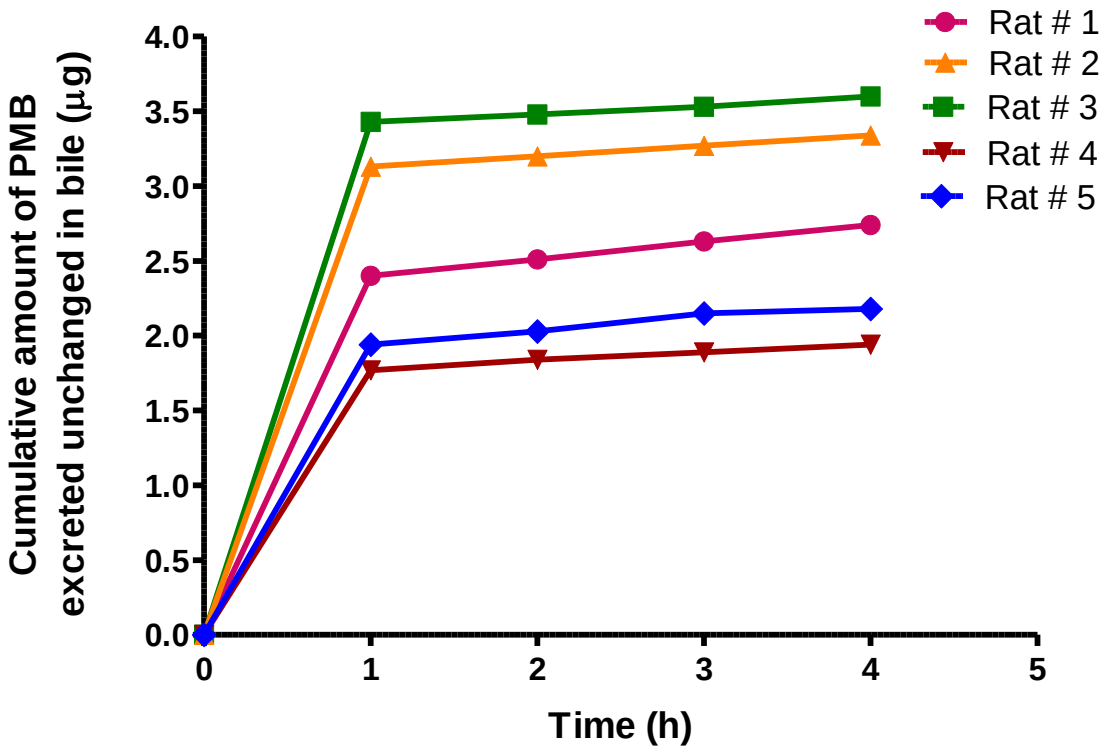

7.2.3 Research Design

7.2.3.1 *Antimicrobial Agent*

Polymyxin B sulfate (USP) powder will be purchased from Sigma-Aldrich (St. Louis, MO). Prior to each experiment, the drug will be reconstituted and diluted to the desired concentrations with normal saline. The reconstituted drug solutions will be stored at -80ºC until analysis.

7.2.3.2 *Animals*

Female Sprague-Dawley rats (225-250g; Harlan, Indianapolis, IN, USA) will be used as our *in vivo* model to study drug disposition in bile. In selected experiments, jugular veins of selected animals will be cannulated to facilitate intravenous drug administration. The animals will receive food and water *ad libitum* and will be maintained in a 12 h dark/light cycle and a temperature-and-humidity-controlled environment. All animals will be cared for in accordance with the highest humane and ethical standards, as approved by Institutional Animal Care and Use Committee (IACUC) of the University of Houston.

7.2.3.3 Biliary disposition of polymyxin B and its metabolites in rats

Once the metabolites of polymyxin B are identified, we would further assess the biliary disposition of parent as well metabolites at steady state. The steady state will be achieved by dosing polymyxin B for 11 consecutive days. Rats will undergo bile duct cannulation to collect the bile over 24 h post-dosing. The parent drug and the metabolites will be quantified in the bile using a validated UPLC-MS/MS method.

7.2.4 Expected Outcome

We expect to account for the majority of the administered dose eliminated in the bile either as parent drug or as its glucuronide metabolite.

7.2.5 Potential Problem and Alternate Strategy

One of the potential problems could be the low recovery of parent drug and metabolites in the bile. Under such circumstances, we could not establish a mass balance between dose administered and amount eliminated. This may warrant investigating drug disposition in feces.

7.3 ***Aim 3*: To investigate *in vitro* cell uptake study of polymyxin B**

We have concluded from our previous study that polymyxin B-induced injuries were primarily observed in the proximal tubules (Abdelraouf, Braggs, et al., 2012). Furthermore, extensive accumulation seen in these renal cell types established that the site of accumulation and site of drug-induced injury is identical (Manchandani, Zhou, et al., 2016). Therefore, we propose to further assess the mechanisms of *in vitro* cellular uptake and cellular toxicity due to prolonged polymyxin exposure using immortalized human renal proximal tubular cell line.

7.3.1 Working Hypothesis

A previous study from our lab has demonstrated that the intracellular uptake of polymyxin B in proximal tubular cells is an active and saturable process. It has been reported that the polymyxin B internalization/uptake in kidneys is mediated via an apical membrane-bound uptake system (Abdelraouf, Chang, Yin, Hu, & Tam, 2014). We have also demonstrated in a rat model that this uptake process can be disrupted chemically by using sodium maleate (Manchandani et al., 2016). Maleate is known to induce transient ultrastructural changes in the membrane localization of megalin on the renal brush border epithelium, rendering it non-functional for uptake of drugs and endogenous

ligands (Bergeron et al., 1996). Based on these relevant facts, we hypothesize that polymyxin B accumulation within renal cells is mediated through megalin, a membrane-bound endocytic receptor (Lrp2/ gp330). Therefore, to elucidate the role of megalin we propose to conduct *in vitro* cell uptake and cytotoxicity experiments of polymyxin B using HK-2 cells with varying pretreatment concentrations of sodium maleate.

7.3.2 Justification and Feasibility

73.2.1 *Review of Relevant Literature*

Megalin is 600 kDa glycoprotein and endocytic receptor located on the brush border epithelium of renal proximal epithelium cells. A previous study reported the involvement of megalin in the internalization of polybasic drugs such as polymyxins, gentamicin, and amikacin within kidneys (Moestrup et al., 1995). Colistin, a closely related analogue of polymyxin B, both structurally and pharmacologically, exhibits a high affinity towards megalin (Suzuki et al., 2013).

7.3.2.2 *Preliminary Results*

We performed *in vitro* cytotoxicity assay (MTT assay) using an immortalized HK-2 cells lines (Manassas, VA). In our treatment group, the cells

were incubated first with sodium maleate (Sigma-Aldrich, St. Louis MO) for 24 h at a final concentration of 5µg/ml in each well, followed by incubation with varying concentrations of polymyxin B (3.125 – 100 µg/ml) for 48 h. However, in the control group, the cells were only incubated with varying concentrations of polymyxin B for 48 h. After pretreatment, the cell viability was measured by MTT assay as described previously (Huang et al., 2015).

Our results indicated that there was no significant difference in the cell viability of HK-2 cells in the control and treatment group as shown in Table 7.3. These results indicated that 5 µg/ml of sodium maleate did not alter the mitochondrial activity; therefore, no major changes were observed in % cell viability between the control and the treatment group. We further estimated % cell viability with varying concentrations of sodium maleate as indicated in Table 7.4. Our result indicated that the cells retained their viability up to approximately 99% even when the concentration of sodium maleate exposed was increased 100 times (500 µg/ml) as compared to previous concentration (5 µg/ml).

Table 7.3: MTT Assay of Polymyxin in the using HK-2 Cells

Concentration of polymyxin B (μg/ml)	% Cell viability	
	Control group	Treatment group (pre-treatmentnt with sodium maleate, 5 μg/ml)
3.125	98.12	98.58
6.25	97.22	96.02
12.5	74.95	86.29
25	41.96	57.03
50	21.57	21.31
100	14.82	13.64

Table 7.4: MTT Assay with Varying Concentrations of Sodium Maleate using HK-2 Cells

Concentration of polymyxin B (μg/ml)	% Cell viability
62.5	107.46
125	108.95
250	109.09
500	98.86
1000	81.18
2000	48.65

7.3.3 Research Design

7.3.3.1 *Antimicrobial Agent*

Polymyxin B sulfate (USP) powder will be purchased from Sigma-Aldrich (St. Louis, MO). Prior to each experiment, the drug will be reconstituted and

diluted to the desired concentrations with normal saline. The reconstituted drug solutions will be stored at -80ºC until analysis.

7.3.3.2 *HK-2 Cell Culture*

HK-2 cells (ATCC CRL-2190, Manassas, VA) will be grown in Dulbecco's Modified Eagle's Medium (DMEM) with 10% fetal bovine serum, 0.02% epidermal growth factor (EGF), 2 mM glutamine, 50 U/ml penicillin, 50 pg/ml streptomycin and 1% non-essential amino acids (Thermoscientific, Waltham, MA). The cells will first be seeded in 96-well plate at the density of 5000 cells/well and allowed to grow for 2-3 days. The media will be replaced, and later the cells will be maintained in 10% DMEM/F12 media supplemented with 10% fetal bovine serum, 100 U/ml penicillin, 100 g/ml streptomycin, 100 g/ml neomycin and 1-2 g of sodium bicarbonate (Thermoscientific, Waltham, MA). The pH of the media will be adjusted to 7.2 either by 0.1N NaOH or HCl (Sigma-Aldrich, St. Louis, MO). The cells will be seeded on a 96-well plate maintained at 37ºC and 5% CO2 atmosphere with a density of 4000 cells/well. The cultures will be grown to approximately 80-90% confluency which usually takes 1-2 days. After attaining confluence, the splitting of the cells will be achieved by adding 5ml of PBS buffer supplemented with trypsin. The plates will be left undisturbed for 5 min and then scrapped to remove the cells. The cells will be centrifuged at 300 X g for 5 min

and split into 3 plates. Each plate will be added with 10 ml of PBS buffer, and the experiment will be performed in triplicates.

7.3.3.3 *Treatment Procedure*

The HK-2 cells will be grown at 37ºC in a humidified incubator under an atmosphere of 95% air and 5% CO2; maintained at pH 7.4. To determine the role of megalin in cellular uptake of polymyxin B, we used the specific molecular tool such as megalin siRNA (Santa Cruz Biotechnology, Dallas, Texas) to silence/ knock down the megalin gene/ protein function in HK-2 cells. The cells will then be transfected with either 10 μM of 19-25 nucleotide megalin siRNA or 4 μg/well of scrambled megalin siRNA as described previously (X. C. Li & Zhuo, 2014). The specificity and effectiveness of these target-specific megalin siRNAs on the megalin knockdown has been previously reported elsewhere (M. Li, Balamuthusamy, Simon, & Batuman, 2008). Fresh DMEM medium will be added to the cells, and subsequently, the cell will be treated with escalating concentrations of polymyxin B (3.125-100 μg/ml) for 48 h. For the control group, the entire procedure will remain same except the omission of the transfection with megalin siRNA. The cells will then be lysed using ultrasonication and passing through insulin syringe. The intracellular concentration of polymyxin B would be further assessed in both the groups using validated UPLC-MS/MS

assay. To evaluate % cell viability in both the groups, we would perform MTT assay on control as well as treated cells. Furthermore, we expect to establish a correlation between cell viability and intracellular concentration of polymyxin B.

7.3.4 Expected Outcome

We expect to see an attenuated polymyxin B uptake into the HK-2 cells transfected with megalin siRNA as compared to the control group. We anticipate that cell viability will be correlated to the intracellular uptake of polymyxin B; revealing an inverse association. We anticipate observing the higher levels of polymyxin B within control cells as compared to pretreated cells which will indicate a greater degree of intracellular drug uptake in control cells. This will subsequently result in lower cell viability and would show aggravated levels of toxicity in the control cells as compared to the pretreated cells.

7.3.5 Potential Problem and Alternate Strategy

One of the anticipated problems could be the lack of significant difference in the % cell viability of control and treatment group using MTT assay. Under such circumstances, we may need a more design a more specific mitochondrial toxicity assay on the isolated rat primary proximal tubular cell line. Other potential

problems could be the lack of significant difference in the intracellular polymyxin B concentrations between control and treatment group. This could be due to compensation of renal drug uptake by the secondary transport mechanism if any. Polymyxin B is a polycationic drug, presumed to be a ligand for carnitine/organic cation transporter-1 (OCTN1/SLC22A4) (Ma et al., 2009) or oligopeptide transporter-2 (PEPT-2) (Lu et al., 2016). If we observe potential compensation by other transport mechanisms, we might need to re-examine intracellular uptake of polymyxin B using either cell lines overexpressing OCTN1/PETP-2 or genetically modified [OCTN1 gene (-/-)]/ [PEPT-2 gene (-/-)] mouse model.

REFERENCES

Abdelraouf, K., Braggs, K. H., Yin, T., Truong, L. D., Hu, M., & Tam, V. H. (2012). Characterization of polymyxin B-induced nephrotoxicity: implications for dosing regimen design. *Antimicrob Agents Chemother, 56*(9), 4625-4629. doi:10.1128/AAC.00280-12

Abdelraouf, K., Chang, K. T., Yin, T., Hu, M., & Tam, V. H. (2014). Uptake of polymyxin B into renal cells. *Antimicrob Agents Chemother, 58*(7), 4200-4202. doi:10.1128/AAC.02557-14

Abdelraouf, K., He, J., Ledesma, K. R., Hu, M., & Tam, V. H. (2012). Pharmacokinetics and renal disposition of polymyxin B in an animal model. *Antimicrob Agents Chemother, 56*(11), 5724-5727. doi:10.1128/AAC.01333-12

Bergeron, M., Mayers, P., & Brown, D. (1996). Specific effect of maleate on an apical membrane glycoprotein (gp330) in proximal tubule of rat kidneys. *Am J Physiol, 271*(4 Pt 2), F908-916.

Li, M., Balamuthusamy, S., Simon, E. E., & Batuman, V. (2008). Silencing megalin and cubilin genes inhibits myeloma light chain endocytosis and ameliorates toxicity in human renal proximal tubule epithelial cells. *Am J Physiol Renal Physiol, 295*(1), F82-90. doi:10.1152/ajprenal.00091.2008

Li, X. C., & Zhuo, J. L. (2014). Mechanisms of AT1a receptor-mediated uptake of angiotensin II by proximal tubule cells: a novel role of the multiligand endocytic receptor megalin. *Am J Physiol Renal Physiol, 307*(2), F222-233. doi:10.1152/ajprenal.00693.2013

Lu, X., Chan, T., Xu, C., Zhu, L., Zhou, Q. T., Roberts, K. D., Zhou, F. (2016). Human oligopeptide transporter 2 (pept2) mediates cellular uptake of polymyxins. *J Antimicrob Chemother, 71*(2), 403-412. doi:10.1093/jac/dkv340

Manchandani, P., Zhou, J., Ledesma, K. R., Truong, L. D., Chow, D. S., Eriksen, J. L., & Tam, V. H. (2016). Characterization of Polymyxin B Biodistribution and Disposition in an Animal Model. *Antimicrob Agents Chemother, 60*(2), 1029-1034. doi:10.1128/AAC.02445-15

Nilsson, A., Goodwin, R. J., Swales, J. G., Gallagher, R., Shankaran, H., Sathe, A., Gupta, A. (2015). Investigating nephrotoxicity of polymyxin derivatives by mapping renal distribution using mass spectrometry imaging. *Chem Res Toxicol, 28*(9), 1823-1830. doi:10.1021/acs.chemrestox.5b00262